

**SUMMARY OF LITHOLOGIC LOGGING OF NEW AND
EXISTING BOREHOLES AT YUCCA MOUNTAIN,
NEVADA, MARCH 1994 TO JUNE 1994**

U.S. GEOLOGICAL SURVEY

Open-File Report 94-451

Prepared in cooperation with the
NEVADA OPERATIONS OFFICE,
U.S. DEPARTMENT OF ENERGY under
Interagency Agreement DE-AI08-92NV10874



9505150314 950424
PDR WASTE PDR
WM-11

SUMMARY OF LITHOLOGIC LOGGING OF NEW AND EXISTING BOREHOLES AT YUCCA MOUNTAIN, NEVADA, MARCH 1994 TO JUNE 1994

by Jeffrey K. Geslin and Thomas C. Moyer

U.S. GEOLOGICAL SURVEY

Open-File Report 94-451

**Prepared in cooperation with the
NEVADA OPERATIONS OFFICE,
U.S. DEPARTMENT OF ENERGY under
Interagency Agreement DE-AI08-92NV10874**

**Denver, Colorado
1995**



U.S. DEPARTMENT OF THE INTERIOR

BRUCE BABBITT, Secretary

U.S. GEOLOGICAL SURVEY

Gordon P. Eaton, Director

The use of trade, product, industry, or firm names is for descriptive purposes only and does not imply endorsement by the U.S. Government.

For additional information write to:
Chief, Earth Science Investigations
Program
Yucca Mountain Project Branch
U.S. Geological Survey
Box 25046, MS 421
Denver Federal Center
Denver, CO 80225

Copies of this report can be purchased from:
U.S. Geological Survey
Earth Science Information Center
Open-File Reports Section
Box 25286, MS 517
Denver Federal Center
Denver, CO 80225

CONTENTS

Abstract.....	1
Introduction.....	1
Study methods.....	2
Continuing logging.....	7
References.....	10
Appendix 1. Graphical lithologic logs for boreholes at Yucca Mountain, Nevada.....	10
Notes for graphical lithologic logs.....	10
UE-25 NRG #2C.....	10
UE-25 NRG #2D.....	10
USW NRG-77A.....	10
All graphical lithologic logs.....	10

FIGURES

1. Borehole location map.....	3
-------------------------------	---

TABLES

1. Location and information for boreholes logged at Yucca Mountain, March 1994 to June 1994.....	2
2. Lithostratigraphic nomenclature of the Paintbrush Group at Yucca Mountain.....	4
3. Generalized lithostratigraphy of boreholes at Yucca Mountain, Nevada.....	5
4. Summary of depths to basal contacts for boreholes at Yucca Mountain, Nevada.....	6

CONVERSION FACTORS AND VERTICAL DATUM

Multiply	By	To obtain
millimeter (mm)	0.03937	inch
centimeter (cm)	0.3937	inch
meter (m)	3.281	foot
kilometer (km)	0.6214	mile

Sea level: In this report "sea level" refers to the National Geodetic Vertical Datum of 1929 (NGVD of 1929)—a geodetic datum derived from a general adjustment of the first-order level nets of both the United States and Canada, formerly called Sea Level Datum of 1929.

Summary of Lithologic Logging of New and Existing Boreholes at Yucca Mountain, Nevada, March 1994 to June 1994

By Jeffrey K. Geslin and Thomas C. Moyer

Abstract

This report summarizes lithologic logging of core from boreholes at Yucca Mountain, Nevada, conducted from March 1994 to June 1994. Units encountered during logging include Quaternary-Tertiary alluvium and colluvium, Tertiary Rainier Mesa Tuff, all units in the Tertiary Paintbrush Group, and Tertiary Calico Hills Formation. Logging results are presented in a table of contact depths for core from unsaturated zone neutron (UZN) boreholes and graphic lithologic logs for core from north ramp geology (NRG) boreholes.

INTRODUCTION

Yucca Mountain, Nevada, is being investigated as a potential site for a high-level radioactive waste repository. This report summarizes the lithologic logging of new and existing boreholes at Yucca Mountain that was done from March to June 1994, by the Yucca Mountain Project Branch of the U.S. Geological Survey (USGS). This logging was undertaken with the objective to determine the spatial distribution and characteristics of stratigraphic units within the Yucca Mountain site area. Stratigraphic data obtained from lithologic logging are used in a preliminary three-dimensional lithostratigraphic model of Yucca Mountain. These data also can be integrated into hydrologic studies at Yucca Mountain and applied to engineering and construction of the Exploratory Studies Facility.

Lithostratigraphic units identified during logging include Quaternary-Tertiary alluvium and colluvium, the Tertiary Rainier Mesa Tuff of the Timber Mountain Group, all units in the Tertiary Paintbrush Group, and the Tertiary Calico Hills Formation. Criteria used to identify contacts between these units, and between lithostratigraphic units within the Paintbrush Group, are discussed in Geslin and others (in press). Stratigraphic nomenclature and lithologic descriptions of stratigraphic units in the Tiva Canyon, Yucca Mountain, Pah Canyon, and Topopah Spring Tuffs of the Paintbrush Group are from Sawyer and others (in

press) and also are summarized in Buesch and others (USGS, written commun., 1994).

The boreholes logged from March to June 1994 are listed, with their location and elevation, in table 1. Table 1 also lists the Data Tracking Number (DTN) for stratigraphic data from each borehole that have been released to the Yucca Mountain Project, submitted to the USGS Local Records Center in Denver, Colorado, and stored in the Yucca Mountain Project Central Records Facility in Las Vegas, Nevada. The locations of these boreholes are shown in figure 1. Cores from boreholes logged during this study are stored at the Yucca Mountain Project Sample Management Facility at the Nevada Test Site.

STUDY METHODS

Lithostratigraphic units identified in core follow the stratigraphic hierarchy and nomenclature for the Paintbrush Group defined in Sawyer and others (in press) and followed by Buesch and others (USGS written commun., 1994) (table 2). The criteria used to identify contacts between stratigraphic units are described in Geslin and others (in press). Lithologic logging includes either identification of the depths of stratigraphic contacts (herein referred to as type 1 logging) or identification of the depths of contacts and detailed unit descriptions (herein referred to as type 2 logging). The lithostratigraphic units encountered during type 1 and type 2 logging of core from boreholes are summarized in table 3. The results of type 1 logging are reported as tables of contact depths (summarized in table 4), whereas the results of type 2 logging are reported in graphical form (appendix 1).

Type 1 logs were completed for core recovered from unsaturated zone neutron (UZN series) boreholes (table 4). Core recovered from UZN-series boreholes is stored in lexan tubing that limits viewing of the core and modifies colors by retaining moisture. Contacts that are difficult to identify through lexan or that were removed by sampling were confirmed or constrained by examination of processed samples at the Hydrologic Research Facility or by viewing videotapes of core photographed prior to sample removal.

Table 1. Location and information for boreholes logged at Yucca Mountain, March 1994 to June 1994

[Northing, easting, and elevation data are from EG&G and were provided as information to the Yucca Mountain Project. Northing and easting are based on the Nevada State Coordinate System. Locations and elevations are in feet.]

Borehole number	Northing	Easting	Elevation	Data tracking number
<i>Identification of lithologic contacts (type 1 logging)</i>				
USW UZ-N11	780,573.93	559,020.93	5,224.0	GS940308314211.010
USW UZ-N15	778,090.54	559,551.76	5,109.4	GS940308314211.019
USW UZ-N16	778,150.80	559,625.98	5,116.6	GS940308314211.019
USW UZ-N17	778,224.12	559,995.10	5,127.9	GS940308314211.019
USW UZ-N36	773,899.50	563,582.66	4,642.0	GS940308314211.018
USW UZ-N38	767,466.37	563,343.41	4,148.9	GS940308314211.011
UE-25 UZN #63	768,836.54	566,169.39	3,944.1	GS940308314211.017
USW UZ-N64	765,728.46	559,435.76	4,790.9	GS940308314211.016
<i>Detailed lithologic logging (type 2 logging)</i>				
UE-25 NRG #2C	765,771.68	569,189.76	3,801.2	GS940308314211.012
UE-25 NRG #2D	765,825.10	569,132.29	3,792.1	GS940308314211.013
USW NRG-7A	768,879.96	562,984.13	4,207.0	GS940408314211.020

Type 2 lithologic logs (appendix 1) were created for core recovered from north ramp geology (NRG) boreholes. These logs use the criteria of Buesch and others (USGS, written commun., 1994) to identify the welding and crystallization zones in each unit. Accompanying lithologic unit descriptions include the phenocryst content and assemblage; lithophysae content and size; pumice content, size, and composition; lithic clast content, size, and composition; and matrix color and content. The percentage of phenocrysts, lithic clasts, pumice clasts and lithophysae are visually estimated using charts included in the Munsell Soil Color Charts (Kollmorgen Instruments Corp., 1992). Phenocryst, pumice, and lithic clast types are identified with the aid of a hand lens. Phenocryst, pumice, and lithic clast types are identified with the aid of a hand lens or binocular microscope. The maximum and minimum dimensions of pumice, lithic clast, and lithophysae (void) sizes are measured along two perpendicular axes and recorded as either typical or maximum sizes observed. Pumice, lithic clast, and matrix colors are determined on dry core using Munsell Color Charts

(Geological Society of America, 1991; Kollmorgen Instruments Corp., 1992). Other features of the core, including fracture geometry and morphology, fracture mineralization, and development and orientation of foliation (dip angle measured from horizontal), also are recorded and included in unit descriptions.

CONTINUING LOGGING

Continued logging in 1994 and 1995 will produce a table of contact depths for boreholes NRG #5A, SD-9, SD-10, SD-12, UZ-7A, SRG-1, SRG-2, SRG-3, and SRG-4 (depending on drilling progress) that will be submitted to the USGS Yucca Mountain Project Branch Local Records Center upon completion of drilling and following internal review. Graphical lithologic logs that summarize detailed logging will be prepared for UZ-14, SD-9, SD-12, and UZ-7A (depending on drilling progress). These data will be integrated into the preliminary three-dimensional lithostratigraphic model of Yucca Mountain.

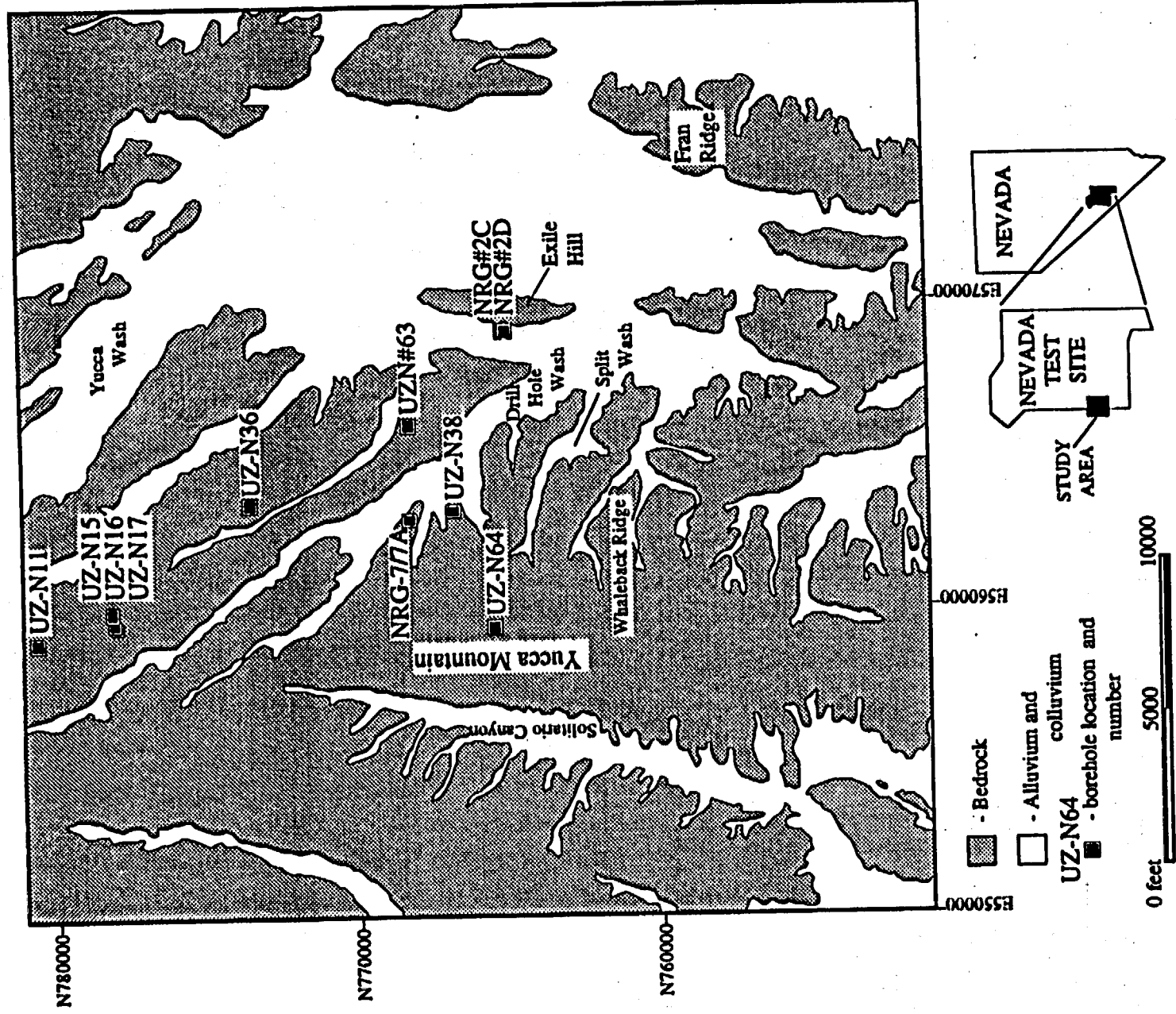


Figure 1. Borehole location map (modified from Nelson and others, 1991).

Table 2. Lithostratigraphic nomenclature of the Paintbrush Group at Yucca Mountain (from Sawyer and others, in press; Buesch and others, USGS, written commun., 1994)

Tuff unit "x" (Tpki)	
Pre-Tuff unit "x" bedded tuff (Tpbt5)	
Tiva Canyon Tuff (Tpc)	Topopah Spring Tuff (Tpt)
crystal-rich member (Tpcr) (quartz latite)	crystal-rich member (Tptr) (quartz latite)
vitric zone (rv)	vitric zone (rv)
non- to partially welded subzone (rv3)	non- to partially welded subzone (rv3)
moderately welded subzone (rv2)	moderately welded subzone (rv2)
vitrophyre subzone (rv1)	vitrophyre subzone (rv1)
nonlithophysal zone (rn)	nonlithophysal zone (rn)
subvitrophyre transition subzone (rn4)	crystal transition subzone (rn1)
pumice-poor subzone (rn3)	lithophysal zone (rl)
mixed pumice subzone (rn2)	crystal transition subzone (rl1)
crystal transition subzone (rn1)	crystal-poor member (Tptp) (high-silica rhyolite)
lithophysal zone (rl)	
crystal transition subzone (rl1)	upper lithophysal zone (pul)
crystal-poor member (Tpcp) (high-silica rhyolite)	cavernous lithophysae subzone (pul2)
upper lithophysal zone (pul)	small lithophysae subzone (pul1)
spherulite-rich subzone (pul1)	middle nonlithophysal zone (pma)
middle nonlithophysal zone (pma)	upper subzone (pma3)
upper subzone (pma3)	lithophysae-bearing subzone (pma2)
lithophysae-bearing subzone (pma2)	lower subzone (pma1)
lower subzone (pma1)	lower lithophysal zone (pll)
lower lithophysal zone (pll)	lower nonlithophysal zone (pln)
lower nonlithophysal zone (pln)	vitric zone (pv)
hackly subzone (plnh)	vitrophyre subzone (pv3)
columnar subzone (plnc)	moderately welded subzone (pv2)
spherulitic pumice interval (plnc3)	non- to partially welded subzone (pv1)
argillic pumice interval (plnc2)	
vitric pumice interval (plnc1)	Pre-Topopah Spring Tuff bedded tuff (Tpbt1)
vitric zone (pv)	
vitrophyre subzone (pv3)	
moderately welded subzone (pv2)	
non- to partially welded subzone (pv1)	
Pre Tiva Canyon Tuff bedded tuff (Tpbt4)	
Yucca Mountain Tuff (Tpy)	
Pre-Yucca Mountain Tuff bedded tuff (Tpbt3)	
Pah Canyon Tuff (Tpp)	
Pre-Pah Canyon Tuff bedded tuff (Tpbt2)	

Table 3. Generalized lithostratigraphy of boreholes at Yucca Mountain, Nevada

	Borehole number										
	UZ-N 11	UZ-N 15	UZ-N 16	UZ-N 17	UZ-N 38	UZ-N 38	UZ-N #63	UZ-N 64	NRG #2C	NRG #2D	NRG -77A
Rainier Mesa Tuff (Tmr)									I	I	
Pre-Rainier Mesa Tuff bedded tuff (Tmbt1)									I	I	
Tuff unit "x" (Tpk1)											
Pre-Tuff unit "x" bedded tuff (Tpbt5)											
Tiva Canyon Tuff (Tpc)											
crystal-rich member (Tpcr)											
vitric zone (rv)											
nonlithophysal zone (m)		I	I	I	I				I		
lithophysal zone (ri)											
crystal-poor member (Tpcp)											
upper lithophysal zone (pul)											
middle nonlithophysal zone (pmm)											
lower lithophysal zone (pll)											
lower nonlithophysal zone (pln)											
hackly subzone (plnh)											
columnar subzone (plnc)											
vitric zone (pv)											
Pre-Tiva Canyon Tuff bedded tuff (Tpbt4)											
Yucca Mountain Tuff (Tpy)											
Pre-Yucca Mountain Tuff bedded tuff (Tpbt3)											
Pah Canyon Tuff (Tpp)											
Pre-Pah Canyon Tuff bedded tuff (Tpbt2)											
Topopah Spring Tuff (Tpt)											
crystal-rich member (Tptr)											
vitric zone (rv)											
nonlithophysal zone (m)											
lithophysal zone (ri)											
crystal-poor member (Tptp)											
upper lithophysal zone (pul)											
middle nonlithophysal zone (pmm)											
lower lithophysal zone (pll)											
lower nonlithophysal zone (pln)											
vitric zone (pv)											
Pre-Topopah Spring Tuff bedded tuff (Tpbt1)											
Calico Hills Formation (The)											

CONTINUING LOGGING

Table 4. Summary of depths to basal contacts for boreholes at Yucca Mountain, Nevada

UNIT* no core	USW UZ-N11	USW UZ-N15	USW UZ-N16	USW UZ-N17	USW UZ-N36	USW UZ-N38	UE-25 UZN #83	USW UZ-N64
Alluvium/colluvium (QIac)	1.7	2.3	4.2	2.5	0.9	17.9	4.4 8.6†	1.8
Tiva Canyon Tuff (Tpc)								
crystal-rich member (Tpcr)								
nonlithophysal zone (m)								
subvitrophyre transition subzone (m4)		16.2†		19.3†	16.1†			
pumice-poor subzone (m3)		57.6	36.5†		47.5			39.8†
mixed pumice subzone (m2)								
crystal transition subzone (m1)								
crystal-poor member (Tpcp)								
lower nonlithophysal zone (pln)								
hackly subzone (plnh)						27.3†	25.0††	
columnar subzone (plnc)								
spherulitic pumice interval (c3)						49.1	44.3	
argillic pumice interval (c2)	25.2†					80.9		
vitric zone (pv)								
moderately welded subzone (pv2)	29.7							
non- to partially welded subzone (pv1)	46.4							
Bedded tuff (Tpbtd)	60.6							
Yucca Mountain Tuff (Tpy)								
Total depth	84.4	59.9	60.0	59.9	59.8	89.4	60.0	60.0

* Stratigraphic subdivisions follow the nomenclature defined by Buesch and others (USGS, written commun., 1994). All measurements are in feet.

† The first unit encountered in the borehole.

†† The contact between the hackly and columnar subzones of the crystal-poor lower nonlithophysal zone is gradational from 25.0 to 37.3 feet. This unit is overlain by alluvium or colluvium.

REFERENCES

- Geological Society of America, 1991, Rock-color chart: Boulder, Colo., Geologic Society of America. (MOL.19940810.0002)
- Geslin, J.K., Moyer, T.C., and Buesch, D.C., 1994, Summary of lithologic logging of new and existing boreholes at Yucca Mountain, Nevada, August 1993 to February 1994: U.S. Geological Survey Open-File Report 94-342, in press. (MOL.19940810.0011)
- Kollmorgen Instruments Corporation, 1992, Munsell soil color charts: New York, Kollmorgen Instruments Corporation. (MOL.19940810.0003)
- Nelson, P.H., Muller, D.C., Schimschal, Ulrich, and Kibler, J.E., 1991, Geophysical logs and core measure-

- ments from forty boreholes at Yucca Mountain, Nevada: U.S. Geological Survey, Geophysical Investigations Map GP-1001, 64 p. (NNA.920211.0022)
- Sawyer, D.A., Fleck, R.J., Lanphere, M.A., Warren, R.G., Broxton, D.E., and Hudson, M.R., Episodic caldera volcanism in the Miocene southwestern Nevada volcanic field—Revised stratigraphic framework, $^{40}\text{Ar}/^{39}\text{Ar}$ geochronology, and implications for magmatism and extension: Geological Society of America Bulletin, in press. (MOL.19940725.0004)

NOTE: Parenthesized numbers following each cited reference are for U.S. Department of Energy OCRWM Records Management purposes only and should not be used when ordering the publication.

APPENDIX

APPENDIX 1. GRAPHICAL LITHOLOGIC LOGS FOR BOREHOLES AT YUCCA MOUNTAIN, NEVADA

Notes for Graphical Lithologic Logs

UE-25 NRG #2C

Core was recovered from the borehole with a hollow-stem auger, and includes nonlithified pyroclastic-flow and fall deposits of the Rainier Mesa Tuff (Timber Mountain Group), nonlithified bedded tuffs that underlie Rainier Mesa Tuff, and lithified tuff unit "x" (Paintbrush Group).

UE-25 NRG #2D

Core that was recovered from the borehole with a hollow-stem auger includes nonlithified pyroclastic-flow and fall deposits of the Rainier Mesa Tuff (Timber Mountain Group), nonlithified bedded tuffs that underlie Rainier Mesa Tuff, and lithified tuff unit "x" (Paintbrush Group).

USW NRG-77A

NRG-7 is a vertical hole located at approximately 768,846.20 N; 563,004.90 E that was drilled from the surface to 17.0 ft and then abandoned. NRG-7A is an adjacent vertical hole located at approximately 768,879.96 N; 562,984.13 E that was cored from 17.0 to 1513.4 ft (total depth). Samples were collected from NRG-7, however, it is not known if these samples represent colluvium or bedrock. Therefore, surface to 17 ft depth was not included in this log. Lithostratigraphic units in the core include the lower zones of the Tiva Canyon Tuff, Yucca Mountain Tuff, Pah Canyon Tuff, Topopah Spring Tuff, interbedded

nonwelded tuffs of the Paintbrush Group, and the upper part of the Calico Hills Formation.

(V)—Contacts depths designated with this symbol were identified using videotape of the core prior to sample removal.

*—The top of the Topopah Spring Tuff is typically marked by a 2-cm-thick lithic-rich fallout deposit. This deposit apparently is represented by an unrecovered interval at approximately 280 ft. This depth is estimated from stratigraphic relationships in adjacent NRG boreholes.

All Graphical Lithologic Logs

Welding Definitions

Nonwelded = nondeformed pumice, no to slight sintering of matrix.

Partially welded = nondeformed pumice, sintered/incipiently welded matrix (some macroscopic porosity).

Moderately welded = partial deformation of pumice (some macroscopic porosity), densely welded matrix (no porosity).

Densely welded = collapsed pumice (no macroscopic porosity), densely welded matrix.

Mineral Notation

qtz = quartz

san = sanidine

plag = plagioclase

feld = sanidine and plagioclase, undifferentiated

hbl = hornblende

cpx = clinopyroxene

bio = biotite

(oxy)bio = partially oxidized biotite

oxybio = completely oxidized biotite

Borehole : UE-25 NRG #2C
 Data Tracking Number: GS940308314211.012

Zones of welding (W)

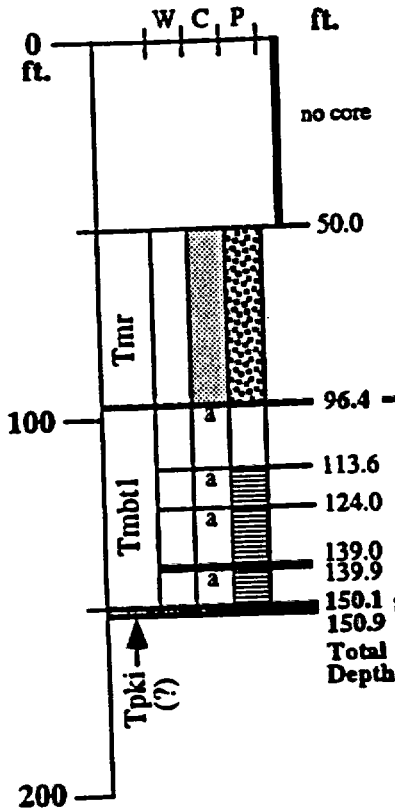
- Moderately to Densely (o-lithophysae)
- Partially to Moderately
- Non- to Partially
- Nonwelded

Zones of crystallization (C)

- Devitrified / Devit. + vapor-phase mins.
- Vitric / Vitric + vapor-phase mins.
- Altered (a) / to clay (c) / to zeolite (z)

Phenocryst content (P)

- greater than 10 percent
- 5 - 10 percent
- less than 5 percent



Rainier Mesa Tuff (Tmr) -

Nonlithified pyroclastic-flow deposit: 50.0-96.4 ft
 Matrix, which changes downward from pale yellowish brown to pinkish white, contains distinctive colorless, bubble-wall glass shards. Pumice clasts (10-15 percent) are vitric, colorless, light gray, light brown, or brownish orange. Crystals (10-15 percent) include qtz, plag, san, and bio. Deposit may be lithified above 51.5 ft.

Bedded Tuff (Tmbt1) -

96.4-113.6 ft: Nonlithified fallout tephra. White, vitric pumice lapilli and volcanic lithic clasts. Moderately sorted. Lithic content is 10-20 percent above 108.5 ft, but less than 2 percent below 108.5 ft. Pumice clasts are typically less than 3 mm diameter. Grades upward into a light brown paleosol (96.4-100.8 ft). *113.6-124.0 ft: Nonlithified pumice-rich fallout.* Moderately well sorted, normally graded. Pumice grades upward from less than 5 mm to less than 3 mm diameter. Contains grayish yellow-green lithic clasts. Crystals of feld, qtz, bio. Light brown paleosol from 113.6-118.8 ft. *124.0-139.9 ft: Nonlithified pyroclastic-flow (?) deposit.* Light brown with glass shards and white pumice less than 5 mm. Crystals of feld, qtz, bio. Pumice fallout from 139.0 to 139.9 ft. *139.9-150.1 ft: Nonlithified pyroclastic-flow (?) deposit.* Medium brown with glass shards and 10-20 percent white pumice, most less than 5 mm. Crystals of feld, qtz, bio. Poorly consolidated.

Tuff Unit "x" (Tpki) (?) -

Lithified pyroclastic-flow deposit: 150.1 ft-Total Depth
 Pumice clasts (10-15 percent), white to pale yellowish or greenish (zeolitized?), in a brownish gray altered matrix. Volcanic lithic clasts (5-7 percent) are dark gray, dark reddish gray, or medium light gray.

Zones of welding (W)

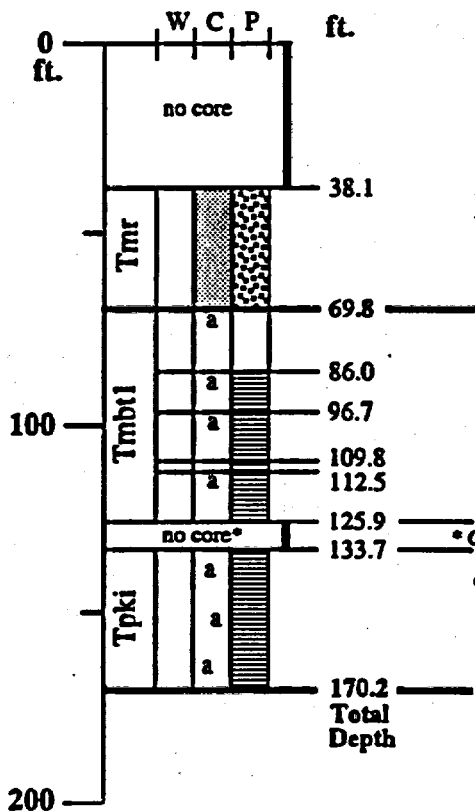
-  Moderately to Densely (o-lithophysae)
-  Partially to Moderately
-  Non- to Partially
-  Nonwelded

Zones of crystallization (C)

-  Devitrified / Devit. + vapor-phase mins.
-  Vitric / Vitric + vapor-phase mins.
-  Altered (a) / to clay (c) / to zeolite (z)

Phenocryst content (P)

-  greater than 10 percent
-  5 - 10 percent
-  less than 5 percent



Rainier Mesa Tuff (Tmr) -

Nonlithified pyroclastic-flow deposit: 38.1-69.8 ft
 Matrix, which changes downward from pale yellowish brown to pinkish white, contains distinctive colorless, bubble-wall glass shards. Pumice clasts (10-20 percent) are vitric, colorless, white, light brown, or brownish orange. Crystals (10-15 percent) include qtz, plag, san, and bio.

Bedded Tuff (Tmbt1) -

69.8-86.0 ft: Nonlithified fallout tephra. White, vitric pumice lapilli and volcanic lithic clasts. Moderately sorted, lithic content increases from about 5 percent to about 20 percent upward, pumice clasts are typically less than 3 mm diameter. Grades upward into a light brown paleosol (69.8-74.0 ft). *86.0-96.7 ft: Nonlithified pumice-rich fallout.* Moderately well sorted, normally graded. Pumice grades upward from less than 5 mm to less than 3 mm diameter. Crystals of feld, qtz, bio. Light brown paleosol from 86.0-91.0 ft. *96.7-112.5 ft: Nonlithified pyroclastic-flow (?) deposit.* Light brown with glass shards and white pumice less than 5 mm. Crystals of feld, qtz, bio. Pumice-rich fallout from 109.8 to 112.5 ft. *112.5-125.9 ft: Nonlithified pyroclastic-flow (?) deposit.* Medium brown with glass shards and 10-20 percent white pumice, most less than 5 mm. Crystals of feld, qtz, bio. Poorly consolidated below 118.0 ft.

* Core run marker notes lithified material at 127.4 ft.

Tuff Unit "x" (Tpki) -

Lithified pyroclastic-flow deposit: 133.7 ft-Total Depth
 Pumice clasts (10-15 percent), white to pale yellowish or greenish (zeolitized?), in a brownish gray altered matrix. Volcanic lithic clasts (5-7 percent) are dark gray, dark reddish gray, or medium light gray.

Zones of welding (W)

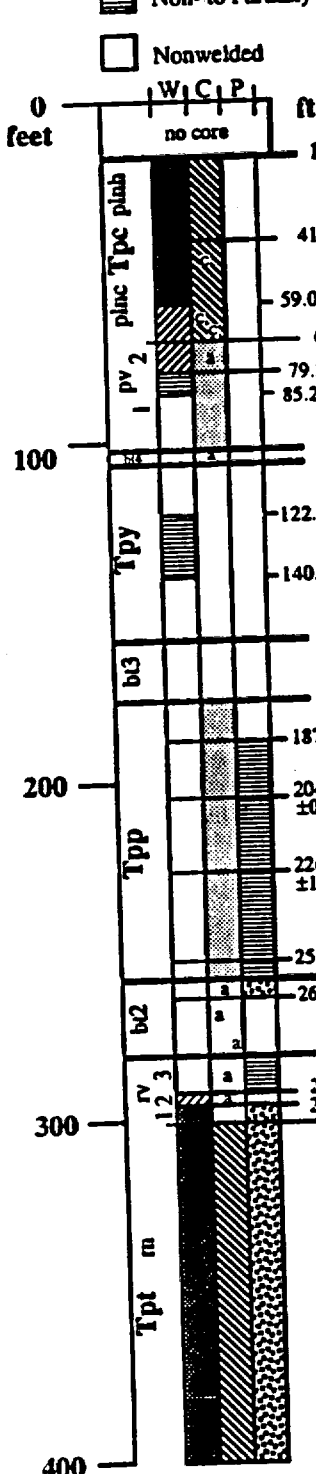
- Moderately to Densely (o-lithophysae)
- Partially to Moderately
- Non- to Partially
- Nonwelded

Zones of crystallization (C)

- Devitrified / Devit. + vapor-phase mins.
- Vitric / Vitric + vapor-phase mins.
- Altered (a) / to clay (c) / to zeolite (z)

Phenocryst content (P)

- greater than 10 percent
- 5 - 10 percent
- less than 5 percent



Tiva Canyon Tuff (Tpc)-

Crystal-poor lower nonlithophysal zone (pln) (17.0-69.7):
 17.0-41.0? - *hackly subzone (plnh)* - Lower contact gradational from 29.0-45.3. Matrix is pale red (10R5/2 to 10R6/2) grading downward to pale brown (5YR5/2). 3-5 percent pumice clasts, gray (N4), devitrified and vapor-phase altered or spherulitic, and grayish pink (5R7/2) and argillic (most less than 20 mm). 3-4 percent phenocrysts include feld and bio. Abundant rough, subhorizontal fractures. Less than 1 percent lithophysae above 19.2. 41.0?-69.7 *columnar subzone (plnc)* - Matrix is light brownish gray (5YR6/1) grading downward to pinkish gray (7.5YR7/1). 5-15 percent pumice clasts define foliation, gray (N5) to grayish red (5R4/2), devitrified, locally vapor-phase altered, mostly pink (5R7/6) and argillic below 66.3. 3-4 percent phenocrysts of feld and bio. Moderately welded with remnant shard texture below 59.0. Moderately smooth fractures.
Crystal-poor vitric zone (pv) (69.7-102.7): 69.7-79.2±0.8 *moderately welded subzone (pv2)* - Glass shards, moderate brown (5YR5/6) grading downward to dark grayish brown (7.5YR3/1) in light brown shreds, moderate (5YR5/6), partly devit. matrix. 10 percent pumice, white (vitric) to pinkish gray (5R7/2, altered). Welding decreases downward. 79.2±0.8-102.7 *non- to partially welded subzone (pv1)* - Black (N1) bubble-textured glass shards in pinkish gray (5YR7/2) to light gray (N8) vitric to partly devitrified matrix. Matrix foliation decreases downward. 3 percent pumice as above.

Yucca Mountain Tuff (Tpy) -

Matrix grades downward from light brown (5YR6/4) to grayish orange pink (5YR7/2) to medium light gray (N6-N7). Glass shards are colorless to black with bubble textures. 1-3 percent pumice clasts, vitric (medium gray-N5) to altered (moderate orange-pink-10R7/4, 5YR8/4; very pale orange-10YR8/2; light brown-5YR6/4). Less than 1 percent phenocrysts include feld. Lower contact in noncovered interval.

Bedded tuff (Tpb3) -

A sequence of six or seven beds varying from 0.2 to 3.6 ft thick. Distinctive units include: pumice- and lithic-rich fallout (163.1-165.6), pyroclastic-flow deposit (167.4-172.3), and reworked tuffaceous material overlying a pumice fallout (172.5-176.1).

Pah Canyon Tuff (Tpp) -

Matrix is moderate orange-pink (5YR8/4 to 5YR7/4 to 10R7/4) grading downward to very pale orange (10YR8/2), pinkish gray (5YR8/1), and grayish orange-pink (10R8/2). Phenocrysts include feld, bio, and cpx. Variations in pumice size, amount, and color indicate flow unit breaks at 187.6, 204.6±0.8, 226.3±1.1, and 252.0. Pumice (typically 10 to 50 mm, but up to 200 mm diameter) varies downward: pale yellowish brown (10YR6/2); grayish orange (10YR7/4) with feld; grayish orange and dark yellowish orange (10YR6/6) with feld and bio; dark yellowish orange and moderate yellowish brown (10YR5/4) with feld and bio; grayish pink (5YR8/1) and white (N9).

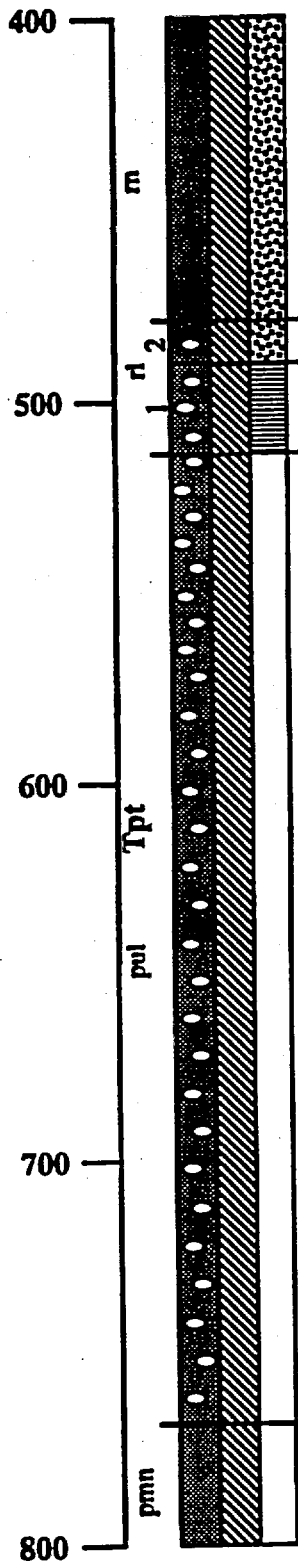
Bedded tuff (Tpb2) -

258.8-263.1 - reworked(?), pale orange-brown (10YR7/2) matrix with white (N9) microvesicular pumice with crystals of feld and bio, moderate orange-pink (10R7/4) pumice, and lithic clasts of dark gray (N2-4) glass with crystals of feld and bio. 263.1-280* - Altered pumice-rich fallout(?), top is moderate red (10R5/4) to moderate pink (10R7/4) and clay-rich.

Topopah Spring Tuff (Tpt) -

Crystal-rich vitric zone (rv) (280*-300.4): *-see notes on cover page
 280*-292.6 *non- to partially welded subzone (rv3)* - Matrix grades downward from light brown (5YR5/6) to moderate brown (5YR4/6) and gradually decreases in amount from 70 to 50 percent before decreasing sharply to 20 percent at 290. Vitric pumice clasts are light gray (N6-N8), 10-30 percent above 290, 70 percent below 290. Phenocrysts include feld, (oxy)bio, and cpx.
 292.6-296.2 *moderately welded subzone (rv2)* - Deformed, vitric, pumice clasts (80 percent), moderate yellowish brown (7.5YR4/4) to light gray (N7). Volcanic lithic clasts (15-20 percent) are grayish red (5R4/2) to medium light gray (N6), commonly with thin opal coating.
 296.2-300.4 *vitrophyre subzone (rv1)* - Dark reddish brown (2.5YR3/2) glass with 2-3 percent grayish black (N2), vitric pumice clasts. 12-15 percent phenocrysts include feld, (oxy)bio, cpx.

Borehole :USW NRG-77A

**Crystal-rich nonlithophysal zone (rn) (300.4-478.2):**

Vapor-phase altered pumice clasts (10-15 percent, locally 5-7 percent) are corroded, mostly less than 30 mm (up to 45 x greater than 80 mm) above about 380 and mostly greater than 30 mm (up to greater than 80 mm, width of the core) below. Pumice clasts grayish red (10R4/2), pale red (10R6/2), white (N9), and light gray to very light gray (N7 to N8). Phenocrysts include feld, oxybio, rare cpx, and rare hbld (7). Matrix grades downward from brownish gray and moderate brown (5YR4/1 and 5YR3/4) to pale red (10R6/2) to pale reddish brown and light brown (10R5/4 and 5YR5/4). Matrix contains white (N9) streaks of vapor-phase minerals. Degree of devitrification and vapor-phase mineralization increases downward, zone of intense vapor-phase mineralization at about 332-360.

Crystal-rich lithophysal zone (rl) (478.2-518.4):

478.2-489.5 crystal-rich lithophysal subzone (rl2) - Lithophysae (1-3 percent) up to 42 x 37 mm. Vapor-phase altered pumice clasts (about 10 percent) are corroded, most less than 40 mm (up to greater than 80 mm, width of the core), white to very light gray (N9 to N8) or rarely pale red (10R6/2). Phenocrysts (10 percent) include feld, oxy bio, and rare altered cpx. Matrix is light brown (5YR5/6) with white (N9) streaks of vapor-phase minerals.

489.5-518.4 crystal transition subzone (rl1) - Phenocrysts decrease downward from 10 percent to 2-3 percent, and include feld, oxybio, and rare altered cpx. Lithophysae (5 percent at top, 10-15 percent downward) are mostly less than 35 mm (up to 39 x 55 mm), and have very light gray (N8) rims. Pumice clasts (10 percent), most less than 40 mm (up to 24 x greater than 80 mm, width of core), are pale brown (5YR5/2) and white (N9). Matrix is grayish orange-pink (5YR7/2) to very light gray (N8).

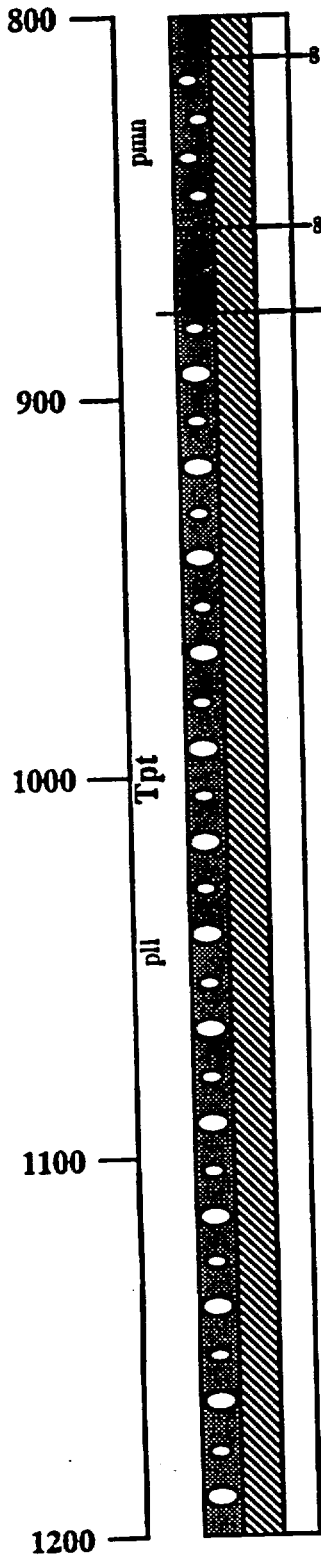
Crystal-poor upper lithophysal zone (ppl) (518.4-768.5):

Lower contact gradational from 763-780. Lithophysae range from 2-3 percent to 15-25 percent, mostly greater than 10 percent above about 570. Lithophysae are mostly less than 40 mm (up to 60 mm) above about 570, mostly less than 25 mm (up to 50 mm) below, with pinkish gray (5YR8/1) rims. Up to 25 percent spots in matrix that are pinkish gray (5YR8/1). Pumice clasts (5-7 percent at top of unit) decrease downward, pumice textures absent below about 610. Pumice clasts are mostly less than 30 mm (up to greater than 80 mm, width of the core), pale brown (5YR5/2) to moderate brown (5YR4/4). Phenocrysts (2-3 percent) include feld and (oxy)bio. Matrix grades downward from grayish orange pink (5YR7/2) to pale red purple and moderate orange pink (5YR6/2 and 10YR7/4) to a variable mixture of red purple (5YR5/2) and pale red (10R6/3).

Crystal-poor middle nonlithophysal zone (pmn) (768.5-811.6):

768.5-811.6 upper subzone (pmn3) - Less than 1 percent lithophysae above 785. Matrix is light brown (5YR6/4) with 1-5 percent pinkish gray (5YR8/1) spots. Phenocrysts (1-2 percent) include feld and (oxy)bio. Lithic clasts (less than 1 percent) include very light gray to light brownish gray (N8 to 5YR6/1), most less than 10 mm.

Borehole :USW NRG-77A



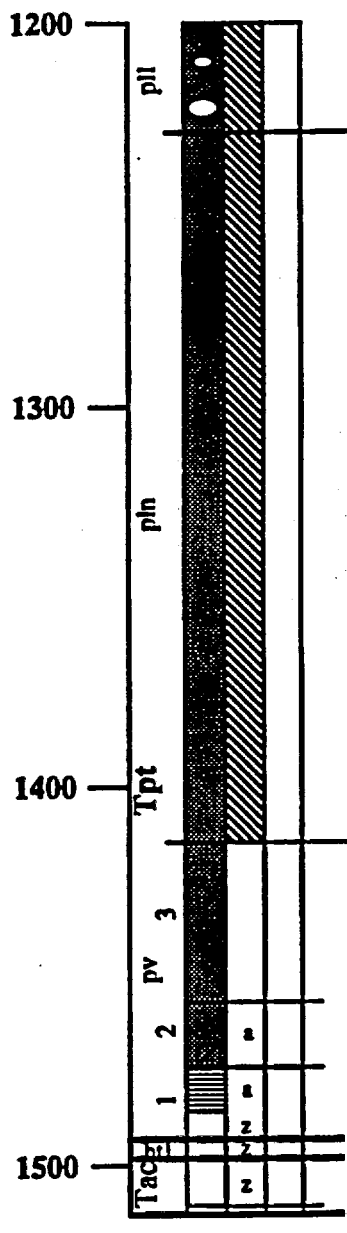
811.6-855.8 lithophysae bearing subzone (ptn2) - 1-3 percent lithophysae, most less than 40 mm (up to 47 x 63 mm), with 5-15 mm pinkish gray (5YR8/1) rims. Matrix is light brown (5YR6/4) with 2-5 percent pinkish gray (5YR8/1) spots. Phenocrysts (1-2 percent) include feld and (oxy)bio. Less than 1 percent (locally up to 2 percent) volcanic lithic clasts, very light gray (N8) or light brownish gray (5YR6/1), most less than 10 mm.

855.8-877.6 lower subzone (ptn1) - Matrix is light brown (5YR6/4) with grayish orange pink to light gray (5YR7/2 to N7) streaks and rims on high-angle fractures. Phenocrysts (1-2 percent) include feld. Less than 1 percent light gray (N7) volcanic lithic clasts. Less than 1 percent pumice clasts, pinkish gray (5YR8/1), most less than 15 mm.

Crystal-poor lower lithophysal zone (pll) (877.6-1228.5):

Lower contact is gradational from 1224-1235. Core is predominantly rubble with large unrecovered intervals suggesting lithophysae larger than the core diameter (80 mm) are present. Core contains less than 1-3 percent visible lithophysae, most less than 25 mm, with grayish orange pink (5YR7/2) rims (generally 1-5 mm wide). Matrix is a variable mixture of light brown (5YR5/4) and pale red (5R6/2), with 10-15 percent grayish orange pink (5YR7/2) spots (up to 35 mm) and rims on lithophysae. Pumice clasts (1-5 percent above about 1150, 5-10 percent between about 1150-1200, 1-4 percent below about 1200) are pinkish gray (5YR8/1) to light brownish gray (5YR6/1) and rarely pale yellowish brown (10YR6/2), mostly less than 25 mm (up to 9 x 48 mm). Lithic clasts (1-5 percent) are mostly very light gray (N8). Phenocrysts (1-2 percent) include feld and rare (oxy)bio.

Borehole : USW NRG-77A



Crystal-poor lower nonlithophysal zone (pln) (1228.5-1414.8±1.6):

Less than 1 percent lithophysae above about 1260, most less than 25 mm. Matrix in upper part of zone is pale brown (5YR5/4) with grayish orange pink (5YR7/2) vapor-phase streaks, grading downward (at about 1320) to a variable mixture of light brown (5YR6/4) and pale red (5R6/2), then grading downward (at about 1380) to a variable mixture of pale red (5R6/2), grayish orange (10YR7/4) and pale yellowish brown (10YR6/2). Pumice clasts comprise 5-7 percent above about 1270, 3-5 percent between about 1270-1340, and 7-10 percent below about 1340, most less than 25 mm (up to 45 x greater than 55 mm, width of core). Pumice clasts are devitrified, light brownish gray to medium light gray (5YR6/1 to N6) and light brown to pale brown (5YR6/4 to 5YR5/2) above 1398. Pumice clasts are vitric, dark gray (N3), devitrified, pale red (5R6/2), or argillic, reddish yellow (7.5YR7/8) below 1398, and below 1410 are vitric and dark gray (N3). Lithic clasts comprise 1-4 percent above 1300, 3-7 percent below 1300, locally as high as 10-15 percent. Lithic clasts are very light gray (N8) and pale red (5R6/2), some contain crystals of feld, most less than 10 mm above 1300 and most less than 20 mm below 1300 (up to 50 x 150 mm). Phenocrysts (1-2 percent) include feld and rare (oxy)bio.

Crystal-poor vitric zone (pv) (1414.8±1.6-1493.6±0.9):

1414.8±1.6-1457.0 vitrophyre subzone (pv3) - Grayish black (N2) glass with light brown (5YR5/4) spherulites. Lithic clasts (5-7 percent near top, 7-10 percent near base) are very light gray (N8) and grayish red (10R4/2), most less than 10 mm (up to 85 x greater than 55 mm, width of core). Phenocrysts (1-2 percent) include feld.

1457.0-1474.6 moderately welded subzone (pv2) - Matrix grades downward from a mixture of grayish black (N2) and reddish yellow (7.5YR7/6) to pinkish gray (7.5YR8/2) with grayish black (N2) glass shards. Pumice clasts (10-15 percent) are vitric and grayish black (N2) or grayish orange (7.5YR7/4), most less than 30 mm (up to 20 x 51 mm). Lithic clasts (5-7 percent) are very light gray (N8), grayish red (10R4/2), and grayish brown (5YR4/4), most less than 10 mm. Phenocrysts (1-2 percent) include feld.

1474.6-1493.6±0.9 non- to partially welded subzone (pv1) - Matrix is light brown (5YR6/4 to 5YR5/6) with grayish black (N2) glass shards at top to grayish yellow (5Y8/4) at base. Pumice clasts (10-20 percent) are altered and light gray (N7) at top and grayish orange pink (10R8/2) at base, most less than 15 mm (up to 46 x greater than 55 mm, width of core). Lithic clasts (5-7 percent at top, 10-15 percent at base) are grayish black (N2), light brownish gray (5YR6/2), and rarely moderate orange pink (10R7/4) and light brown (5YR5/6), most less than 15 mm (up to 48 x 50 mm). Phenocrysts (1-2 percent) include feld and rare qtz (?) and (oxy)bio.

1493.0(V) - 1498.0(V) Bedded tuff (Tpbt1) - Fallout deposit. Pumice clasts (75-85 percent) are white (N9), pinkish gray (5YR8/1) and grayish yellow (5Y8/4), most less than 5 mm. Lithic clasts (15-25 percent) are dark gray (N3) and grayish red (10R3/2), most less than 3 mm. Phenocrysts (2-5 percent) include feld, qtz, (oxy)bio.

Calico Hills Formation (Tac) -

1498.3±0.8-1511.6 pyroclastic flow deposit - Matrix is grayish orange pink (5YR7/2 to 5YR8/3). Pumice clasts (15-20 percent) are grayish yellow to moderate yellow (5Y8/4 to 5Y7/6) or light gray (N7), most less than 15 mm (up to 7 x 27 mm). Lithic clasts (3-5 percent) are dark gray (N3 to N4) or dark reddish brown (10R3/4), most less than 5 mm. Phenocrysts (1-3 percent) include feld, qtz, and (oxy)bio.

1511.6-1513.4(TD) fallout deposit - Inversely graded. Pumice clasts (85-90 percent) are pinkish gray (5YR8/1) and grayish yellow to moderate yellow green (5Y8/4 to 5GY7/4), most less than 3 mm above 1512.3 and less than 1 mm below. Lithic clasts (7-10 percent) are dark reddish brown to grayish red (10R3/4 to 5R4/2), most less than 3 mm above 1512.3 and less than 1 mm below. Phenocrysts (1-3 percent) include feld, qtz, and (oxy)bio.

The following number is for U.S. Department of Energy Office of Civilian
Radioactive Waste Management records management purposes only, and should not
be used when ordering this publication: Accession number - MOL.19941214.0057.
The distribution code for this report is UC-814.

Summary of Lithologic Logging of New and Existing Boreholes at Yucca Mountain,
Nevada, March 1994 to June 1994

USGS/OHR 98-151



Debris-flow deposits in alluvial fans on the west flank of the White Mountains, Owens Valley, California, U.S.A.

JOHN F. HUBERT¹ and ALLAN J. FILIPOV²

¹Department of Geology and Geography, University of Massachusetts, Amherst, MA 01003 (U.S.A.)
²Amoco Production Company, New Orleans, LA 70150 (U.S.A.)

Received June 13, 1988, revised and accepted November 7, 1988

Abstract

Hubert, J.F. and Filipov, A.J., 1989. Debris-flow deposits in alluvial fans on the west flank of the White Mountains, Owens Valley, California, U.S.A. *Sediment. Geol.*, 61: 177-205.

Sections measured in incised channels on 10 alluvial fans show that debris-flow beds, mostly 30-200 cm thick, are more important than stream-flow deposits in construction of fans along the west flank of the White Mountains. The debris-flow beds have a matra-supported fabric with a sandy mud matra that comprises about 40% of individual beds. Complete grain-size analyses of 19 debris-flow beds show that they average 50% gravel, 25% sand, 11% silt, and 4% clay. Inverse grading at the base of most beds is interpreted as due to a layer of high-shear stress beneath an overlying semi-rigid, high-strength plug that supported cobbles and boulders. Sicks and logs embedded in the plugs are oriented parallel with flow directions, reflecting the laminar-viscous motion of the plugs. In the shear layer, the average inclination of discoidal clasts is subhorizontal, varying from 2 to 7° in the up flow direction. In the plugs, discoidal clasts have a subhorizontal fabric with average dips of 5-13°. Compared to the shear layer, plugs have more scatter in clast orientation with numerous clasts dipping at 60-90°. Levees along the margins of debris-flow lobes contain concentrations of the larger clasts in the flows. In the levees, discoidal clasts have an average up flow dip of 21-31° with substantial variability in orientation similar to the plugs. Maximum clast size in individual debris-flow beds is fairly constant down fan until the flows spread and thinned on the sandflat at the fan toe. Clast lithologies show that debris flows originate on steep slopes underlain by granitic and metavolcanic rocks at high elevations in the canyons. In contrast, stream flows obtained most of their clasts from talus slopes on metasedimentary rocks near the apices of the fans. Debris flows are generated during intense rainstorms in the spring and summer when landslides in the water-saturated regolith move down slope, shear, dilate, and by adding water are transformed into debris flows which then move with surging laminar motion along canyon floors to the fans. The recurrence interval for debris flows is about 320 years as evidenced by ¹⁴C dates on plant material buried beneath debris-flow beds.

Introduction

The fault-bounded Owens Valley lies between the Sierra Nevada and the White Mountains. The vertical relief from the crest of the White Mountains at 3600-4300 m to the floor of the valley is 1800-2400 m over distances of 1.5-2 km, making the relief the most precipitous in the southwestern part of the Basin and Range Province (Fig. 1). The alluvial fans along the west side of the White

Mountains have radii of 5-6 km and maximum slopes of 3-10°.

➤ The valley climate is semiarid cold desert in the Koppen classification, with mean annual precipitation of 150 mm at Bishop (Beatty, 1963; Filipov, 1986). The crest of the White Mountains has a cold steppe climate with about 350-500 mm of rain-equivalent precipitation. A significant proportion of the precipitation in the White Mountains is concentrated in a few spring and summer

91102 1649

01102 1650

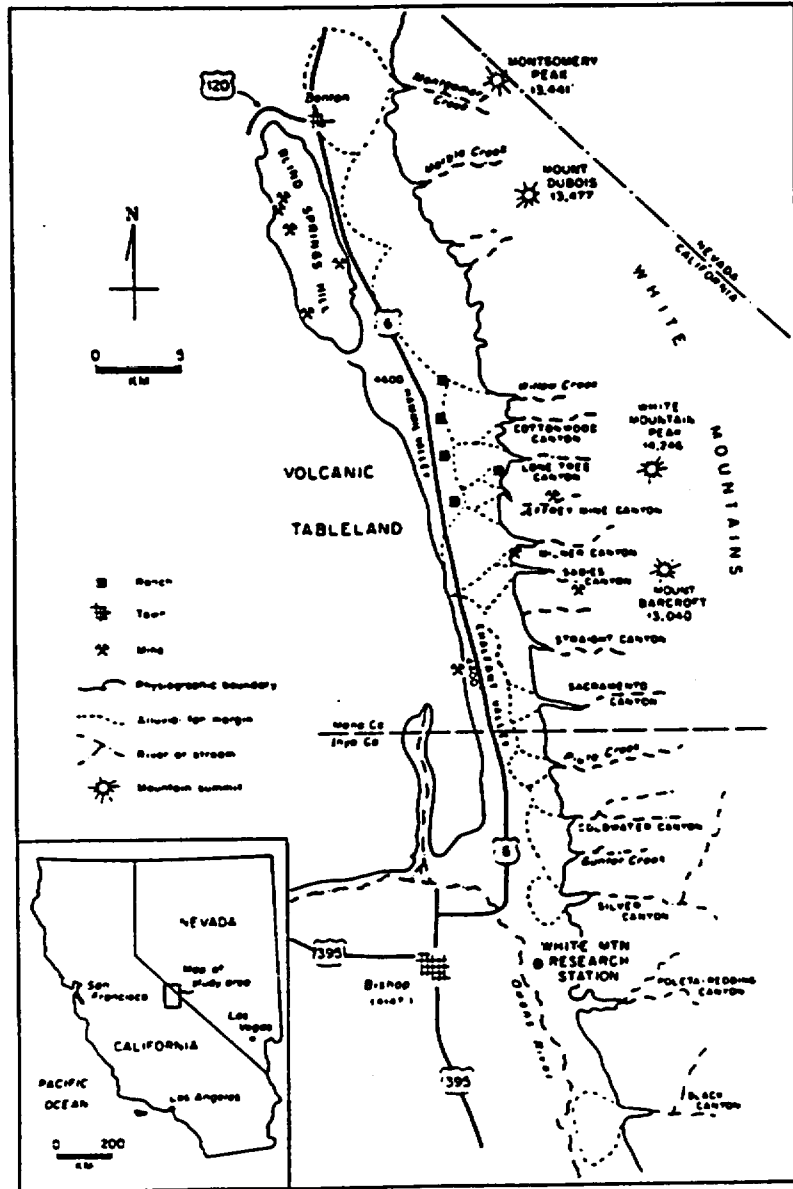


Fig. 1. Map of the Owens Valley near Bishop, California, showing the crest of the White Mountains and the canyons on the west flank.

thunderstorms. Although records are limited, the heaviest recorded precipitation occurred on July 19, 1955, when 250 mm of rain fell in two hours at the recording station near White Mountain Peak. Today, the main channels on the alluvial fans at

Willow, Cottonwood, Lone Tree, and Pine canyons are dry except during cloudbursts because local stockmen have constructed catchment pools at the mouths of the canyons for use in irrigation. The stockmen say that, previously, an

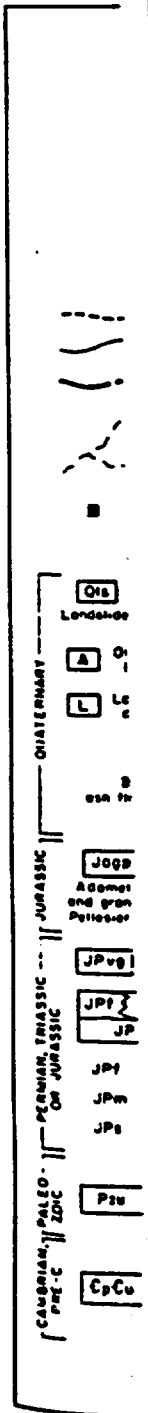
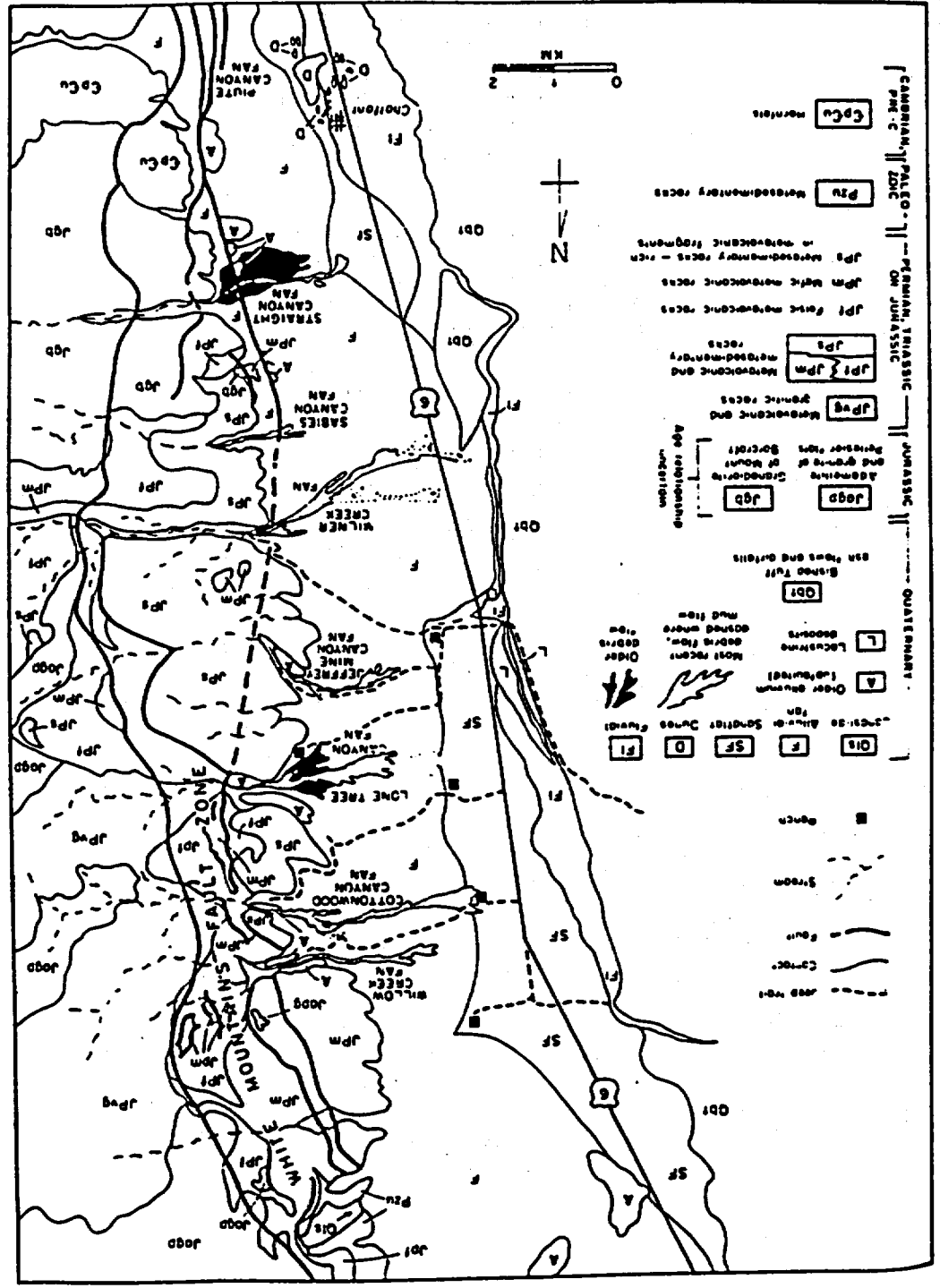


Fig. 2. Map of the debris-flow deposits. Kraushopf (1972)

Fig. 2. Map of the alluvial fans examined in this study. Various map symbols and patterns show the sedimentary facies and recent debris-flow deposits. The bedrock geology of the White Mountains is after Crowder et al. (1972). Crowder and Shendan (1972), and Kowaloff (1972).



Trc. and Pite
ing choudhursts be-
nstructed catchment
canyons for use in
that, previously, an-

IONS ON THE WEST

01102 1651 MINIMUM

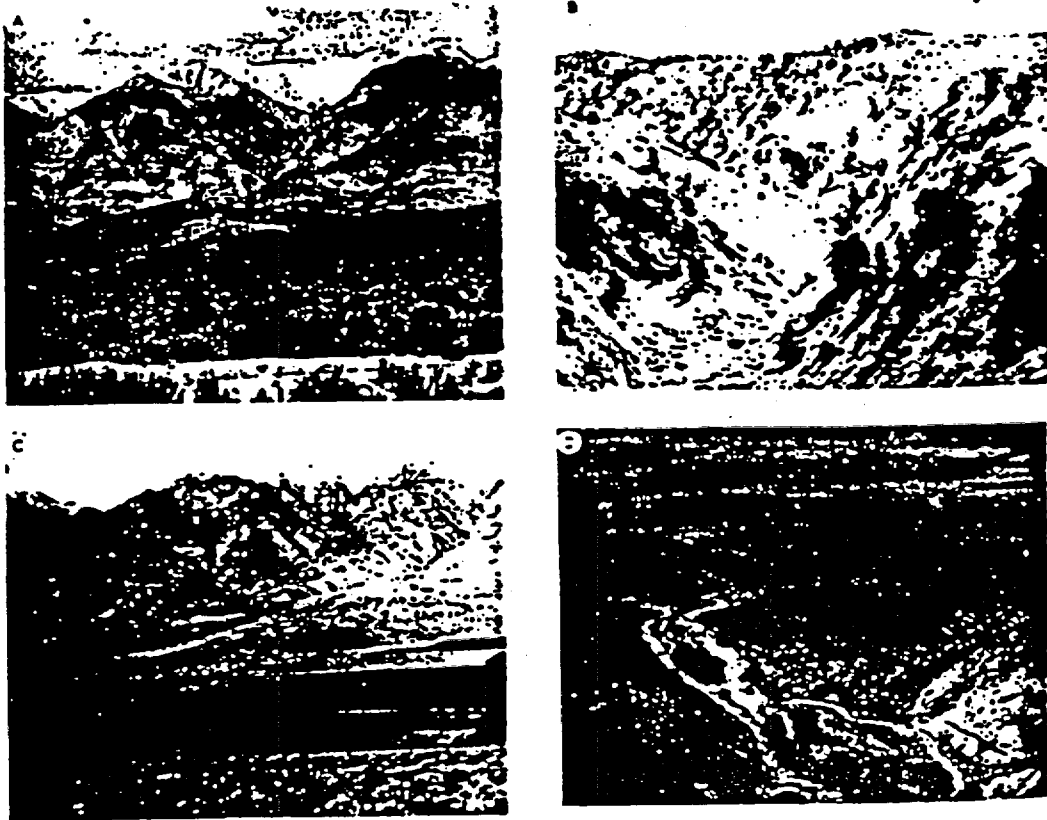


Fig. 3. A. View east of White Mountains and Lone Tree Canyon fan. White Mountain Peak is the highest peak. Note the lobe of the 1952 debris flow (center of photo) that spilled out of the incised channel on the Lone Tree Canyon fan. This debris flow is light-colored because it has not yet been covered with dark-colored vegetation. B. View east up Lone Tree Canyon from near the fan apex. Note the steep slopes on the light-colored granitic and metavolcanic rocks. Near the fan apex in the foreground are dark-colored metasedimentary rocks. C. View east of White Mountains and Cottonwood Canyon fan, showing light-colored 1952 debris flow that flowed downslope to the left (just above ranch buildings). Irrigated fields and ranch in foreground are on sandflat at the toe of the fan. D. View west down the Cottonwood Canyon fan from fan apex. Metasedimentary rocks crop out to the north (right) and south (left) of the channel at the fan apex. The 1952 debris flow is the light-colored elongate pattern that extends down the channel of the fan to the sandflat, covered by irrigated fields.

nual melting of the snow in the mountains generated runoff in the main channels of these fans.

In the spring and summer, intense rainstorms with a rate of precipitation of more than 50 mm per hour have at times generated debris flows, as on July 25, 1952, when debris flows occurred on fans at Milner Creek, Cottonwood Canyon, and Lone Tree Canyon (Figs. 2, 3). Other debris flows took place on the fans at Jeffrey Mine Canyon (May, 1958), Willow Creek Canyon (June, 1956)

and Montgomery Creek Canyon (July 30, 1965) and both Straight and Sahies canyons (summer, 1918). The deposits are easily recognized on the ground and in aerial photographs (Beatty, 1963, 1964).

Beatty (1963) interviewed two stockmen who witnessed the 1952 debris flows on Cottonwood Canyon fan and Lone Tree Canyon fan. They observed that the flows were mixtures of sandy-muddy water with suspended cobbles and boulders

that moved in the fans "as kilometers per breaching of the channels course out of up and down likened to "t. bumping together debris flows in solid and fluid with logs and edge (Bill Syrr The stockmen for 45 minutes followed by 1 hours, deposit the sandflats.

In this paper proposed in incised physical properties. For each bed, semi-rigid plus by sedimentary volume of material are then interpreted as viscous model. 1970: Johnson. live is to control debris-flow be interpret ancient

Field descriptions

Inverse gradient study area shows boulders in the 20% or so of the 20 cm (Fig. 4A) each bed was moving flow, a was the semi-rigid all beds, the lateral of the bed, debris-flow bed fan, which con



Figure 1. The lobe of the debris flow is from near the fan edge foreground are light-colored 1952 are on sandflat at 2 out to the north that extends down

1653
1102

July 30, 1965.

Bill Symons (summer, 1965) recognized on the photographs (Beaty, 1963).

Two stockmen who work on Cottonwood Canyon fan. They are mixtures of sandy-

that moved in surges down the main channels of the fans "as fast as a man can dog trot", a few kilometers per hour. The surges developed from breaching of temporary dams made of debris in the channels and in some cases the flow shifted course out of the channel. The boulders hopped up and down in the flows accompanied by noises likened to "the sound of a thousand freight cars bumping together" (Beaty, 1963). One of the debris flows moved as a "large wave" of admixed solid and fluid material "like ocean breakers", with logs and bushes tossed about at the leading edge (Bill Symons, personal communication, 1984). The stockmen noted that the discrete flows moved for 45 minutes to an hour, then stopped to be followed by high water that continued for 24-48 hours, depositing mud on their ranches located on the sandflats at the toes of the fans.

In this paper, we describe the stratigraphy exposed in incised channels on the fans and the physical properties of selected debris-flow beds. For each bed, the basal high-shear layer, overlying semi-rigid plug, and lateral levees are characterized by sedimentary structures, grain-size distributions, volume of matrix, fabric of discoidal clasts, and variation in thickness. These physical properties are then interpreted in terms of the Coulomb-viscous model for formation of debris flows (Johnson, 1970; Johnson and Rodine, 1984). Our objective is to contribute to the data-base for modern debris-flow beds in order to help recognize and interpret ancient debris flows.

Field description of debris-flow beds

Inverse grading. Most debris-flow beds in the study area show inverse grading where the largest boulders in the bed are excluded from the lower 20% or so of the bed or up to a thickness of about 20 cm (Fig. 4A, B). We infer that the lower part of each bed was the basal high-shear layer of the moving flow, and the overlying ungraded portion was the semi-rigid, high strength-plug. In almost all beds, the largest boulders do not touch the base of the bed, a feature illustrated in the 1952 debris-flow bed at section V on Lone Tree Canyon

comprises 85% of the thickness of the bed without extending into the lower 20 cm.

Elongate-lobate shape. Debris-flows move down the incised channels on the fans, with the larger flows surging over the channel walls to deposit lobes on the fan surface, as shown on the fans at Willow Creek, Cottonwood Creek, Lone Tree Canyon, Jeffrey Mine Canyon, Milner Creek, Sabies Canyon, and Straight Canyon (Fig. 2). Subsequent stream flows in the channel floors tend to remove any debris-flow material so that the preserved parts of debris-flow deposits are mostly elongate lobes on the fan surface.

Sandy mud matrix. The debris-flow beds have a fabric of matrix-supported clasts, with a sandy mud matrix that averages about 40% by volume of each bed. Stream flows locally have removed the matrix from around the clasts at the top of a debris-flow bed. In a few cases, these clasts are reworked into imbricated matrix-free gravel. Debris flows grade transitionally into mudflows as the proportion of mud increases.

Levees of coarse boulders. Levees with a concentration of the larger clasts in the flow occur along the margins and snouts of debris-flow lobes (Fig. 4C). On two debris-flow lobes on fans at Cottonwood Canyon and Willow Creek, the number of clasts with *a*-axis larger than 35 cm was counted in squares with 2-m sides on the lobe surfaces, plotted at the center of each square, and contoured (Filipov, 1986). The concentration of coarser clasts in the levees is evident on these maps.

Embedded sticks and logs. Sticks and logs are commonly embedded within debris-flow beds. A spectacular photograph by Chester Beaty on the cover of the October, 1985, issue of *Geology* shows logs orientated parallel with the paleoflow direction on the upper surface of the debris flow of July 8, 1984, near the apex of the Busher Creek fan on the east flank of the White Mountains. The sticks and logs embedded in the upper surface of the 1958 debris-flow bed on Jeffrey Mine Canyon fan were mapped to show the paleoflow pattern of this debris flow (Filipov, 1986). The long axes of the wood are subhorizontal and subparallel to the elongation of the lobes, without circular patterns that would suggest flow vortices. In the levees

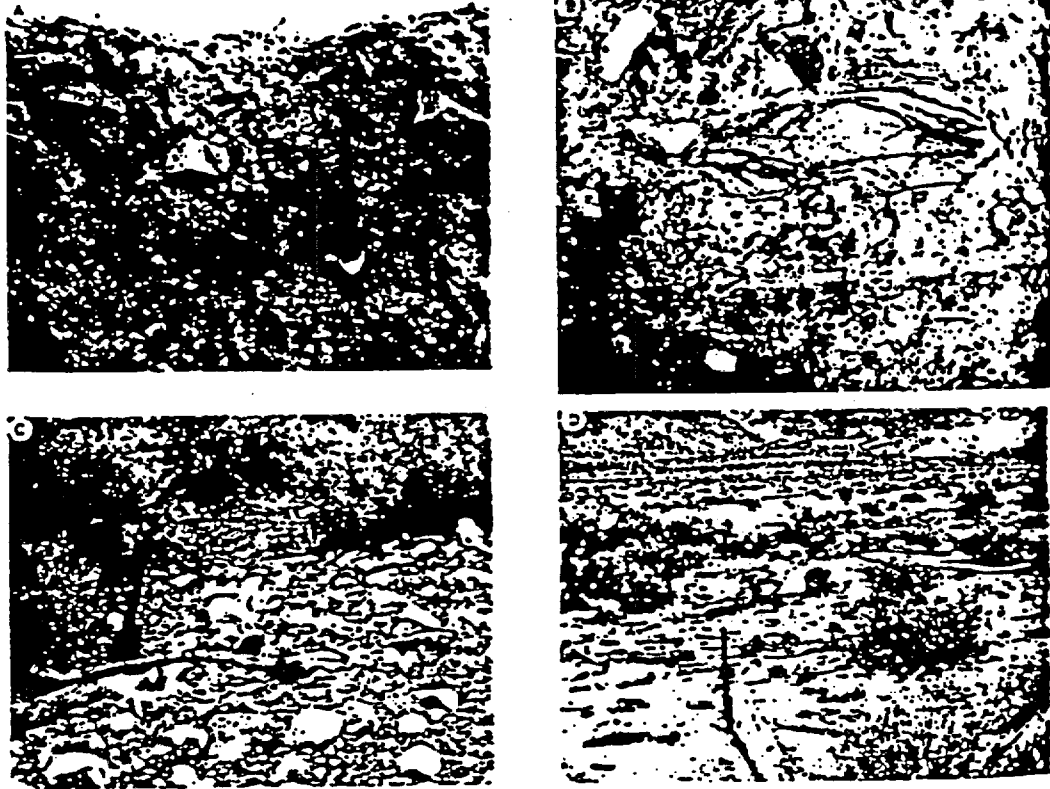


Fig. 4. A. The 1952 debris flow at section IV on Lone Tree Canyon fan. The flow buried some plant debris on the upper surface of the underlying debris flow (top of metal blade of shovel). Cobbles and boulders occur throughout the 1952 debris flow except in the lower 20 cm, forming inverse grading interpreted as a shear layer overlain by a semi-rigid plug. B. Non-erosional contact (horizontal surface one third up in photograph) between two debris-flow beds at section IVA on Cottonwood Canyon fan. The photograph shows part of the thickness of each bed. Inverse grading in the lower 20 cm of upper flow is interpreted as due to a layer of high shear. C. Concentration of boulders on margin of the 1952 debris flow on Lone Tree Canyon fan. D. View east showing wood embedded in upper surface of a mudflow on Milner Canyon fan.

pieces of wood are subparallel to the flow margin, piled up among the boulders. This debris flow was selected for mapping because it has a high proportion of sandy mud matrix and lacks large boulders that otherwise would interfere with the movement of the sticks during flow. In general in the interior of flows, wood tends to pile up behind obstructions with the long axes perpendicular to flow, for example behind a large boulder in the flow or a pre-flow boulder on the fan surface.

Non-erosion base. A debris-flow bed buries the relief of the pre-existing surface with no or minor erosion (Fig. 4B). Where a debris flow traversed

over a debris-flow bed, the contact tends to be particularly smooth, inclined at the slope of the fan surface.

Projection of boulders above the flow surface. Cobbles and boulders project above the surface of many debris-flow beds as sketched on the measured sections. Examples are the 1952 debris-flow beds on the fans at Lone Tree Canyon, Cottonwood Canyon, and Milner Canyon (Figs. 5, 9).

Bubbles of air. A few of the muddy, thinner debris-flow beds and mudflow beds have a bubbly texture due to entrapment of air as a flow moved across the fan surface.

Mats of vegetation centimeters in debris-flow beds, and animal droppings and roots and root fragments on debris-flow fan surface but

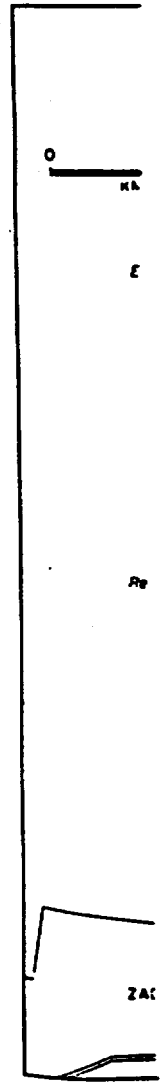


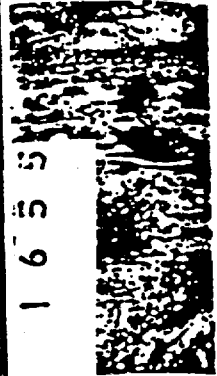
Fig. 5. Locations of debris flows on July

Mats of vegetation. Layers of vegetation several centimeters in thickness are common beneath debris-flow beds. These mats consist of leaves, twigs, and animal droppings and are associated with roots and root casts in the underlying stream-flow or debris-flow bed. Debris flows spread over the fan surface burying vegetation and in most cases

also entraining some organic material up in the flow, as shown on the measured sections.

Description of measured sections

Thirty-nine sections were measured on 10 fans, using exposures in incised channels, pits dug on



upper surface of
ow except in the
tract (horizontal)
The photograph
a layer of high
t showing wood

tends to be
slope of the

flow surface
the surfaces
d on the mea-

the 1952 debris-flow
Tree Canyon. Cot-
Canyon (Figs. 5-9),
the muddy, thinner
beds have a bubbly
air as a flow moved

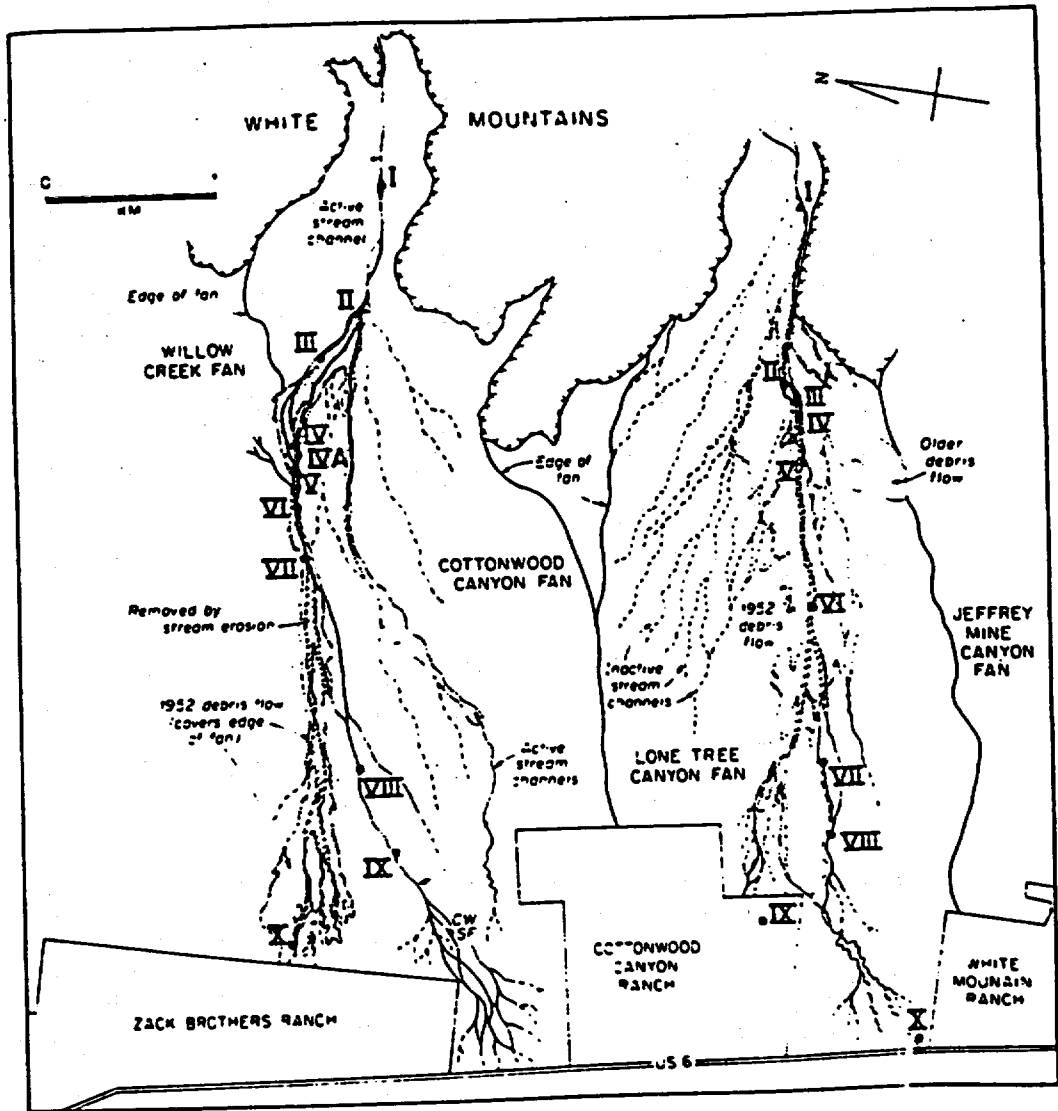


Fig. 5. Locations of measured sections on the Cottonwood Canyon fan and Lone Tree Canyon fan. The stippled pattern shows the debris flows on July 25, 1952.

LONE TREE CANYON FAN

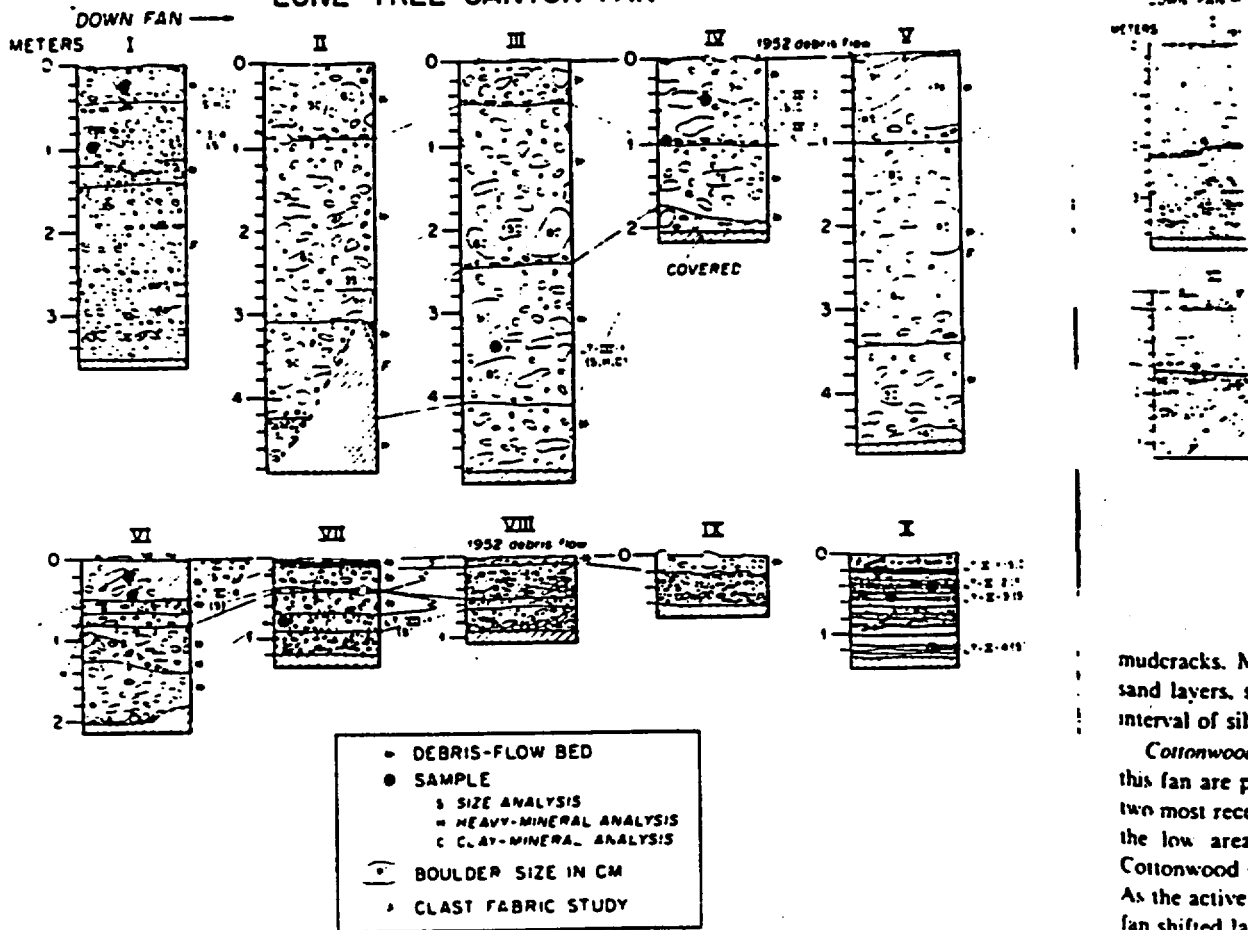


Fig. 6. Measured sections on the Lone Tree Canyon fan.

sandflats, the commercial gravel pit on Milner Creek fan, and road cuts. At each section the horizontal distance sketched in the field was 3-5 m, but the final line drawings show a reduced width to retain equal vertical and horizontal scales. The major features of each fan are noted in the following paragraphs.

Lone Tree Canyon fan. Sections II, III, IV and V expose only debris-flow beds without stream-flow deposits (Figs. 5, 6). In contrast, section I at the fan apex, flanked on both sides by crystalline rocks, has mostly stream-flow gravels and sands and only two thin debris-flow beds. The reason

for this distribution is that debris flows pass through the relatively deep channel at the fan apex without overtopping the walls and any debris-flow deposits in the channel tend to be subsequently removed by stream flows.

The thickest debris-flow bed at section II (47 cm from 90 to 137 cm) can be followed down fan to section VII. This flow has steep 1-m high margins and thinned as it spread on the fan surface. The debris-flow bed at 120 cm in section I has a markedly scoured upper surface.

In the sandflat at the toe of the fan, section X has several thin mud layers with desiccation

mudcracks. N sand layers, s interval of silt

Cottonwood this fan are p. two most recent the low area Cottonwood C. As the active c fan shifted later flow beds into debris-flow bed IVA. The debris-flow bed I is decreasing in cm (section VI (section X)).

An organic the 1952 debris were incorporated upper portion flows into material measured in an active channel. from debris fl. Saline Valley, C

COTTONWOOD CANYON FAN

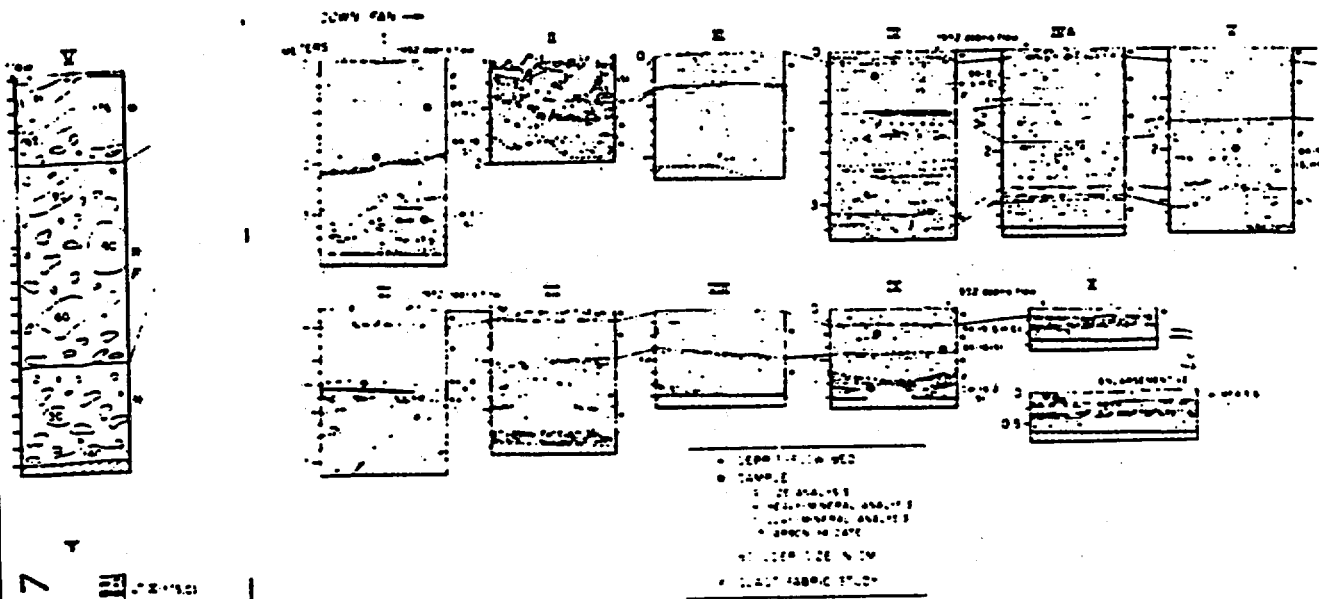


Fig. 7. Measured sections on the Cottonwood Canyon fan.

mudcracks. Mudcurl chips occur in the overlying sand layers, some of which are capped by a thin interval of silt that passes up into a clay drape.

Cottonwood Canyon fan. Debris-flow beds on this fan are particularly elongate (Figs. 5, 7). The two most recent debris flows deposited material in the low area along the boundary between the Cottonwood Creek fan and the Willow Creek fan. As the active channel on the Cottonwood Canyon fan shifted laterally, it eroded the elongate debris-flow beds into isolated remnants, such as the debris-flow bed from 120 to 185 cm at section IV. The debris-flow bed from 0 to 215 cm in section I is continuous down fan for 4.6 km, decreasing in thickness to 95 cm (section V), 62 cm (section VIII), 50 cm (section IX), and 10 cm (section X).

An organic mat 2-5 cm in thickness lies below the 1952 debris-flow bed and leaves and twigs were incorporated into the base of the flow. The upper portion of this flow was reworked by stream flows into matrix-free gravel at section II, measured in an isolated "butte" in the middle of the active channel. Similar matrix-free gravels derived from debris flows occur in some of the fans in Saline Valley, California (Smoot, 1982).

In section IV at mid-fan, there is a 180-cm sequence of stream-flow deposits of gravel and sand together with some graded beds of gravel-sand. Here, as is generally the case, the largest stream-flow clasts are smaller than the largest clasts in the debris-flows beds at the same section.

A 3- to 7-cm lens of silty clay is exposed for several tens of meters at and near section VI. The overlying silty sand contains charcoal sampled for ¹⁴C dating.

The 1952 debris flow spread as a thin layer around bushes and boulders on the sandflat. At section X, a pit dug on the sandflat, the 1952 debris-flow is relatively fine grained, but still contains more than 50% sand and a few cobbles.

Milner Creek fan. Debris-flow beds comprise about 80% of the exposures in the six sections (Figs. 8, 9). The thickness of each of the three debris-flow beds from 0 to 165 cm at section I remains fairly uniform over the 2.7 km down fan to section IV where they abruptly thin. A 3- to 5-cm organic mat underlies the 1952 debris flow.

A commercial pit for gravel and sand about two-thirds of the way down the fan exposes about 80% stream-flow plane-bedded gravel and sand and 20% debris-flow beds (Fig. 10). Cross sections

1657
1658
1659
1660
1661
1662
1663
1664
1665
1666
1667
1668
1669
1670
1671
1672
1673
1674
1675
1676
1677
1678
1679
1680
1681
1682
1683
1684
1685
1686
1687
1688
1689
1690
1691
1692
1693
1694
1695
1696
1697
1698
1699
1700

flows pass at the fan and any debris to be sub-

at section II (47) followed down fan as steep 1-m high spread on the fan (120 cm in section I surface.

of the fan, section X with dessication

01102 1651

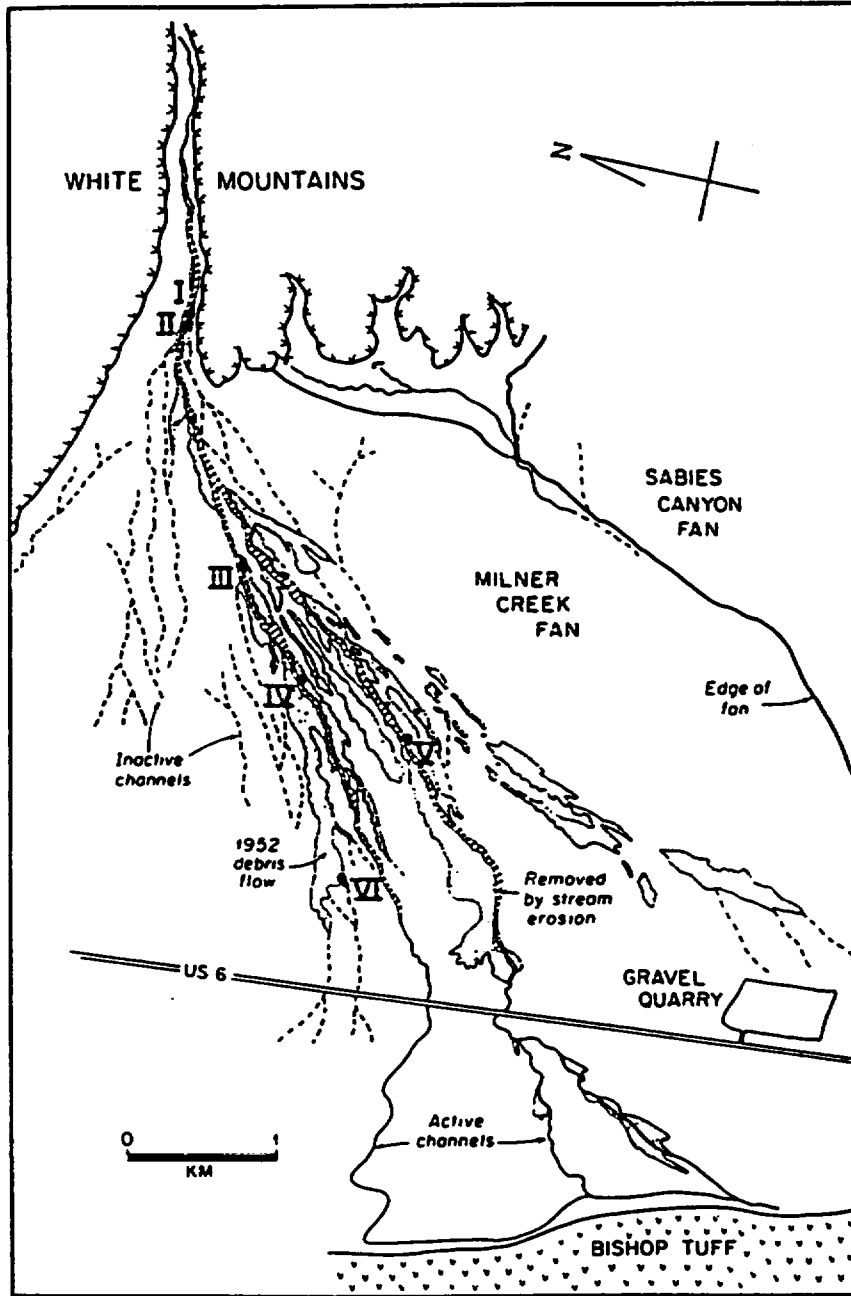


Fig. 8. Map of the Milner Creek Canyon fan with the 1952 debris flow shown by the stippled pattern. Roman numerals show the locations of the measured sections.



of shallow ch.
many debris-f.
nants, evident
average paleol
gravel, measu
ration of sma.



Fig. 10. Measured section A debris-flow (C) The paleocurrent bull-dozed surface.

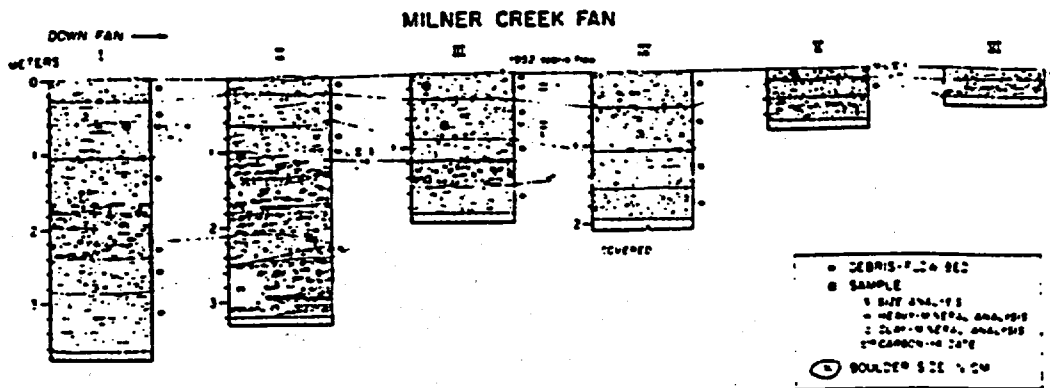


Fig. 9. Measured sections on the Milner Canyon fan.

of shallow channels are evident in Fig. 10 and many debris-flow beds survive as erosional remnants, evidently scoured by stream flows. The average paleoflow direction for the stream-flow gravels, measured by vectors for the average orientation of small areas of imbricated clasts, was

southwest towards 208°, parallel to the surface channels in this part of the fan. There is substantial scatter in the paleoflow vectors.

Montgomery Creek fan. The section at fan apex exposes five debris-flow beds separated by organic mats; there are no stream-flow deposits (Fig. 11).

91102 1650

nan numerals show the

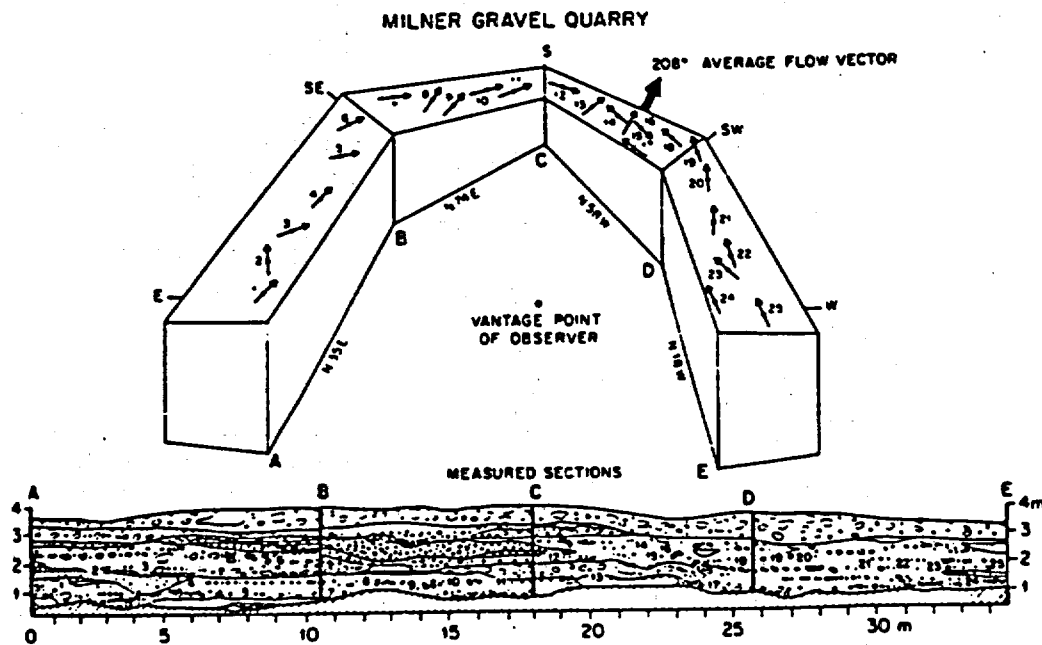


Fig. 10. Measured sections in the gravel quarry on the Milner Canyon fan. The deposits are mostly stream-flow gravel and pebbly sand. A debris-flow bed is continuous across the top of the sections and another is an erosional remnant between 1 and 2 m in section C. The paleocurrent vectors are based on imbrication of discoidal clasts in the stream-flow gravels. The top of all the sections is a bull-dozed surface.

OTHER FAN SECTIONS

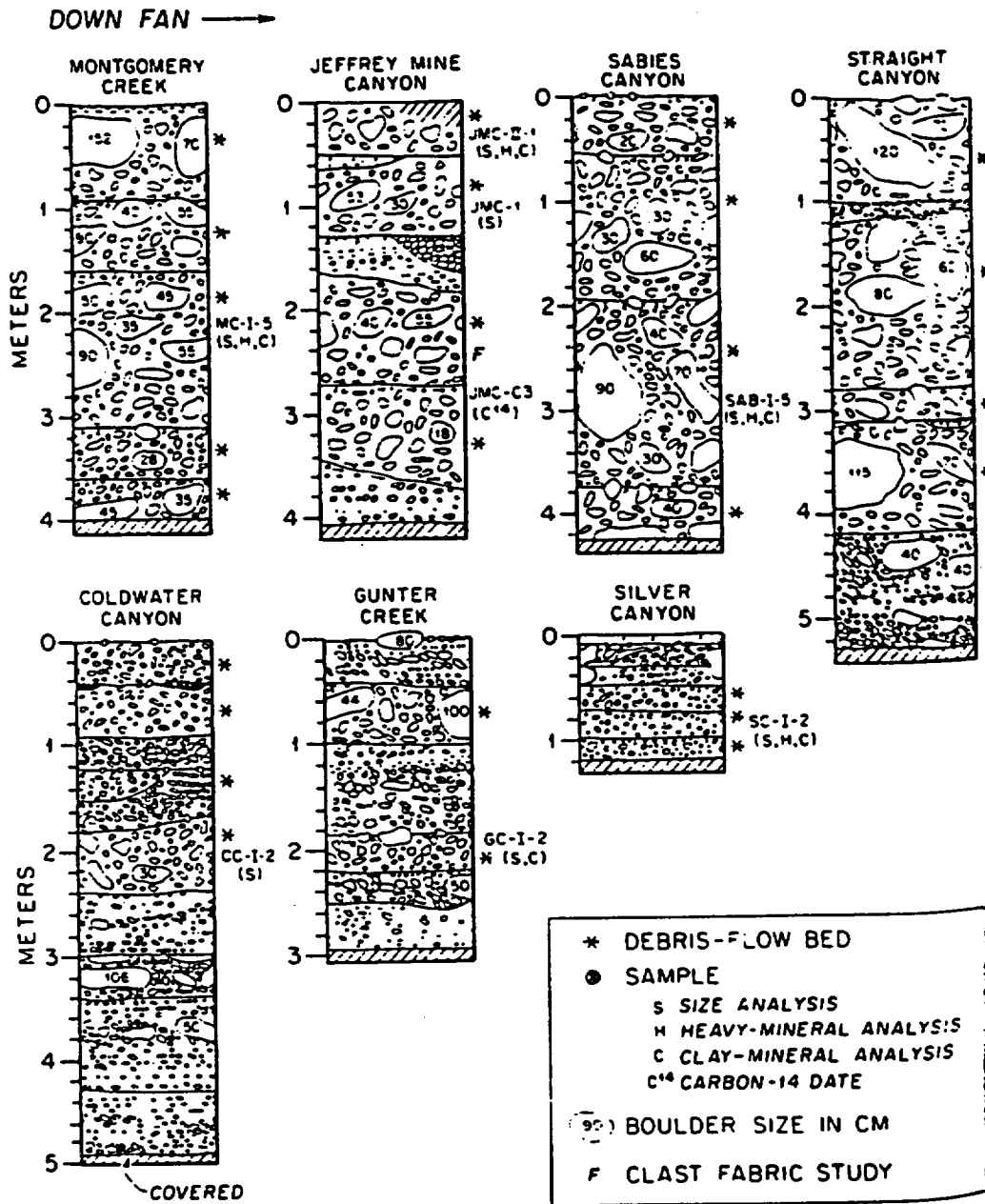


Fig 11. Measured sections on each of seven fans

cm
15C

10C

5C

C

N



Fig 12. Measure dug in the road

The debris flow spilled levees about allowing it to Jeffrey Mine debris-flow b and sand (Fig reported an arr used by the their andalusit the canyon. Tl over a distanc 1 m (where it Sections in of shallow ps channels with that cross the paleochannels plane beds are smaller tha

1650
1102

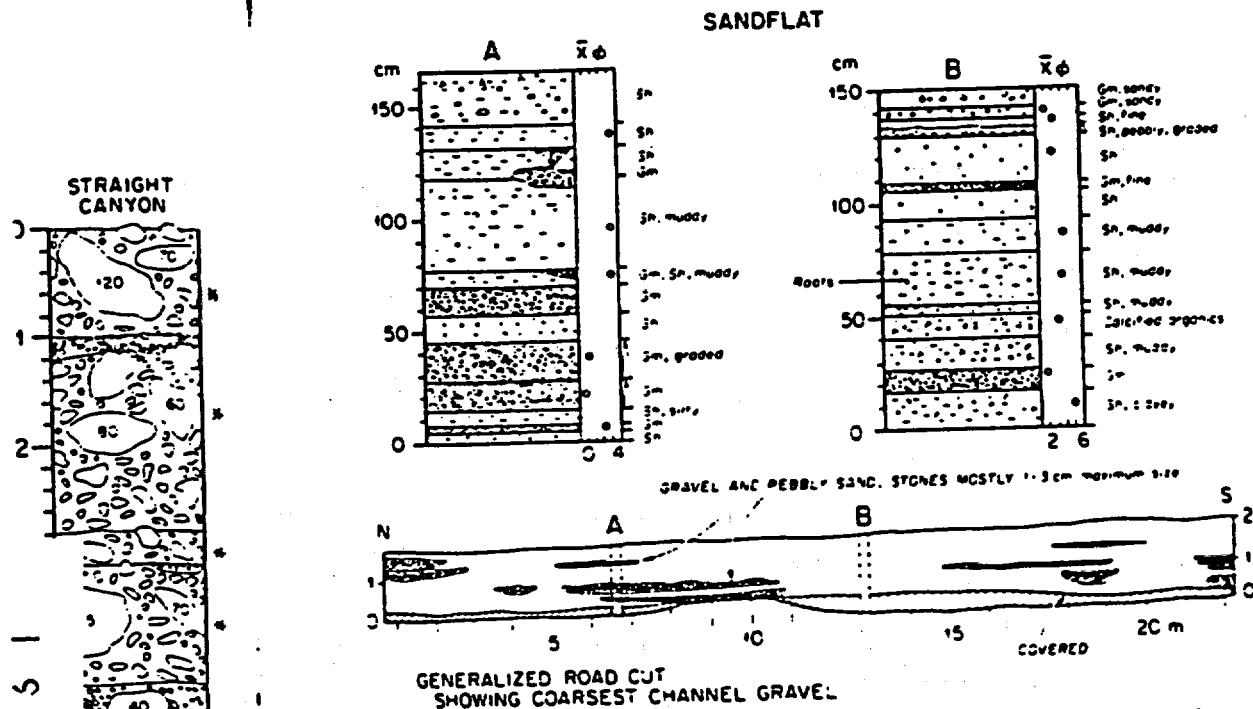


Fig. 12. Measured sections in the sandflat at the toe of the Jeffrey Mine Canyon fan. Sections A and B are logs of vertical trenches dug in the roadcut along Highway 6. The facies codes are from Miall (1978).

The debris flow of 1965 is 90 cm thick. When this flow spilled out of the channel, it constructed levees about 70 cm thick that confined the flow, allowing it to continue down fan for over 2 km.

Jeffrey Mine Canyon fan. The section has four debris-flow beds with minor stream-flow gravel and sand (Fig. 11). The 1958 debris flow transported an array of mining equipment formerly used by the Champion Sparkplug Company at their andalusite mine located on the steep walls of the canyon. This debris flow deposited a lobe that over a distance of 0.5 km thinned down fan from 1 m (where it overtopped the channel) to 2 cm.

Sections in the sandflat contain cross sections of shallow paleochannels similar to the active channels with longitudinal bars of gravel and sand that cross the surface of the sandflat (Fig. 12). The paleochannels are filled with gravel and sand in plane beds and graded beds. Most of the pebbles are smaller than 3 cm. During flooding, the surface

of the sandflat between channels is the locus of deposition of plane-bedded sand and muddy sand.

The undersides of many pebbles in the sandflat have calcite crusts precipitated from groundwater droplets. Roots and plant fragments in the inter-channel deposits are also commonly calcified.

Sabies Canyon fan. This section has four debris-flow beds and no stream-flow deposits (Fig. 11). Two flows are 1.4 and 1.8 m thick, among the thickest in all the fans.

Straight Canyon fan. The section near the fan apex exposes four debris-flow beds with subordinate stream-flow gravel and sand (Fig. 11).

Coldwater Canyon fan. Four debris-flow beds comprise 40% of the 5-m section. Atypically, the largest clasts in the debris-flow beds are smaller than those in the stream-flow gravels.

Gunter Creek Canyon fan. This section is a faulted exposure of older fan material mapped as unit A on the facies map (Fig. 2). Like the younger

GENERAL ANALYSIS
 RAL ANALYSIS
 DATE
 IN CM
 STUDY

sections on the fans, it contains interbedded debris-flow and stream-flow deposits.

Silver Canyon fan. Silver Canyon is at the southern end of the study area where it drains a relatively gently sloping area that contrasts with the steep front of the White Mountains to the north. Three debris-flow beds occur in the section, which is at the fan apex, but no meter-size boulders are present in the canyon or on the fan.

Texture of the debris-flow deposits

Methods

Grain-size cumulative curves were constructed to include the entire range of particles present in the debris-flow beds using the following method. The volumetric proportion and size distribution of clasts larger than 1 cm were determined by measuring the sizes of these clasts in the field. A string marked in 35-cm intervals was placed along a vertical exposure of the debris-flow bed. Each mark fell on a clast larger than 1 cm, or on smaller particles arbitrarily defined as matrix. The volume percent of clasts larger than 1 cm was determined by counting 100 marks. Each clast was removed from the outcrop and the long *a*-axis, intermediate *b*-axis, and short *c*-axis were measured by calipers, with the *b*-axis used in constructing the cumulative grain-size curve.

To complete the analysis, approximately 1 kg of matrix was removed from each debris-flow bed. These samples were weighed, wet-sieved to separate silt and clay, and then dried for sieve analysis by quarter-phi screens. A cumulative curve for the silt-clay fraction was determined using a Sedigraph rapid sediment analyser. The complete cumulative grain-size curve for the debris-flow bed thus combines field measurement of the clasts larger than 1 cm, sieve data for the 0.062-1000 mm fraction, and Sedigraph data for the silt-clay.

The mean, median, standard deviation, skewness and kurtosis were calculated using the formulas of Folk and Ward (1957). The individual cumulative curves for 62 samples from various depositional environments can be seen in Filipov (1986).

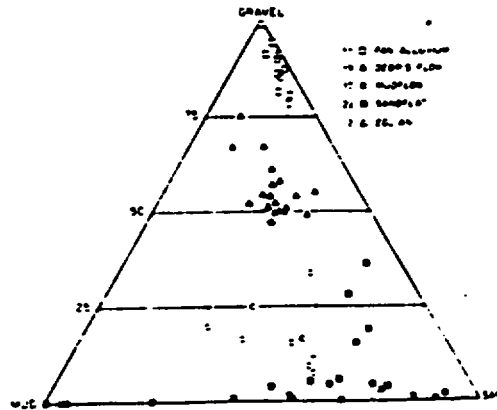


Fig. 13 Triangular plot of gravel, mud and sand for the five sedimentary facies.

The roundness of each clast larger than 1 cm in both debris-flow and stream-flow deposits was visually estimated in the field using a roundness chart (Folk, 1974). The lithology of each clast was also tabulated. The sphericity was computed as the cube root of the quantity: *a*-axis squared divided by the *c*-axis times the *b*-axis (Folk, 1974).

Results

On a triangular plot of gravel, sand, and mud, there is a clear separation of the deposits of debris-flows, fan stream-flows, mudflows, sandflats, and eolian dunes (Fig. 13). The 19 debris flows average 60% gravel, 25% sand, 11% silt and 4% clay. The 10 mudflows are mixtures of sand and mud with varying amounts of gravel. The deposits of the sandflats are also mixtures of sand and mud, but contain more gravel, mostly in the channels that cross the sandflats.

In four debris-flow beds, the grain-size cumulative curve for the plug is compared to that for the basal shear layer in the same flow (Fig. 14). In each flow, the largest clasts in the plug are about 1 ϕ unit coarser than in the shear layer. The parts of the curves that correspond to the sandy mud matrices of the flows are similar in both the plug and shear layers. Each of the debris flows contained about 16% silt and 3-4% clay.

Fig. 15 shows the envelopes that include all of the cumulative curves for each of the five deposi-

CUMULATIVE PERCENT

Fig. 14 Grain-size clasts in the semi-Clay, finer than 5 ϕ

tional environ-
tinctive group
sorted mixture
they are fine-
very platykurtic
and less than 5
except that the

Fig. 15 Envelopes 1
samples encloses a gr
to strength fine-skew.

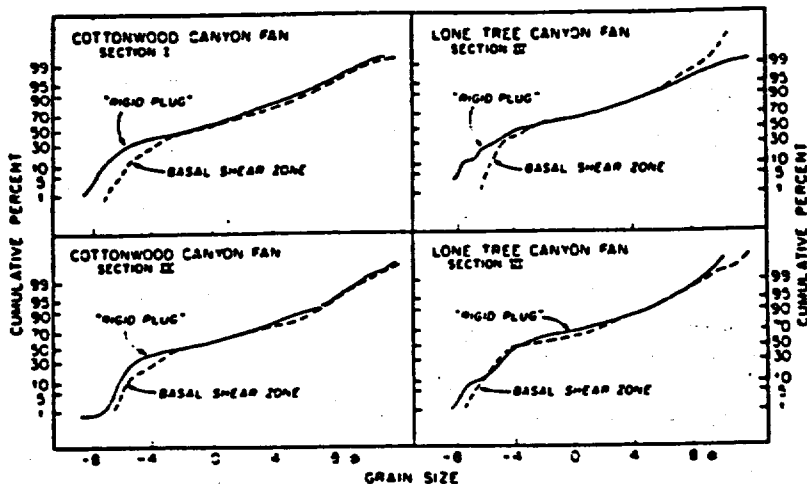


Fig. 14. Grain-size cumulative curves for the basal shear zone and semi-rigid plug in four debris-flow beds. In each bed, the larger clasts in the semi-rigid plug are about 1 ϕ unit coarser than in the shear zone. The debris-flow beds contain about 20% silt plus clay. Clay finer than 20 μ comprises 3-4% of each sample.

nominal environments. The debris-flows are a distinctive group of polymodal, extremely poorly sorted mixtures of gravel, sand and mud. Also, they are fine-skewed to strongly fine-skewed and very platykurtic. The debris-flows average 20% silt and less than 5% clay. The mudflows are similar except that they lack coarse gravel and thus are

finer grained and not as poorly sorted. The stream-flow fan alluvium is consistently coarser on the average than the debris-flow deposits, although the largest clasts are about the same size in both types of deposits.

The cumulative curves for debris-flow beds in the Owens Valley are similar to debris flows in

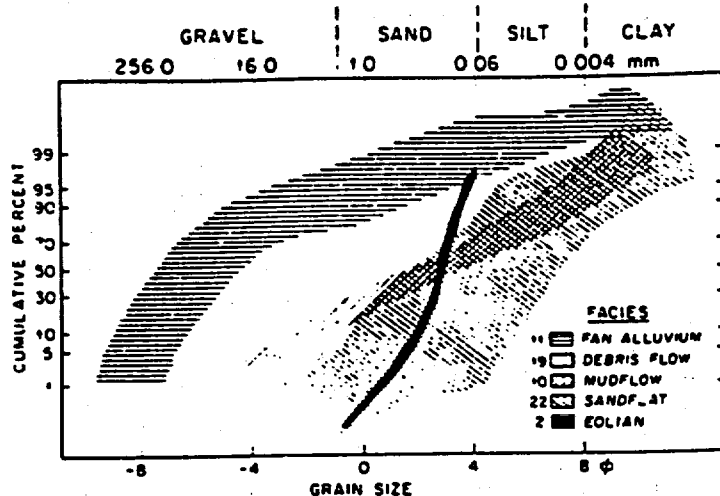


Fig. 15. Envelopes for the grain-size cumulative curves for each depositional facies. For example, the envelope for debris-flow samples encloses a group of polymodal, muddy sands with extremely poor sorting. These debris-flow deposits are fine-skewed to strongly fine-skewed and very platykurtic.



larger than 1 cm in deposits was a roundness each clast was computed as axis squared (Folk, 1974).

and mud. osits of debris sandflats, and flows average 4% clay. The and mud with deposits of the and mud, but channels that

n-size cumulative to that for the (Fig. 14). in he plug are about 1 r layer. The parts of to the sandy mud ar in both the plugs : debris flows con- % clay. s that include all of 1 of the five deposi-

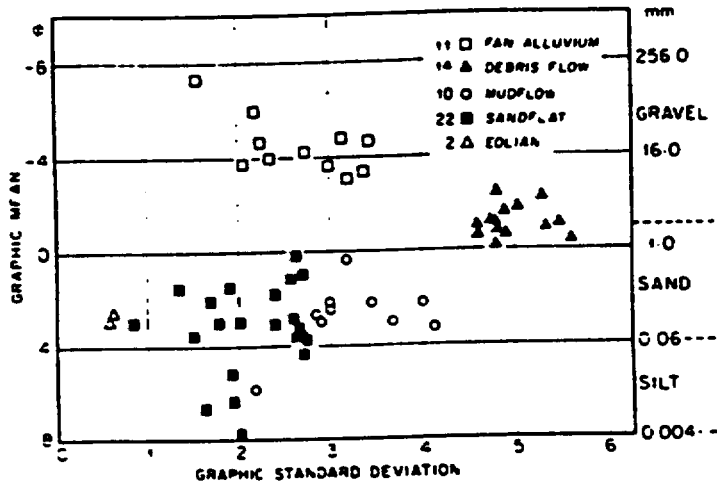


Fig. 16 Scatter diagram of mean grain size and standard deviation of the samples from the five depositional facies

California, New Zealand, the Yukon, and Alaska, except that some of the debris flows in these other areas are finer-grained where the source terranes lacked coarse gravel (Sharp and Nobles, 1953; Bull, 1964; Broscoe and Thomson, 1969; Pierson, 1980, 1981). Many published cumulative curves for debris-flow deposits are only for the matrix, omitting cobbles and boulders.

The mean grain sizes and standard deviations of the 59 samples from the five depositional environments are plotted on the scatter diagram of Fig. 16. The poor sorting of the 19 debris flows is

shown by the standard deviations which are all larger than 4.5 ϕ . Mudflows are not quite as poorly sorted and have standard deviations of 2-4 ϕ ; they did not transport as much nor as coarse gravel as the debris flows. The mean grain size of 9 of the 10 mudflows is in the sand range and one is sandy mud. The fan stream-flow and sandflat deposits have standard deviations of about 1-3.5 ϕ , indicating better sorting than the mudflows. The eolian sands are fine-grained and moderately well sorted with standard deviations of just over 0.6 ϕ .

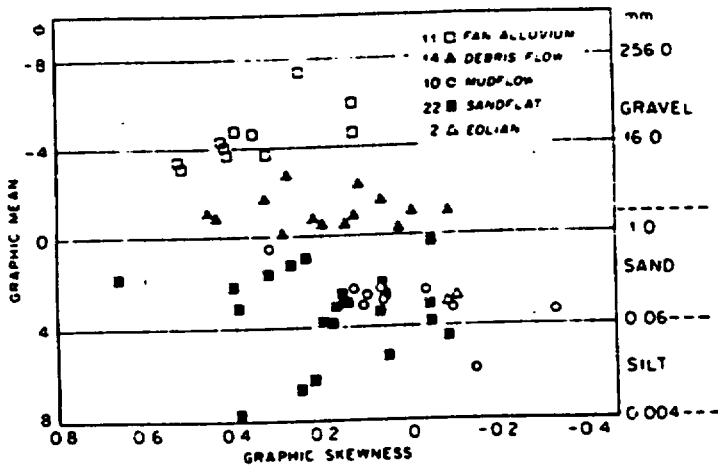


Fig. 17 Scatter diagram of mean grain size and skewness of the samples from the five depositional facies

Fig. 18. Down 1, Cottonwood Canyon

Mean grain size and scatter diagrams and sandflat are strongly fine-silt and clay and make up most curves of the skewed due to mudflows vary metrical to fine-grained mud. eolian sands are As a debris-measured section, clasts decrease between the debris-flow as it and less steep Cottonwood Canyon. The axes of the 1 beds remains at 1 in the upper 1 distance of 4.2 a marked decrease

71109 1654



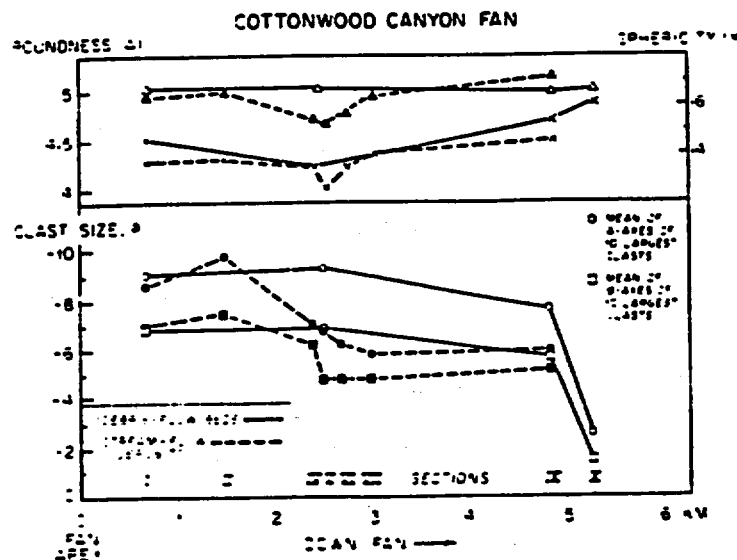


Fig. 18. Down fan changes of roundness, size, and sphericity of the larger clasts in debris-flow and stream-flow deposits on Cottonwood Canyon fan.

Mean grain size and skewness are plotted on the scatter diagram of Fig. 17. The debris-flow and sandflat deposits tend to be fine-skewed to strongly fine-skewed, reflecting the admixture of silt and clay to the coarser-grained material that make up most of the deposits. The cumulative curves of the fan stream-flow gravels are fine-skewed due to the presence of a sand "tail". The mudflows vary widely from coarse-skewed to symmetrical to fine-skewed, depending on the proportions of mud, sand, and gravel (Fig. 13). The eolian sands are coarse-skewed.

As a debris-flow bed is followed down fan in measured sections, the average size of the largest clasts decreases only slightly until the junction between the fan and sandflat. Here, the larger clasts run aground and stop moving within a debris-flow as it spreads and thins on the smoother and less steep surface of the sandflat. On the Cottonwood Canyon fan, the mean size of the *b*-axes of the 10 largest clasts in the debris-flow beds remains about 9.0 cm (-6.5ϕ) from section 1 in the upper fan to section IX in the lower fan, a distance of 4.2 km (Fig. 18). At section X, there is a marked decrease to 3 cm (-1.5ϕ). A similar

trend is seen on the Lone Tree Canyon fan where the debris-flow beds show a moderate decrease in mean size of the *b*-axes from 12.8 cm (-7.0ϕ) to 6.4 cm (-6.0ϕ) from section I to section VI over a distance of 2.2 km (Fig. 19). At section XI, there is a decrease in size to 3.2 mm (-1.7ϕ).

In contrast to debris-flows, the mean size of the 10 largest clasts in the stream-flow gravels on the Lone Tree Canyon fan and Cottonwood Canyon fan decrease in size down fan until near the toes of the fans where rather unexpectedly the clasts increase in size. On the Lone Tree Canyon fan, this increase in mean size is from 3.2 cm (-5.0ϕ) to 11.1 cm (-6.8ϕ) between sections VII and VIII (Fig. 19). There is a smaller increase on the Cottonwood Canyon fan from 5.6 cm (-5.8ϕ) to 6.4 cm (-6.0ϕ) between sections VII to IX (Fig. 18). These unexpected down fan increases seem to be due to stream flows exhuming large clasts from the older debris-flow deposits. Support for this inference is provided by down fan comparison of the lithologies of clasts larger than 1 cm in the debris-flow and stream-flow deposits on the Cottonwood Canyon fan as discussed later. The proportion of felsic metavolcanic clasts increases in

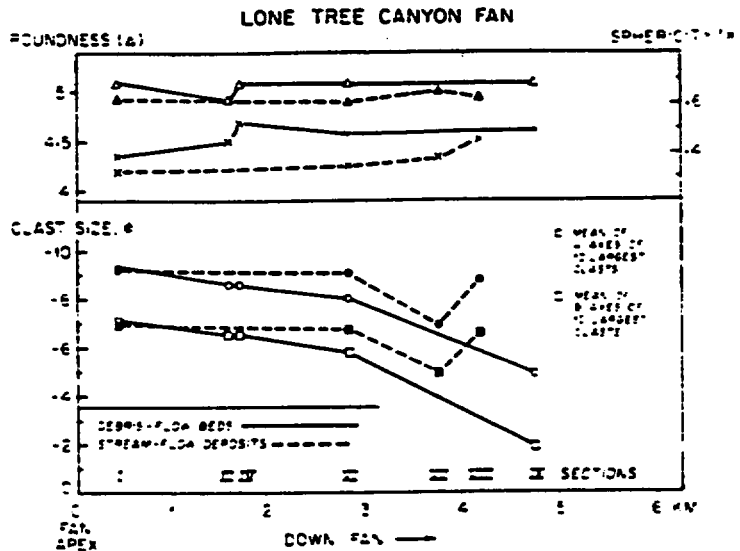


Fig. 19 Down fan changes of roundness, size, and sphericity of the larger clasts in debris-flow and stream-flow deposits on Lone Tree Canyon fan

the lower third of the fan, evidently due to removal of them from the debris-flow deposits where they are abundant.

The sphericity of clasts larger than 1 cm in both debris-flow and stream-flow deposits remains fairly constant down fan on the Lone Tree Canyon and Cottonwood Canyon fans, averaging about 0.5 and 0.4, respectively (Fig. 19). Compared to stream flows, debris flows carry more granitic and gneissic clasts and fewer metasedimentary clasts, as discussed later. The slightly greater sphericity of the granitic and gneissic clasts produces a slightly higher average sphericity of the clasts in the debris flows. Similar trends occur on the Cottonwood Canyon fan except that the data points show more scatter (Fig. 18).

Roundness data suggest that transport in debris flows does not produce significant abrasion of the clasts larger than 1 cm. The average roundness of clasts in debris-flow beds on Cottonwood Canyon fan and Lone Tree Canyon fan remains about subround (0.5) from near the fan apex to the sandflat (Figs. 18, 19). In general, on a specific fan, clasts of the same size in stream-flow gravels are slightly more angular and show more variability among measured sections than in debris-flow

beds. Comparisons of the roundness of clasts of the same lithology in stream-flow and debris-flow deposits show no significant differences except that granite and gneissic clasts are slightly more round in the debris-flow beds. Some clasts evidently break during transport by stream flows, thereby decreasing the average roundness for all clasts.

Clast fabric in debris-flow deposits

Methods

The clast fabrics of debris-flow beds were determined by measuring the orientations of the discoidal clasts with *a*-axes longer than 1 cm. Fabrics were measured at 21 locations, including basal shear layers, semi-rigid plugs, levees and snouts. For comparison, the clast fabric was also measured in two stream-flow gravels. The strike and dip of the *ab*-plane of each of 100 discoidal clasts were measured at each locality. Each clast was completely removed from the sandy mud matrix of the debris-flow to obtain an accurate strike and dip and to verify its discoidal shape. The *ab*-poles to the planes were plotted on the lower

Fig. 20 Fabric of Cottonwood Canyon

hemisphere of stereonet. Each plot for the vector *n* is a 95% chance of orientation.

Results for individual

Comparison of fabrics of rigid plug were

COTTONWOOD CANYON FAN
CLAST FABRIC IN ONE DEBRIS-FLOW BED
AT TWO SECTIONS

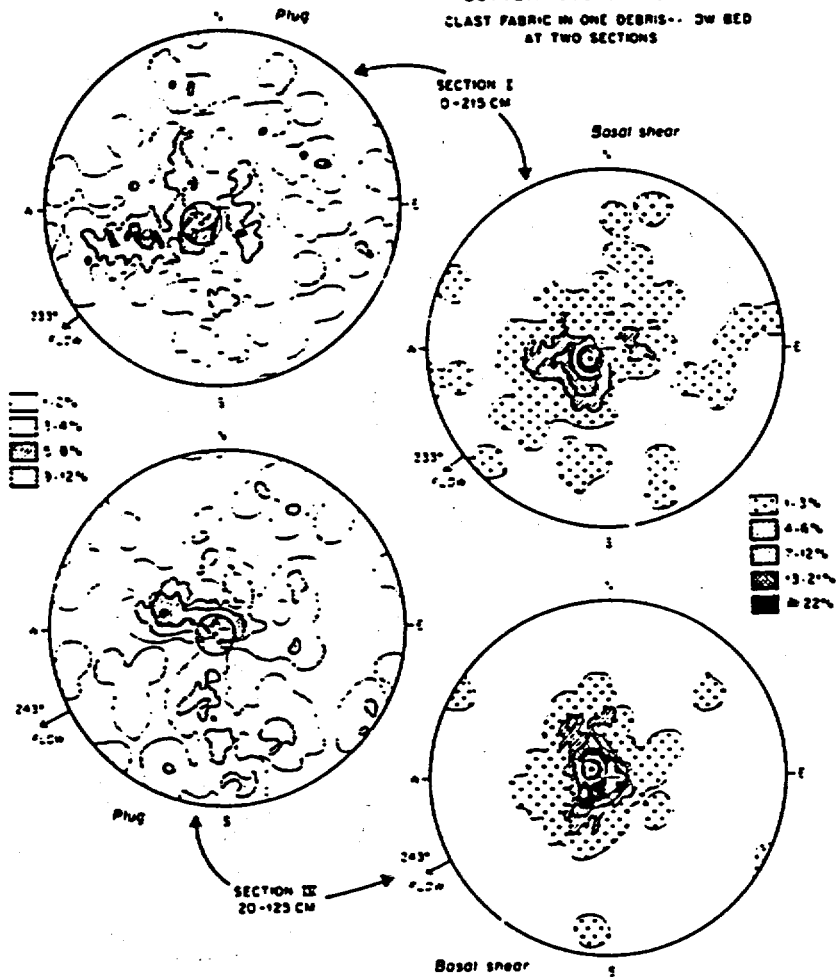


Fig. 20. Fabric of discoidal clasts in the shear zone and semi-rigid plug of the 1917 debris-flow deposit at sections I and IV on Cottonwood Canyon fan. See text for discussion.

beds were depositions on Lone Tree

s of clasts of debris-flow lenses except slightly more fine clasts evidence stream flows. readiness for all

beds were depositions of the r than 1 cm. ons, including s. levees and abric was also gravels. The strike each of 100 discoidal a locality. Each clast n the sandy mud main an accurate strike discoidal shape. The plotted on the lower

hemisphere of a Schmidt net and computer contoured. Each plot shows the 95% confidence circle for the vector mean, delineating the area that has a 95% chance of including the "true" average pole orientation.

Results for individual debris-flow beds

Comparison of shear layer and plug in the same bed. The fabrics of the shear layer and overlying semi-rigid plug were compared at sections I and IV in

the 1-m debris-flow bed of 1917 on the Cottonwood Canyon fan (Fig. 20). In the 20-cm shear layer, the discoidal clasts at each of the two sections have average dips of 9° to the northeast and southeast, respectively. The poles to the individual clasts are clustered around the means, and the 95% confidence circles do not include the centers of the nets where the orientation is horizontal. As these debris flows "froze", the discoidal clasts were inclined in the upflow direction with an average dip of 9°.

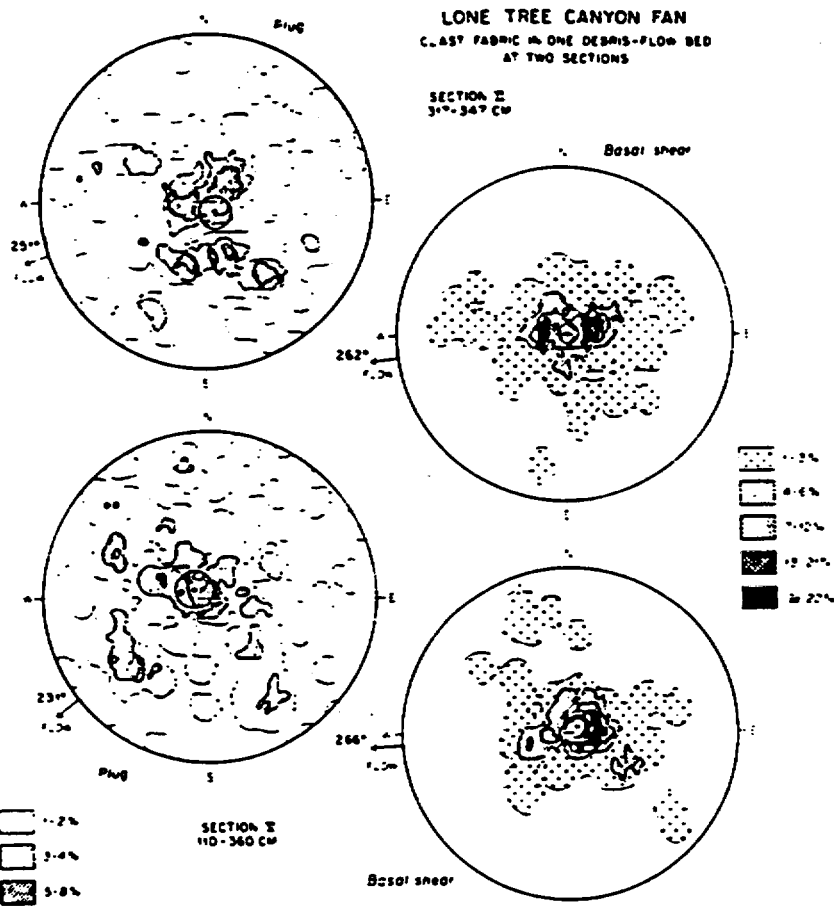


Fig. 21. Fabric of discoidal clasts in shear zone and semi-rigid plug of a debris-flow bed at sections II and IV on Lone Tree Canyon fan. See text for discussion.

In the semi-rigid plug of this bed, at the same sections I and IV, the discoidal clasts average a subhorizontal position as shown by the two 95% confidence circles which touch and include the centers of the nets. The average dips of the clasts are 10 and 5°, respectively. The clasts in the plug show more scatter in orientation than do those in the shear layer, and many dip at 60-90°.

A similar sampling design compares the fabrics of the shear layer and semi-rigid plug of a 1.5- to 2.5-m debris-flow bed at sections II and IV on Lone Tree Canyon fan (Fig. 21). The discoidal clasts in the shear layer have average dips of 8 and 9°, but the 95% confidence circles include the

centers of the nets so that the fabric is subhorizontal. In the plug, the discoidal clasts are also subhorizontal with dips of 7 and 9°. The clasts in the plug show more scatter in orientation than do those in the shear layer.

Comparison of the plugs, levees, and snouts of the debris-flows of 1952 on Cottonwood Canyon and Lone Tree Canyon fans. The 1952 debris-flow bed on Cottonwood Canyon fan is one of only two sampling locations where the discoidal clasts in a plug have a statistically significant inclination from horizontal. The inclined fabric is poorly developed as shown by the 95% confidence circle around the

Fig. 22. Fabric of clasts in debris-flow bed. See text for discussion.

mean which all clasts dip to the western level and snout dip to the southwestern level.

TABLE 1
Orientation parameters

Location	Orientation parameter
Plug	
Shear zone	
Levee and snout	

11102 1551

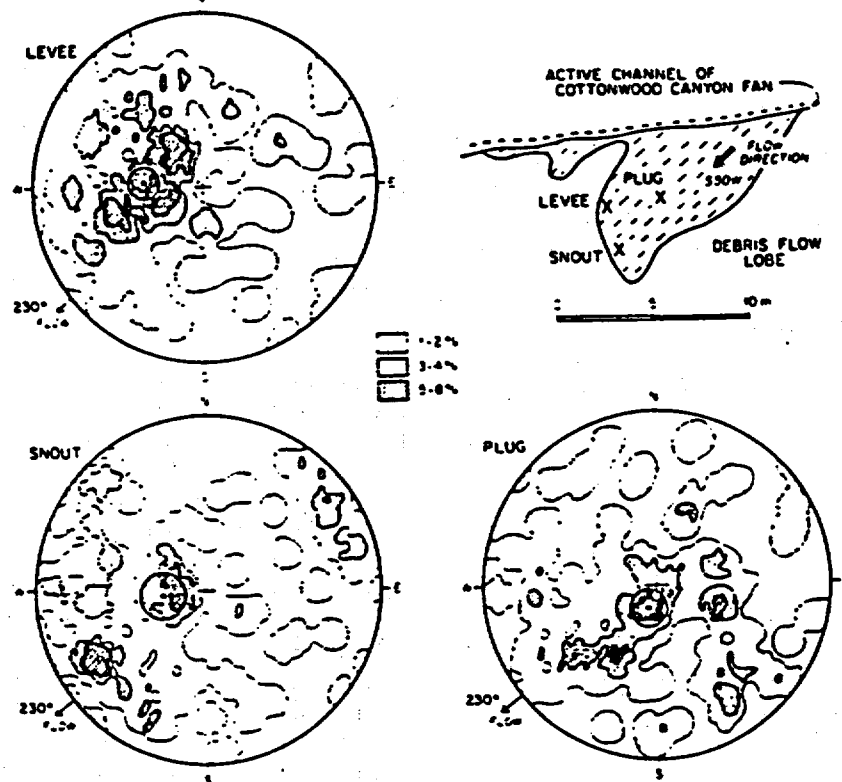


Fig. 22. Fabric of discoidal clasts in semi-rigid plug, levee and snout of a lobe of the 1952 debris-flow on Cottonwood Canyon fan. See text for discussion.

mean which almost touches the center of the net (Fig. 22). In contrast, the clast fabrics of the levee and snout dip up flow at 29° towards the east at the western levee and 21° to the northeast at the southwestern snout.

At the two locations in the semi-rigid plug of the 1952 debris flow on Lone Tree Canyon fan, the clasts have a subhorizontal orientation with average dips of 10° at location 4 and 6° at location 8 (Figs. 23, 24). In each plot, the 95%

Tree Canyon

subhorizon-
re also sub-
clasts in the
in than do

and snouts of the
ood Canyon and
2 debris-flow bed
one of only two
scoidal clasts in a
at inclination from
poorly developed
circle around the

TABLE 1

Orientation parameters for plots of fabrics of discoidal clasts in debris-flow beds

	N	Mean dip (°)	Mean concentration	Mean σ_{95} (°)	Number of plots with statistically significant inclined mean dips	Range of statistically significant non-horizontal mean dips (°)	Range of mean dips (°) of plots that lack a statistically significant inclined mean dip
Plug	8	8.4	2.9	10.1	2 of 8	10.3-13.3	4.7-9.8
Shear zone	5	5.3	8.5	5.8	2 of 5	8.7- 9.9	2.0-7.0
Levee and snout	10	24.0	3.0	9.9	9 of 10	8.9	

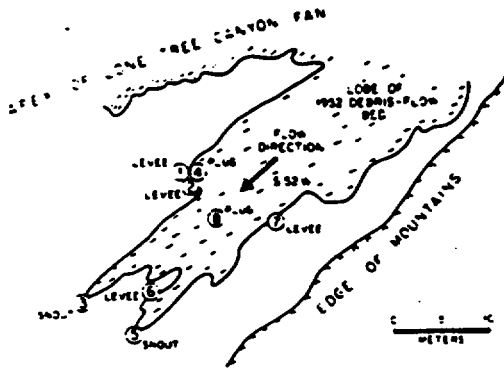


Fig. 23. Index map of the locations of fabric diagrams in a lobe of the 1952 debris flow near the apex of Lone Tree Canyon fan.

confidence circles include the center of the net. At the four locations in the levees and two snout locations, the clasts on average have statistically significant inclined mean dips striking subparallel to the flow margins and dipping upflow at angles from 21 to 31° (Figs. 23, 24).

Summary of results

Shear layers. The orientation of discoidal clasts was measured in the shear layers of debris-flow beds at five locations (Table 1). In three plots, the fabrics are subhorizontal with the mean dips of 2-7° and the 95% confidence circles include a horizontal orientation. Mean dips of 8.7° and 9.9° were statistically significant at two localities. The concentration factor, k , in these five plots of shear layers averages 8.5, whereas the concentration factor averages 2.9 for the eight localities in plugs and 3.0 for ten localities in levees. These data show that the clasts in shear layers show less scatter in orientation than clasts in plugs and levees.

Plugs. In six of eight plug localities, the discoidal clasts have subhorizontal fabrics, with mean dips of 4.7° and 9.8° and with the centers of the nets included in the 95% confidence circles (Table 1). Two localities have statistically significant dips of 10.3° and 13.3°. In each of the eight plugs, the clasts show substantial scatter in orientation with

many dipping at 60-90°. Discoidal clasts evidently move about as they are carried along in a semi-rigid plug, maintaining an average subhorizontal to low-angle orientation, retained as the flow "freezes". In some plots, the poles to the discoidal clasts form a rough ellipse oriented with its long axis perpendicular to the flow direction. This feature also is seen in a few plots of the shear layer.

Levees. In ten locations in levees along the margins and snouts of debris-flow beds, the discoidal clasts have orientations that average a dip of 24° in the up flow directions (Table 1). The sample sites are eight on the Lone Tree Canyon fan and two on the Cottonwood Canyon fan. In nine of the 10 analyses, the means are statistically significant and 95% confidence circles exclude the centers of the nets. Variability in clast orientation is about the same in levees as plugs, with the concentration factor, k , averaging 2.9 and 3.0, respectively (Table 1). Numerous clasts in the levees dip at angles of 60-90° and strike subparallel to flow margins; these clasts are visually impressive and tend to mask the average lower dip of the clasts.

Stream-flow gravel. The orientations of discoidal clasts were measured at two localities, one each in the active channels of the fans at Lone Tree Canyon and Cottonwood Canyon. As anticipated, the clasts have a statistically significant up flow imbrication, averaging 21° and 41°, in contrast to the subhorizontal to low-angle imbrication of clasts in the plugs of debris-flow beds.

Lithology of the clasts

Results. Figs. 25 and 26 show the lithology of clasts larger than 1 cm in the debris-flow beds and stream-flow gravels on Cottonwood Canyon fan and Lone Tree Canyon fan. The data are for the upper, middle, and lower thirds of each fan. A rather unexpected result is that on each fan the debris flows have a different assemblage of clasts than the interbedded stream-flows. On the Cottonwood Canyon fan, the debris flows carried an average of 60% granitic clasts and 6% metased-



232°



233°



Fig. 24. Fabric of Canyon fan. See

LONE TREE CANYON FAN LOBE OF 1952 DEBRIS-FLOW BED

Discoidal clasts were carried along in an average subhorizontal position, retained as the poles to the slip surface oriented with the flow direction. Plots of the shear

along the margins of the discoidal clasts show a dip of 24° in the nine sample sites on the fan and two on the snout. In nine of the 10 statistically significant sites the centers of concentration are about 10 cm from the margins; they dip at angles of 23° to 24° and tend to be parallel to the margins.

of discoidal clasts one each in the Lone Tree Canyon fan is anticipated. The contrast in the up flow direction of clasts

0110210101

lithology of the flow beds and the data are for the center of each fan. A comparison on each fan the assemblage of clasts was made. On the Lone Tree flows carried an average of 6% metasedimentary

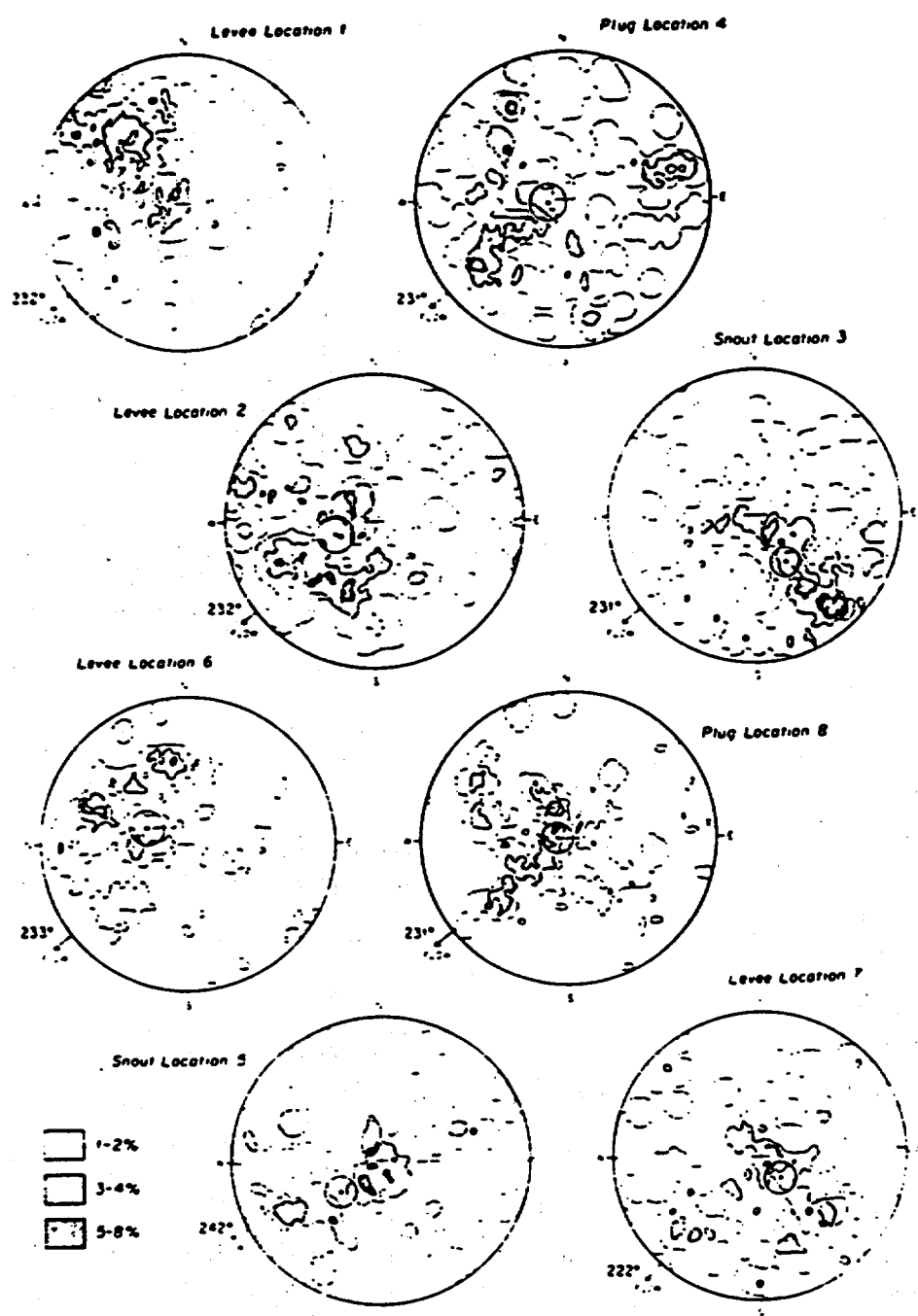


Fig. 24. Fabric of discoidal clasts in the semi-rigid plug, levee, and snout in a lobe of the 1952 debris flow near the apex of Lone Tree Canyon fan. See text for discussion.

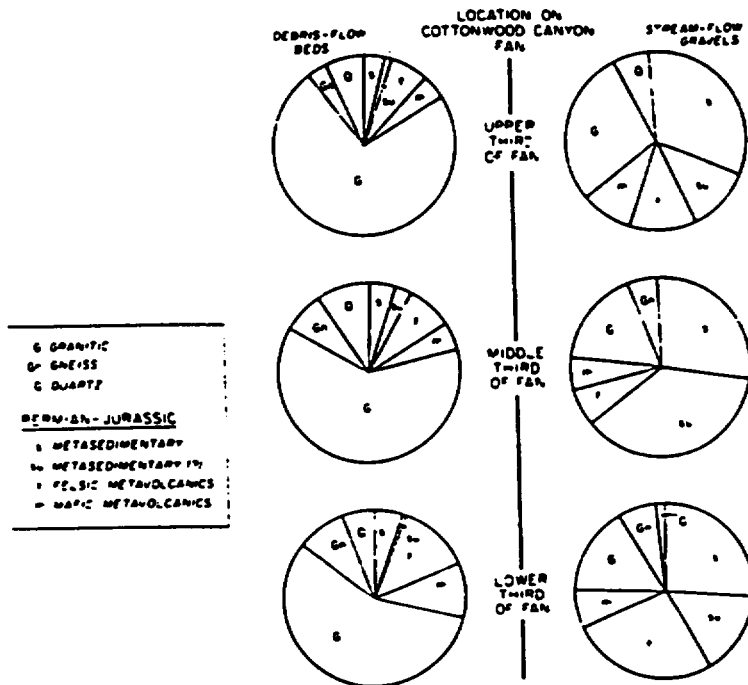


Fig. 25. Lithology of clasts larger than 1 cm in three debris-flow beds and three stream-flow gravels on Cottonwood Canyon fan. The debris flows carried more granitic and fewer metasedimentary clasts than the stream flows. As discussed in the text, debris flows originate high in the mountains on steep slopes developed on granitic rocks.

mentary clasts whereas the stream-flows transported 19% and 50%, respectively. On the Lone Tree Canyon fan, the debris-flow beds contain an average of 85% granitic plus metavolcanic clasts and 3% metasedimentary clasts in contrast to the stream-flow gravels which contain 47% and 37%, respectively.

Interpretation The aerial distribution of bedrock lithologies shown on the geologic map of Fig. 2 suggests a reason for the contrasting lithologic assemblage of the clasts carried by the debris flows and stream flows. The stream flows obtained many of their clasts from the talus slopes on the metasedimentary rocks whose distribution is restricted to near the apices of these two fans. The numerous granitic and metavolcanic clasts in the debris flows came from higher in the mountains. The debris flows originated on steep mountain slopes underlain by granitic and metavolcanic bedrock; on the way to the fans, the debris flows

entrained metasedimentary clasts as they passed through the area of metasedimentary bedrock.

Accessory heavy minerals

Methods. Accessory heavy minerals were analyzed in samples from the sandy mud matrices of 13 debris-flow beds, three stream-flow and sandflat sands, and one eolian sand. These samples are from the fans at Lone Tree Canyon, Jeffrey Mine Canyon, Sabies Canyon, Cottonwood Canyon, Milner Creek Canyon, and Straight Canyon (Fig. 2). The heavy minerals were separated from the isolated fine-sand fraction (2-3 ϕ) by intermittent stirring during gravity settling for four hours in tetrabromoethane (s.g. 2.9). The heavy minerals were cleaned in acetone, dried, and mounted in Canada Balsam. On each slide, 100 grains were randomly counted in ribbon traverses to establish the ratio of micas: opaques: nonopaques. The nonopaque count was then continued until 100

Fig. 26. Lithology trends and conclusions.

nonopaque grain was repeated, by grains. The grain and hypersthene and/or etched a portion of these sample.

Results. The heavy samples is dominated comprise 64% of magnetite judging octahedral form. grains 31%. The blends, 16%: clinzoisite-zoisite garnet, 3% tourmaline, sillimanite, 1% and 1% hypersthene. In the 17 sample blends, epidote.

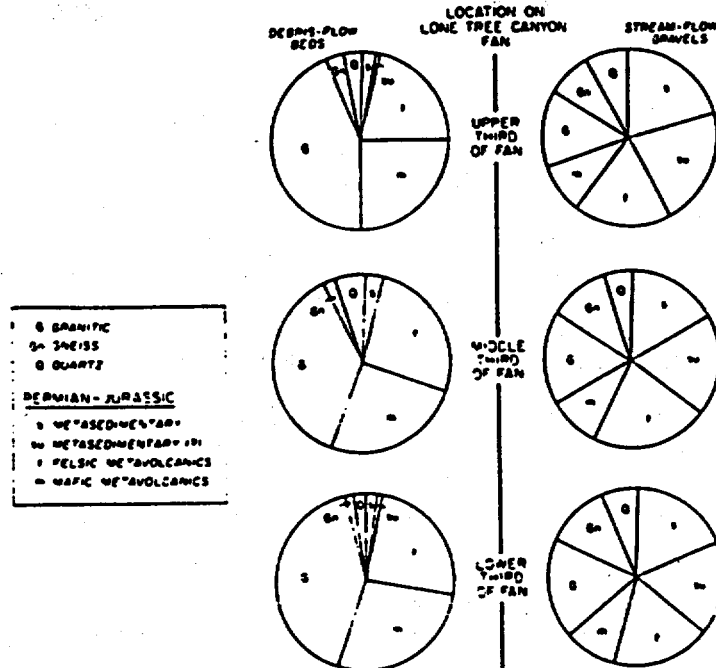


Fig. 26. Lithology of clasts larger than 1 cm in three debris-flow beds and three stream-flow gravels on Lone Tree Canyon fan. The trends and conclusions are similar to those for the Cottonwood Canyon fan (Fig. 25).

Canyon fan. The
all debris flows

they passed
bedrock.

were analyzed
atrics of 13
and sandflat
samples are
Jeffrey Mine
od Canyon.
Canyon (Fig.
ed from the
φ) by intermittent
for four hours in
the heavy minerals
and mounted in
100 grains were
verses to establish
nonopaques. The
ntinued until 100

nonopaque grains were tabulated. This procedure was repeated, bringing the nonopaque total to 200 grains. The grains of hornblende, epidote, augite, and hypersthene with limonite surface stains and/or etched spines were tabulated as a subproportion of these four Fe-silicate minerals in each sample.

Results. The heavy-mineral assemblage of the 17 samples is dominated by opaque grains, which comprise 64% of the total. The opaques are mostly magnetite judging by magnetic susceptibility and octahedral form. Micas form 5% and nonopaque grains 31%. The nonopaques average 35% hornblende, 16% andalusite, 13% epidote, 7% clinzoisite-zoisite, 7% sphene, 6% staurolite, 4% garnet, 3% tourmaline, 3% zircon, 2% rutile, 1% sillimanite, 1% augite, 1% brookite, and less than 1% hypersthene.

In the 17 samples, 54% of the grains of hornblende, epidote, augite, and hypersthene have

limonite surface stains and/or etch spines. The proportions of these altered grains are about the same in the 13 debris-flow beds (53%), three stream-flow and sandflat sands (54%), and in the one eolian sand (57%).

Interpretation. The generalized order of increasing stability of heavy minerals during weathering in acidic waters is (1) olivine and pyroxenes, (2) amphiboles, (3) sphene and biotite, (4) apatite, (5) epidote and garnet, (6) chloritoid and spinel, (7) staurolite, (8) andalusite, (9) kyanite, (10) tourmaline and sillimanite, and (11) zircon and rutile (Morton, 1985). The presence of 35% hornblende and 13% epidote grains, about half with limonite surface stains and/or etch spines, shows that chemical leaching is of moderate importance in the thin regolith on the steep slopes of the White Mountains. Mechanical weathering plays an important role in generating detritus for downslope movement to the tributary and trunk canyons.

Clay minerals

Methods. The less than 2- μm fraction was analyzed in 22 samples, including the sandy mud matrix of 14 debris-flow beds in nine alluvial fans. In Jeffrey Mine Canyon, one sample was collected from the regolith and another from a deeply weathered boulder. Six samples are mud layers on the sandflats at Cottonwood Canyon fan and Lone Tree Canyon fan.

The samples were disaggregated and dry sieved to 62 μm to obtain the silt and clay, which was then treated with a buffered solution of sodium acetate of pH 5 to remove carbonate. The silt and clay were ultrasonically agitated and washed several times with distilled water to remove any salts. The less than 2- μm fraction was obtained by centrifugal sedimentation in distilled water. An oriented specimen was prepared for X-ray diffraction analysis (XRD) by smearing a paste of material onto a glass slide. Diffraction patterns were obtained for three preparations: air dried, ethylene glyco-saturated, and heated to 550°C for one hour. XRD analyses were run on a Siemens X-ray diffractometer using Ni-filtered Cu-K α radiation. Scans were run at a goniometer speed of 2° per minute using a 1° slit and 0.4° receiving slit.

Results. The common clays in the less than 2- μm fraction of the 22 samples are well crystallized illite, kaolinite, smectite, and mixed-layer smectite-illite. The mixed-layer clay has superlattice peaks of 32-35 Å that appear upon glycolation and intensify with heat treatment. Chlorite and Fe-chlorite occur in moderate amounts. Detrital quartz, K-feldspar, and plagioclase are ubiquitous.

Interpretation. The abundance of smectite and mixed-layer smectite-illite reflects incomplete leaching in the regolith, as does the preservation of iron-silicate heavy minerals. The less than 4- μm clay fraction determined by Sedigraph analysis comprises less than 5% of the debris-flow beds, which suggests a low rate of clay production in the regolith. Soil development on the flank of the White Mountains is inhibited by the cold climate, limited precipitation, and steep slopes.

Inspection of the steep slopes of the trunk and tributary canyons shows boulder-rich debris perched on the slopes. This material evidently moves downslope mostly by mass wasting, storm runoff, and infrequent debris flows. Small debris-flow lobes move material downslope, particularly above tree line.

Smectite is present to abundant in the debris-flow beds, but occurs mostly in traces in mud layers deposited by stream flows on the sandflats. Perhaps the coarser-grained clays such as illite, kaolinite and mixed-layer clay settle from flood waters on the sandflats whereas the finer-grained smectite is preferentially carried beyond the sandflats.

Recurrence interval of debris flows

Methods. The superposition of debris-flow beds in the alluvial fans allows estimation of their recurrence interval by dating charcoal and wood in the older debris-flow and stream-flow deposits. The three samples dated by the ¹⁴C method lie beneath 2, 3, 4 debris-flow beds on the Cottonwood Canyon fan, Milner Canyon fan, and Jeffrey Mine Canyon fan, respectively. The samples were collected in the upper parts of the fans because some debris flows are too small to reach the distal portions. The analyses were run by Kruger Laboratory, Cambridge, Massachusetts, incorporating a correction for ¹³C.

Results and interpretation. The recurrence interval for debris flows on these fans is 320 years, based on estimates of 212, 400, and 350 years (Table 2). The 320-year average is similar to the 300-year estimate of Beaty (1970, 1974) who indirectly estimated the recurrence interval. Beaty noted that older fan deposits lie on the Bishop Tuff in uplifted fault blocks, which implies that fans have been building for 700,000 years, the age of the Bishop Tuff. Beaty then assumed that the fans were built mostly by debris flows, each with a volume equal to the 1952 debris flow on the Cottonwood Canyon fan. Beaty calculated by geometry that a debris flow every 300 years would build the fans in 700,000 years.

TABLE 2

¹⁴C dates of sample

Sample

Charcoal in stream-
Charcoal in stream-
Suck within debris-

Beaty's assu
dominated con:
700,000 years m
deposits expose
bris-flow beds.
stream-flow dep
sured sections i
fans. Perhaps th
greater than 300

Applications to i
bris-flows

On the weste
flows occur wit
320 years. The
debris flows sho
steep slopes de
camic rocks at hi
Johnson and Ru
and Rodine (19
scribed the proc
bris flows. We
intense summer
ing 50-100 mm
falls on an alrea
producing one
downslope, shear
and are transfo
channelized debr
trunk canyon, i
Although of inf
are more impor
structing the fa
White Mountain

es of the trunk and
er-rich debris per-
ial evidently moves
ing, storm runoff.
Small debris-flow
particularly above

lant in the debris-
in traces in mud
vs on the sandflats.
lays such as illite,
settle from flood
is the finer-grained
ried beyond the

flow beds in
their recur-
wood in the
eposits. The
lie beneath
ood Canyon
fine Canyon
collected in
some debris
tal portions.
Laboratory,
ating a cor-

ence interval
years, based
rs (Table 2).
he 300-year
o indirectly
y noted that
ishop Tuff in up-
es that fans have
rs, the age of the
ned that the fans
lows, each with a
bris flow on the
ity calculated by
y 300 years would

TABLE 2

¹⁴C dates of samples from three alluvial fans

Sample	Alluvial fan	Number of overlying debris-flow beds	Age	Recurrence interval of debris flows (years)
Charcoal in stream-flow sand	Cottonwood Canyon, section VI	2	425 ± 150	212
Charcoal in stream-flow sand	Milner Canyon, section II	3	1165 ± 150	400
Stick within debris-flow bed	Jeffrey Mine Canyon	4	1385 ± 75	350
				Mean 320

Beatty's assumption that debris flows have dominated construction of the fans for the last 700,000 years may or may not be correct. The fan deposits exposed in the fault blocks contain debris-flow beds, but their volumetric ratio to stream-flow deposits is lower than in our measured sections in incised channels of the modern fans. Perhaps the long-range recurrence interval is greater than 300 years.

Applications to the Coulomb-viscous model for debris-flows

On the western flank of the White Mountains, flows occur with a recurrence interval of about 320 years. The lithologies of the clasts in the debris flows show that these flows originate on the steep slopes developed on granitic and metavolcanic rocks at high elevations on the canyon walls. Johnson and Rahn (1970), Costa (1984), Johnson and Rodine (1984), and French (1987) have described the processes that commonly generate debris flows. We infer that in our study area, an intense summer rainstorm, with intensities reaching 50–100 mm per hour, saturates the regolith, or falls on an already snow-melt saturated regolith, producing one or more landslides that move downslope, shear, dilate by the addition of water, and are transformed into a debris flow. As a channelized debris flow moves along the floor of a trunk canyon, it incorporates additional debris. Although of infrequent occurrence, debris flows are more important than stream flows in constructing the fans on the western flank of the White Mountains (Beatty, 1963).

Debris flows move by deformation within a basal layer of high-shear stress (Johnson, 1970; Fisher, 1971; Naylor, 1980). In the debris-flow beds we studied, this layer after compaction comprises about 20% of the thickness of the beds, up to a maximum of about 20 cm. The larger boulders in each flow tend to move upward and out of the shearing layer, which is the weakest part of the flow, to produce the inverse grading seen at the base of most beds. Discoidal clasts in the shear layer tend to have a subhorizontal orientation, with up flow inclinations of 2–7°. The clasts have less scatter in orientation than do clasts in the overlying semi-rigid plug or in the levees on flow margins.

Above the shearing layer, lower shear stresses seldom exceeded the yield strength of the matrix so that the bulk of each debris flow rafted along as a semi-rigid, high-strength plug described by the Coulomb-viscous model for debris flows (Johnson, 1970; Johnson and Rodine, 1984; Pierson and Costa, 1987). A flow ceases to move when the thickness of the plug becomes equal to the thickness of the flow due to a decrease in slope angle or a drop in excess pore pressure. Maps of the orientations of sticks and logs embedded in the debris-flow beds on the White Mountain fans show a flow-parallel pattern that reflects the laminar-viscous motion of the plugs (Filipov, 1986). The presence of about 40% sandy mud matrix in most of these debris-flow beds suggests that the strength and buoyancy of the debris flows were largely provided by matrix cohesion, aided by frictional resistance (Rodine and Johnson, 1976; Hampton, 1979; Pierson, 1981). The

boulders, remained suspended in the flows, many projecting above the upper surfaces. The matrices of the flows evidently could move about somewhat, allowing the discoidal clasts to develop the observed subhorizontal fabric, with average dips of 5-13°, but also with substantial scatter in the clast orientation, many dipping at 60-90°. In some beds, the poles to the discoidal clasts plot as an ellipse roughly aligned with its long direction perpendicular to the flow direction as predicted by theory (Lindsey, 1968). The maximum size of the cobbles and boulders carried by an individual debris flow remains fairly constant down fan until the flow thins on the sandflat at the toe of the fan.

As debris lobes move down slope, lateral levees develop from snout materials pushed aside and sheared from the flow as the rigid plug passes by. Distinct levees, commonly containing the largest clasts in the flow, continue to form until the flow stops (Johnson and Rodine, 1984). The discoidal clasts in the levees of the debris-flow lobes on the White Mountain fans have average orientations that dip up flow at 21-31° and strike subparallel to the flow margins. The scatter in orientation of the discoidal clasts is substantial, about the same as in the semi-rigid plugs. Where a debris flow spilled out of a channel to spread over the low relief of the fan surface, the levees have in some cases confined the flow within an artificial channel, allowing the flow to continue down fan for a substantial distance.

Acknowledgements

Discussions with Arvid Johnson and Kevin Scott helped clarify our concepts of the sedimentology of debris flows. The staff of the White Mountain Research Station of the University of California, Bishop, California, provided housing and logistical support. The drawings were drafted by Marie Litterer, Scientific Illustrator of the Department of Geology/Geography, University of Massachusetts at Amherst. The manuscript was critically read by Earle F. McBride, Andrew D. Miall, Alan R. Peterfreund, and Kevin M. Scott. The project was supported by grant EAR83-06416 from the Division of Earth Science, U.S. National Science Foundation.

References

- Beats, C.B., 1963. Origin of alluvial fans, White Mountains, California and Nevada. *Ann. Am. Assoc. Geogr.*, 52: 516-535.
- Beats, C.B., 1970. Age and estimated rate of accumulation of an alluvial fan, White Mountains, California, U.S.A. *Am. J. Sci.*, 268: 56-77.
- Beats, C.B., 1974. Debris flows, alluvial fans, and a revitalized catastrophism. *Z. Geomorphol.*, 21: 39-51.
- Bruscoe, A.J. and Thompson, S., 1969. Observations on an alpine mudflow, Steele Creek, Yukon. *Can. J. Earth Sci.*, 6: 219-229.
- Bull, W.B., 1964. Alluvial fans and near-surface subsidence in western Fresno County, California. *U.S. Geol. Surv., Prof. Pap.*, 437-A: A1-A71.
- Costa, J.E., 1984. Physical geomorphology of debris flows. In J.E. Costa and P.J. Fleisher (Editors), *Developments and Applications of Geomorphology*. Springer-Verlag, Berlin, pp. 270-317.
- Crowder, D.F. and Sheridan, M.F., 1972. Geologic map of the White Mountain Peak quadrangle, Mono County, California. *U.S. Geol. Surv., Geol. Quad. Map GQ-1012*.
- Crowder, D.F., Robinson, P.T. and Harris, D.L., 1972. Geologic map of the Benton quadrangle, California-Nevada. *U.S. Geol. Surv., Geol. Quad. Map GQ-1013*.
- Filipow, A.J., 1986. Sedimentology of debris-flow deposits west flank of the White Mountains, California. Master's Thesis, University of Massachusetts, Amherst, Mass., 207 pp.
- Fisher, R.V., 1971. Features of coarse-grained, high-concentration fluids and their deposits. *J. Sediment. Petrol.*, 41: 916-927.
- Folk, R.L., 1974. *Petrology of Sedimentary Rocks*. Hemphill, Austin, Texas, 182 pp.
- Folk, R.L. and Ward, W.C., 1957. Brazos river bar: a study of the significance of grain size parameters. *J. Sediment. Petrol.*, 27: 3-27.
- French, R.H., 1967. *Hydraulic Processes on Alluvial Fans*. Elsevier, New York, N.Y., 244 pp.
- Hampton, M.A., 1979. Bouyancy in debris flows. *J. Sediment. Petrol.*, 49: 753-756.
- Johnson, A.M., 1970. *Physical Processes in Geology*. Freeman and Cooper, San Francisco, Calif., 577 pp.
- Johnson, A.M. and Rahn, P.H., 1970. Mobilization of debris flows. *Z. Geomorphol., Suppl. B*, 9: 168-186.
- Johnson, A.M. and Rodine, J.R., 1984. Debris Flow. In D. Brunsten and D.B. Prior (Editors), *Slope Instability*. J. Wiley and Sons, New York, N.Y., pp. 270-317.
- Krauskopf, K.B., 1972. Geologic map of the Mount Bartlett quadrangle, California-Nevada. *U.S. Geol. Surv., Geol. Quad. Map GQ-960*.
- Lindsey, J.F., 1968. The development of clast fabric in mud flow. *J. Sediment. Petrol.*, 38: 1242-1253.
- Miall, A.D., 1978. Lithofacies types and vertical profile models in braided river deposits: a summary. In: A.D. Miall (Editor), *Fluvial Sedimentology*. Can. Soc. Pet. Geol., Mem. 597-604.

- Menon, A.C., 1985. G.G. Zuffa (Ed.), *Dordrecht*, pp. 1111-1116.
- Salvor, M.A., 198. debris flow def 1111-1116.
- Peterson, T.C., 1986. Mount Thomas. *Sedimentol.*
- Peterson, T.C., 1981. debris flows of tions for mobil. Peterson, T.C. and

ans, White Mountains
n. Assoc. Geogr., 53

te of accumulation of
ifornia. U.S.A. Am J

tans, and a revitalized
4-51.

Observations on an
a. Can. J. Earth Sci., 4

surface subsidence in
U.S. Geol. Surv., Prof

gs of debris flows. In
ent. Developments and
Springer-Verlag, Berlin

gic map of the
County, Cali-
70-1012.

L., 1972. Geo-
formia-Nevada
3.

deposits, west
4aster's Thesis,
s., 207 pp

ugh-concentra-
t. Petrol., 41

cks. Hemphill

har: a study in
Sediment. Pe-

Alluvial Fans.

ss J Sediment

ology Freeman

ation of debris
86.

Flow. In: D

Skope Instability. J
p. 270-317.

of the Mount Barcroft
S. Geol. Surv., Geol

of clast fabric in mud-
-1253

vertical profile models
In: A.D. Miall (Edi-
Pet. Geol., Mem., 5

Morton, A.C., 1985. Heavy minerals in provenance studies: In: G.G. Zuffa (Editor), *Provenance of Arenites*. D. Reidel, Dordrecht, pp. 249-277.

Walzer, M.A., 1980. The origin of inverse grading in muddy debris flow deposits — a review. *J. Sediment. Petrol.*, 50: 1111-1116.

Peterson, T.C., 1980. Erosion and deposition by debris flows at Mount Thomas, New Zealand, and implications for mobility. *Sedimentology*, 28: 49-60.

Peterson, T.C., 1981. Dominant particle support mechanisms in debris flows of Mount Thomas, New Zealand, and implications for mobility. *Sedimentology*, 28: 49-60.

Peterson, T.C. and Costa, J.E., 1987. A rheologic classification

of subaerial sediment-water flows. In: J.E. Costa and G.F. Wieczorek (Editors), *Debris Flows/Avalanches: Process, Recognition, and Mitigation*. Reviews in Engineering Geology, Vol. VII. Geological Society of America, pp. 1-12.

Rodine, J.R. and Johnson, A.M., 1976. The ability of debris, heavily freighted with coarse clastic materials, to flow on gentle slopes. *Sedimentology*, 23: 213-234.

Sharp, R.P. and Nobles, L.H., 1953. Mudflow of 1941 at Wrightwood, southern California. *Geol. Soc. Am. Bull.*, 64: 547-560.

Smoot, J.P., 1982. Sedimentary fabrics of debris flow-dominated, stream-modified alluvial fan, Saline Valley, California. *Am. Assoc. Pet. Geol. Bull.*, 66: 633 (abstract).

BMS SL • 026902

INFORMATION ONLY

WBS: 1232842
QA: N/A

BEST AVAILABLE COPY

NNA.910412.0011

FINAL REPORT JANUARY 1, 1967 - JUNE 30, 1988

TASK 1 Quaternary Geology and Active Faulting at and near Yucca Mountain

Principal Investigator: John W. Bell, Engineering Geologist

Co-Investigators: Alan R. Ramelli, Research Associate
Craig M. dePolo, Research Associate
Harold F. Bonham, Jr., Geologist

Assistants: Keryl Fleming, Computer Specialist
Nick Varnum, Graduate Assistant

Consultants: Ronald I. Dorn, Texas Tech University
Frederick F. Peterson, University of Nevada-Reno
Steven Forman, University of Colorado
Teh-Lung Ku, University of Southern California

90338
2316

Best copy available from original.
4-1-91

Appendices

Appendix A - Consultant's report: A critical evaluation of cation-ratio dating of rock varnish, and an evaluation of its application to the Yucca Mountain repository by the Department of Energy and its subcontractors; R. I. Dorn

Appendix B - Consultant's report: Soil-geomorphology studies in the Crater Flat, Nevada, area; F. F. Peterson

Appendix C - Consultant's report: Assessment of the applicability of the thermoluminescence (TL) dating technique to natural hazard evaluations at the high-level nuclear waste repository site, Yucca Mountain, Nevada; S. L. Forman

Appendix D - Consultant's report: Radiometric dating with U- and Th-series isotopes in the Nevada Test Site region - a review; T. L. Ku

Appendix E - Cedar Mountain field guide: Visit to trenches along the southern part of the 1932 Cedar Mountain earthquake ruptures, Monte Cristo Valley, Nevada; C. M. dePolo, A. R. Ramelli, and J. W. Bell

Appendix F - Abstracts presented and/or submitted

9 0 8 8 8
2 3 1 7

Appendix D

Consultant's report: Radiometric dating with U- and Th-series isotopes in the Nevada Test Site region - a review

by T. L. Ku

2318

90838

**Radiometric Dating with U- and Th-series Isotopes
in the Nevada Test Site Region - A Review**

**Teh-Lung Ku
(June 1988)**

Introduction

This document is a literature review of the uranium and thorium decay series dating of Quaternary deposits in the Nevada Test Site (NTS), Nevada. In evaluating the Yucca Mountain at NTS as a possible suitable site for nuclear waste repository, geological age information of the Site is of fundamental importance. Our ability and efforts to obtain such information have yet to be strengthened. There is a general dearth of both the material and the methods available for absolute dating in continental settings. The methods involving the U- and Th-series isotopic disequilibrium relationships can be looked upon as among the most promising. In the meantime, however, one recognizes their being in the evolving stage, requiring further research to be carried out.

In the following, I will first present the principles of the U/Th dating methods applicable to the NTS material, pointing out their merits, shortcomings, and assumptions involved. I will then review the quality of the data obtained to date and suggest future work for possible improvement.

The Methods

The disequilibrium relationships among ^{230}Th - ^{234}U - ^{238}U are used in two basically different ways to extract the age, or time of sedimentation, for a deposit at NTS. They can be referred to as the closed-system and the open-system approaches. The former approach is used conventionally in the

9 0 8 3 8 2 3 1 9

U-series dating, by noting the extent of daughter ingrowth toward secular equilibrium with its long-lived radioactive parent (Ku, 1976). It applies mostly to authigenically precipitated carbonate deposits. The latter approach is embodied in a method called uranium-trend dating (Rosholt, 1980). In this method, the age of a deposit is derived from the time-dependence of isotopic distribution in the deposit through which a solution (soil water or groundwater) carrying the isotopes has moved. Such a deposit can be largely detrital sediments of alluvial, glacial, and eolian origin, among others.

Closed System Dating - The Conventional U-Series Methods

It is well known that uranium is much more soluble than thorium in natural solutions. So minerals like calcium carbonate or silica precipitated from such solutions usually contain a few ppm of uranium but virtually no thorium. Subsequent to their formation, if the minerals act as a closed system with respect to U and Th isotopes, the age (t) of the minerals can be derived from the following radioactive growth and decay equation:

$$^{230}\text{Th} = ^{238}\text{U}[1 - \exp(-\lambda_0 t)] + (^{234}\text{U} - ^{238}\text{U})\lambda_0 / (\lambda_0 - \lambda_1) [1 - \exp(\lambda_1 t - \lambda_0 t)] \quad (1)$$

where λ_0 and λ_1 are decay constants of ^{238}Th and ^{234}U , respectively, and the notation for nuclides refers to their specific activities (dpm/g). The last term of the above equation accounts for the effect of the excess ^{234}U over ^{238}U generally found in natural waters. The unknown, t, can be solved iteratively or estimated from a graphic solution as shown in Fig. 1. The maximum age dateable using this method is about 350,000 years. This technique has been

9
0
8
8
9
2
5
2
0

used for dating a wide variety of pure carbonate material such as corals and mollusks.

In applying this technique to material from the terrestrial environments in general and from the NTS area in particular, two problems have to be overcome. First, the samples selected for dating must meet the closed system requirement. In the absence of independent cross-checks of age results, the criteria for the sample selection usually call for dense, compact material devoid of leaching and reprecipitation features (Ku et al, 1979). For carbonate precipitates at NTS, an approximate, generalized order of reliability might be: calcite crystals or veins - dense pebble coating from Cca soil horizon - travertine > calcrete - tufaceous travertine > caliche nodules - soil caliche (Knauss, 1981). Secondary silica deposits (opal or opal - euhedral quartz) have also been shown to approximate a closed-system for U and its daughters (Ludwig et al, 1980; Knauss, 1981; Szabo and O'Malley, 1985).

The second problem is detrital ^{230}Th contamination, for terrestrial carbonates are seldom pure and contain detrital minerals (mostly aluminosilicates or 'clay') of significantly older age. There have been several publications dealing with measures to eliminate or correct the detrital contamination effect. A summary paper was published by Ku and Liang (1984). Usually the approach consists of a combined chemical leach and numerical or graphical correction procedure. The procedure that has been used in the NTS studies (e.g., Knauss, 1981; Szabo et al, 1981) is the one originally reported by Rosholt (1976) and Szabo and Sterr (1978). It entails dilute acid leaching of the impure carbonate sample, followed by radiochemical analysis of both the leachate and the residue. Under the assumption that the acid leaching step does not fractionate the U and Th

2321

8

3

3

0

9

isotopes, the $^{230}\text{Th}/^{234}\text{U}$ and $^{234}\text{U}/^{238}\text{U}$ ratios of the pure carbonate phase in the sample can be obtained from the slopes of $^{230}\text{Th}/^{232}\text{Th}$ vs. $^{234}\text{U}/^{232}\text{Th}$ and $^{234}\text{U}/^{232}\text{Th}$ vs. $^{238}\text{U}/^{232}\text{Th}$ plots for the leachate-residue pairs, respectively. An example of the plots is shown in Fig. 2 for a caliche sample from a unit that is cut by the Yucca Fault at NTS (Knauss, 1981). The age of the sample calculated from the $^{230}\text{Th}/^{234}\text{U}$ and $^{234}\text{U}/^{238}\text{U}$ ratios using a rearranged Equation (1) is 108 ky.

There is one aspect in regards to this second problem to be noted. That is, even if no attempt at correction for detrital contamination is made, or if doubts arises as to the correction procedures used, data on ^{230}Th , ^{234}U and ^{238}U in the whole sample (carbonate plus detrital 'clay') should give an upper-limit age estimate, which in some cases should still be of value. Thus in the use of the conventional U-series dating of carbonate and silica material, the key requirement is sample acting as a closed system in a geochemical sense, as the heading of this section denotes.

Open System Dating - The Uranium Trend Method

An 'unconventional' method has been devised to date fine-grained sediments such as alluvial/colluvial deposits and soils of Quaternary age using the U-series isotopes. It is unconventional in the sense that, unlike all the age dating methods which require enclosure of radioisotopes in a sample to be dated, this so-called "uranium-trend dating method" determines the age by modelling the behavior and distribution of isotopes in the sample which acts as an open system for the isotopes. A preliminary model for U-trend dating was presented by Rosholt (1980) and Szabo and Rosholt (1982), which was revised later by Rosholt (1985). This dating technique has been applied rather extensively at NTS (Rosholt et al, 1985; Shroba et al, 1988).

The principles of U-trend dating are briefly summarized below. For more details, referred to Rosholt (1985) and Muhs et al (1987). The U-trend clock starts with the inception of water movement through sediment or soil, the timing of which may coincide with the initiation of sediment deposition or soil development. This water contains some uranium (^{238}U) which decays to ^{234}U and ^{230}Th . These daughter nuclides are adsorbed or driven into (via alpha-decay recoil mechanism) sediment grains. This daughter emplacement process results in solids having $^{234}\text{U}/^{238}\text{U}$ and $^{230}\text{Th}/^{238}\text{U}$ activity ratios higher than the secular equilibrium ratio of unity. At the same time, a counter process takes place by which ^{234}U produced by decay of ^{238}U structurally incorporated in sediment grains is preferentially released from the sediment via leaching and alpha-recoil. This ^{234}U displacement process is responsible for the widely known phenomenon that natural waters often exhibit $^{234}\text{U}/^{238}\text{U}$ activity ratios of >1.00 . According to Rosholt (1985), in arid or semiarid environments, emplacement of ^{234}U and ^{230}Th is the dominant process initially. With time, continuous exposure of leachable ^{234}U sites to percolating water results in eventual domination of the displacement process.

The essence of the uranium-trend method is thus a model which describes the migration of uranium in a solid-fluid matrix through time, leaving in its wake a trail of daughter products such that the distributions of the isotopes involved (^{238}U , ^{234}U , and ^{230}Th) are modelled in terms of the above-mentioned parameters of daughter emplacement and ^{234}U displacement, and uranium-flux factor. This latter parameter is related to the flux of mobile uranium through a deposit, assumed to decrease exponentially with time. Emplacement by recoil-adsorption processes is a function of the concentrations of dissolved uranium and of the sorptive

9 0 3 8 8 2 3 2 3

9
0
3
3
8
2
3
2
4

properties on the solids. Displacement by recoil-leaching is controlled by the concentrations of uranium in the solid phase and by the solubility of uranium in the leachate. The uranium-flux factor depends on the quantity of water migrating through a deposit and the concentration of uranium in this water relative to that in the solid phase. All these parameters should vary from deposit to deposit and are unknown. They also are not amenable to rigorous mathematical description. To circumvent these difficulties, U-trend dating writes empirical model equations expressing $^{234}\text{U} - ^{238}\text{U}$ and $^{230}\text{Th} - ^{234}\text{U}$ as a function of sample age t and U-flux factor $F(0)$; the latter is expressed as "decay" constant λ_0 [$-\ln 2$ /half period of $F(0)$] from the assumed exponential decrease of $F(0)$. As shown in Fig. 3, by plotting $(^{234}\text{U} - ^{238}\text{U})/^{238}\text{U}$ vs. $(^{238}\text{U} - ^{230}\text{Th})/^{238}\text{U}$ for a suite of samples of the same age (i.e., from a given unit), the age t can be determined from the slope of the plot if λ_0 or half period of $F(0)$ for the unit is known. To assign λ_0 for a given suite of samples, the method again uses the empirical approach of getting a relationship between the half period of $F(0)$ and the x-intercept in a $(^{234}\text{U} - ^{238}\text{U})/^{238}\text{U}$ vs. $(^{238}\text{U} - ^{230}\text{Th})/^{238}\text{U}$ plot for suites of samples of known age, as shown by Fig. 4. The half period of $F(0)$ for a sample of known age is calculated from the empirical equations of $^{234}\text{U} - ^{238}\text{U}$ and $^{230}\text{Th} - ^{234}\text{U}$, both are function of t and λ_0 only, as mentioned. Depending on the half period of $F(0)$, or λ_0 , as shown in the example of Fig. 5, the U-trend dating applies to samples with ages ranging approximately from 10 to 800 thousand years.

Merits and Demerits of the Two Approaches

The closed-system approach requires that the sample acts as a closed system with respect to isotopic exchange with the its surroundings. If this requirement is fulfilled, procedures and assumptions used in deriving age

information are much more straight-forward and easier to be substantiated than those used in the open-system approach. On the other hand, the conventional closed-system U-series dating to NTS has the following limitations:

(1) It is generally limited to dating carbonate and perhaps silica deposits, the ages of which may not be close to those of geomorphic surfaces or of neotectonic events in the area.

(2) The maximum age dateable is limited to 350 thousand years.

(3) There are no well-established criteria for sample screening to ensure closed system.

The uranium-trend method is potentially applicable to a wide variety of material including soil, alluvial, lacustrine, marine, eolian, and glacial deposits (Rosholt, 1985). It applies to a relatively large age range (10-800 ky, though more sensitive in the range of 60-600 ky). However, at this stage of development of the method, it can still be considered as experimental, in view of the following major points of concern:

(1) An important component of this empirical model is the uranium flux, $F(t)$. This factor should be related to the concentration and amount of uranium moving through a deposit, which is a function of climate and sediment lithology/compaction. The time variation of this function has to be very complex. The adopted function of a simple exponential decay with time for the uranium flux is certainly an oversimplified one, not to mention the possibility of being incorrect in certain cases. For example, to what extent the uranium-flux in the NTS area could be affected by the pluvial climate during the last glaciation in the western U.S.?

(2) As far as age assignment by the U-trend technique is concerned, the empirical relationship of Fig. 4 forms a key element to that assignment.

Yet there exists room for clarification or improvement of that relationship. First, its physical meaning is by no means clear, so is the significance of the coordinate x_i of the plot. The latter question becomes an even more pertinent one to be clarified when one notes that the algebraic sign of x_i is of no consequences; that is, the plot only takes positive values whereas x_i 's for the data points delineating the curve have both positive and negative values. Here, one assumes *a priori* the existence of a symmetrical relationship between half period U flux and degree of ^{230}Th - ^{238}U disequilibrium. Whether this relationship holds in theory or empirically remains an open question. Second, although the curve in Fig. 4 is defined by 10 data points, only four of the points (units 3, 8, 11 and 12) represent samples independently dated by ^{14}C , K-Ar or fission track and thus can be considered as primary calibration points. (It should be noted that unit 12, Tuff B of Lake Tecopa, was considered to be the distal facies of the Bishop Tuff, and thus was dated indirectly.) The remaining six calibration points are of secondary nature. The ages of these six samples are assessed by local correlation (Rosholt et al, 1985b; J.N. Rosholt, pers. comm., 1988) only, and their accuracies, hence uncertainties in their half period $F(0)$ estimates, are difficult to determine. Thus, it is reasonable to view the Fig. 4 relationship as being preliminary, pending further refinement.

(3) There is the "sensitivity" problem of how well one is able to resolve or determine ages from the analytical data. A linear fit of the data displayed in plots like Fig. 3 give intercept x_1 and slope m ; both of these parameters are needed in calculating the age of the sample. The uncertainties attached to these parameters depend on how well the linearity is defined. Data such as those shown in Fig. 6 for two of the samples from NTS obviously will impart considerable uncertainty to the estimation of x_i

6
2
3
2
2
8
8
0
0
9

and m, hence to their age assignment. It should also be pointed out that even if error in x_1 is small, the corresponding estimate for half period of $F(0)$ could still be large because of the preliminary nature of the empirical relationship shown in Fig. 4, mentioned above. According to the present relationship, an uncertainty of 100% in half period of $F(0)$ may cause an error of the order of 50% in age (J.N. Rosholt, pers. comm., 1988; also cf. Fig. 5 of Rosholt, 1985).

Current Data

Uranium-trending dating has been reported for 40 suite of samples from the Nevada Test Site (Rosholt et al., 1985a; Shroba et al., 1988). Each suite consists of 4 to 12 samples from a stratigraphic unit or section. Eight of the suites have been analyzed in two different size fractions (denoted as m and f). By inspection of the goodness of the linear fits for the 4 to 12 data points of each suite in a $(^{234}\text{U} - ^{238}\text{U})/^{238}\text{U}$ vs. $(^{238}\text{U} - ^{230}\text{Th})/^{238}\text{U}$ plot such as shown in Fig. 4, one gets some idea as to how good the determination of the age for a given unit is. The following list is an evaluation of the data at hand. Very qualitatively, category A includes suite of samples giving sufficiently well defined slopes and x-intercepts in the $(^{234}\text{U} - ^{238}\text{U})/^{238}\text{U}$ vs. $(^{238}\text{U} - ^{230}\text{Th})/^{238}\text{U}$ plots such that their ages will have 10-20% errors. Category C, on the other hand, are those units with "clustered" data arrays, causing age estimations with large uncertainties of >100%, if not impossible. The in-between category B will have age uncertainties of ~50%.

Category A: P2, RV1-AD, RV1-EI, RV1-PU, RV1-VZ, TSV-307, S9, SCP4, TSV396 (m and f), CF1, CF2 (m and f), YM2U (m and f), YM2L (m and f), YM13U (m and f), YM13L (m and f), YM14B, YM14U, CQB, deposit F

Category B: RV2-U, RV2-L, JD, YM14M, YM14L, S3, deposit H

Category C: SFF, FFPG, S1, F3, RV1-JO, Q2E, Q2S, SCF1 (m and f), SCF2 (m and f), SCF3, CF6, FHA, Deposit C, deposit D.

The conventional uranium-series dating carried out thus far at NTS (Knauss, 1981; Szabo et al., 1981; Szabo and Kyser, 1985; Szabo and O'Malley, 1985; Shroba et al., 1988), while showing its value in contributing to the geochronology of the region, has pointed to the need for further systematic sampling and measurement. Because of the method's reliance on the closed-system assumption, consistency of age data based on multiple analyses and field relationships is of utmost importance. By multiple analyses is meant the use of different methodologies on the same sample or on different material from the same stratigraphic unit. They have yet to be performed in a consistent manner.

Suggestions for Future Work

Future geochronological work with U-series isotopes at NTS should strive for consistency check. Both internal and external consistencies should be sought. The internal check refers to (1) reproducibility of results obtained on a single sample and (2) ages obtained for a group of samples are consistent with their relative stratigraphic positions; in both cases, the same dating technique is employed. The external consistency refers to cross-checks made with different age dating methods on a given sample or on samples in the same depositional unit.

The uranium-trend dating uses model approach. Models always involve assumptions, and some of the assumptions used by the U-trend method (such as the exponential uranium fluxes) are difficult to verify. Furthermore, the method completely relies on empirical data for calibration.

2329
2
8888
90888
9

and the quality and appropriateness of such data become very crucial and at this time still need refinement. As it stands, while having an encouraging start (thanks to the efforts of Rosholt and his associates), the method can be looked upon as in the evolving stage. For these considerations, it is suggested that the conventional closed-system dating should be emphasized in future geochronological work at NTS, with priority being placed on samples of pure carbonate (i.e., calcite veins) and/or opal deposits. Preliminary studies made on dating secondary silica (opal) material from the region using uranium-series disequilibrium have obtained encouraging results (Knauss, 1981; Szabo and Kyser, 1985). These include high U/Th ratio and equilibrium ^{238}U - ^{234}U - ^{230}Th relationship in the samples studied, suggesting that opal fulfills initial conditions and closed-system requirements for U-series dating. In the NTS area, waters obtain silica from the hydrolysis and dissolution of glass contained in tuffaceous deposits which can be a source of uranium when they are vitrified (Rosholt et al., 1971; Zielinski, 1978). Further work on the dating of Quaternary secondary silica is warranted. Because opal contains much higher uranium concentration than carbonates in the area, it is possible that the age signal for the silica precipitates will be preserved even if the analyzed opal is not pure.

In the dating of secondary calcium carbonate such as pedogenic precipitates, the strategy should be to select (even though extremely painstaking efforts may be required) samples containing as little detrital silicate impurities as possible, so as to avoid the detrital ^{230}Th correction routine. The correction, if unavoidable, requires little or no fractionation of Th and U isotopes in the acid leaching procedure, which can be best checked by either replicate analyses or successive leaching (see Ku and Liang, 1984).

9
0
8
8
8
2
3
3
0

In order to establish for the uranium-trend dating a stronger footing than it has had, it is suggested that the empirical curve of Fig. 4 should be verified by addition of calibration points with truly independently dated samples. The U-trend plot should show well-defined linearity. Muhs et al. (1987) have suggested a linear correlation coefficient of at least 0.7, with a confidence level of at least 90%. These are reasonable criteria for data acceptance. In this context, the following words of caution are noteworthy (Muhs et al., 1987): "..... a complex geological history can result in an inaccurate U-trend age even when a U-trend plot shows reasonable linearity. For example, the lower part of a deposit to be dated might experience little or no interaction with U-bearing water during its history. At some later time, however, the upper part of the deposit is removed by erosion and the lower part begins to experience interaction with U-bearing water. The U-trend age will reflect the time of sediment/water interaction, not the original time of sediment deposition. This is a condition that can be assessed only by geological evidence and/or independent age control, because the deposit may yield well-defined Th-index and U-trend plots."

The above quote touches on two important aspects. One aspect points to the difficulties one might face in attempting to model a natural system which often has too many variables. The other aspect points out the fact that the ultimate cross-check for reliability is comparison with ages obtained by independent means. In this regard, Rosholt and Szabo (1982) have reported agreement between U-trend ages of U.S. Atlantic coastal sediments and conventional $^{230}\text{Th}/^{234}\text{U}$ ages of corals from the same sediments. Rosholt et al. (1986) and Machette et al. (1986) also reported U-trend ages for terrace alluvium along the Colorado River in Grand Canyon National Park which are in agreement with the depositional sequence of the terraces.

However, these reports are in abstract form, lacking formal documentation. More recently, Muhs et al (1987) have attempted similar comparison studies on terrace deposits in Palos Verdes Hills and San Nicolas Island, California. We anticipate continuous progress made toward the improvement of the U-trend method. This is important, for there is a lack of means to determine the deposition time of fine-grained sediments of Quaternary age.

References Cited

- 9
0
3
8
2
3
3
1
- Knauss, K.G. (1981) Dating fault associated Quaternary material from the Nevada Test Site using uranium-series methods. Lawrence Livermore National Laboratory, Livermore, CA, UCRL-53231. 51p.
- Ku, T.L. (1976) The uranium-series methods of age determination. *Ann. Rev. Earth Planet. Sci.* 4, 347-379.
- Ku, T.L., W.B. Bull, S.T. Freeman and K.G. Knauss (1979) ^{230}Th - ^{234}U dating of pedogenic carbonates in gravelly desert soils of Vidal Valley, southern California. *Geol. Soc. Amer. Bull.* 90, 1063-1073.
- Ku, T.L. and Z.C. Liang (1984) The dating of impure carbonates with decay-series isotopes. *Nucl. Instru. Meth. in Phys. Res.* 223, 563-571.
- Ludwig, K.R., D.A. Lindsey, R.A. Zielinski and K.R. Simmons (1980) U-Pb ages of uraniferous opals and implications for the history of beryllium, fluorine, and uranium mineralization at Spor Mountain, Utah. *Earth Planet. Sci. Lett.* 46, 221-232.
- Machette, M.N., J.N. Rosholt and C.A. Bush (1986) Uranium-trend ages of Quaternary deposits along the Colorado River, Grand Canyon National Park, Arizona. *Geol. Soc. Amer. Abstr. with Programs* 18, 393.

- Muhs, D.R., J.N. Rosholt and C.A. Bush (1987) The uranium-trend dating method: Principles and application for southern California marine terrace deposits. Submitted to *Quat. Sci. Rev.*
- Rosholt, J.N. (1976) $^{230}\text{Th}/^{234}\text{U}$ dating of pedogenic carbonates in desert soils. *Geol. Soc. Amer. Abstr. with Programs* 9, 1976.
- Rosholt, J.N. (1980) Uranium-trend dating of Quaternary sediments. U.S. Geological Survey Open-File Report 80-1087, 65p.
- Rosholt, J.N. (1985) Uranium-trend systematics for dating Quaternary sediments. U.S. Geological Survey Open-File Report 85-298, 34p.
- Rosholt, J.N., C.A. Bush, W.J. Carr, D.L. Hoover, W.C. Swadley and J.P. Dooley, Jr. (1985a) Uranium-trend dating of Quaternary deposits in the Nevada Test Site area, Nevada and California. U.S. Geological Survey Open-File Report 85-540, 37p. + 35 Figs.
- Rosholt, J.N., C.A. Bush, R.R. Shroba, K.L. Pierce and G.M. Richmond (1985b) Uranium-trend dating and calibrations for Quaternary sediments. U.S. Geological Survey Open-File Report 85-299, 48p.
- Rosholt, J.N., W.R. Downs and P.A. O'Malley (1986) Uranium-trend ages of surficial deposits in the central Grand Canyon National Park, Arizona. *Geol. Soc. Amer. Abstr. with Programs* 18, 408.
- Rosholt, J.N., Prijana and D.C. Noble (1971) Mobility of uranium and thorium in glassy and crystallized silicic volcanic rocks. *Econ. Geol.* 66, 1061-1069.
- Rosholt, J.N. and B. Szabo (1982) Comparison of uranium-series dating of coral and uranium-trend dating of coral-bearing terraces on the U.S. Atlantic coastal plain. *Geol. Soc. Amer. Abstr. with Programs* 14, 603.
- Shroba, R.R., D.R. Muhs and J.N. Rosholt (1988) Physical properties and radiometric age estimates of surficial and fracture-fill deposits along a

- portion of the Carpetbag Fault System, Nevada Test Site, Nye County, Nevada. USGS-10583-1, 45p.
- Szabo, B. and T.K. Kyser (1985) Uranium, thorium isotopic analyses and uranium-series ages of calcite and opal, and stable isotopic compositions of calcite from drill cores UE25a#1, USW G-2 and USW G-3/GU-3, Yucca Mountain, Nevada. U.S. Geological Survey Open-File Report 85-224, 25p.
- Szabo, B. and P.A. O'Malley (1985) Uranium-series dating of secondary carbonate and silica precipitates relating to fault movements in the Nevada Test Site region and of caliche and travertine samples from the Amargosa Desert. U.S. Geological Survey Open-File Report 85-47, 12p.
- Szabo, B. and J.N. Rosholt (1982) Surficial continental sediments. In: Ivanovich, M. and R.S. Harmon, eds., Uranium Series Disequilibrium: Application to Environmental Problems. Clarendon Press, Oxford, p.246-267.
- Szabo, B. and H. Sterr (1978) Dating caliches from southern Nevada by $^{230}\text{Th}/^{232}\text{Th}$ versus $^{234}\text{U}/^{232}\text{Th}$ and $^{234}\text{U}/^{232}\text{Th}$ versus $^{238}\text{U}/^{232}\text{Th}$ isochron-plot method. U.S. Geological Survey Open-File Report 78-701, p.416-418.
- Szabo, B., W.J. Carr and W.C. Gottschall (1981) Uranium-thorium dating of Quaternary carbonate accumulations in the Nevada Test Site region, southern Nevada. U.S. Geological Survey Open-File Report 81-119, 35p.
- Zielinski, R.A. (1980) Uranium in secondary silica: A possible exploration guide. Econ. Geol. 75, 592-602.

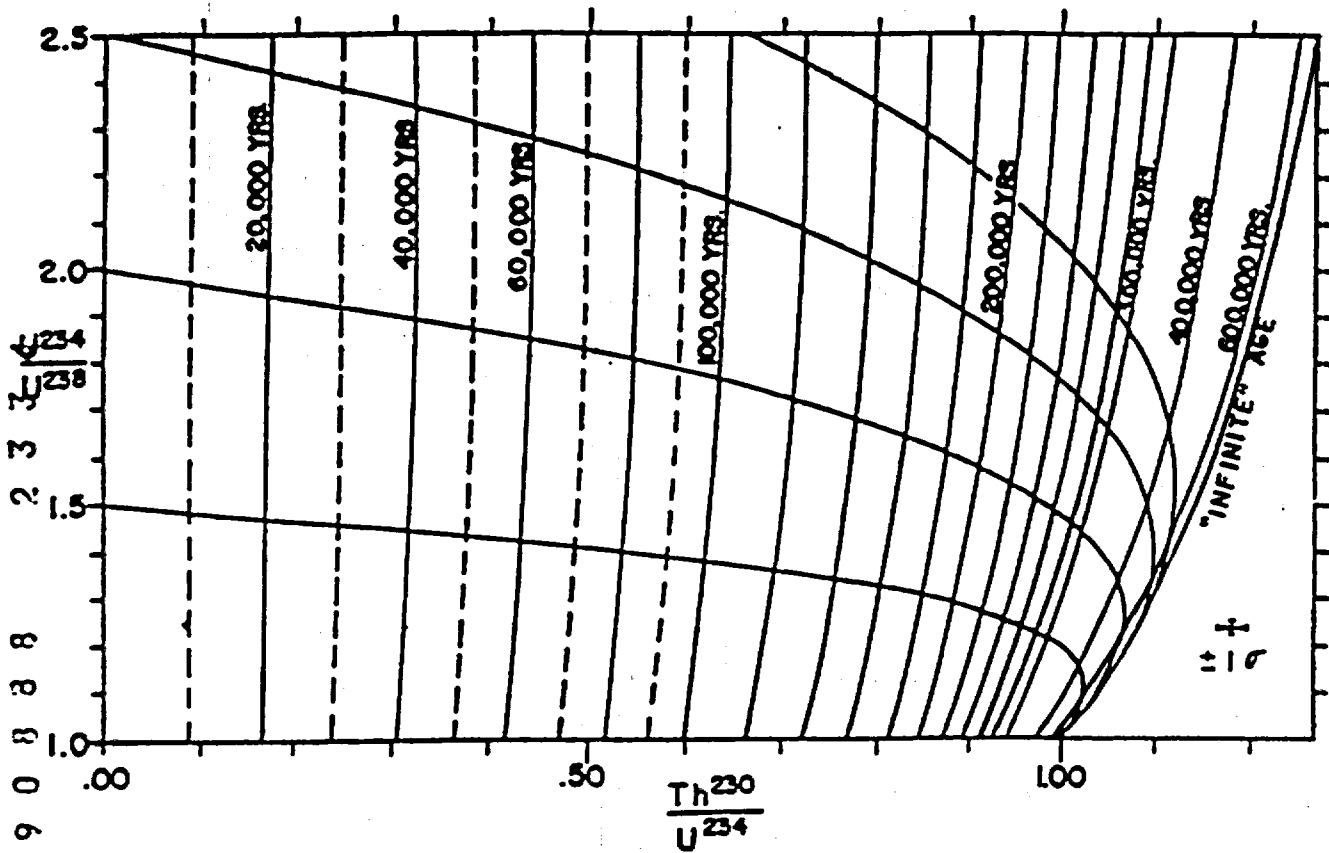


Fig. 1. Graphic solution for Eq. (1). The near-vertical curves are isochrons. The near horizontal lines are growth curves along which carbonates with initial U-234/U-238 ratios of 1.5, 2.0 and 2.5 would evolve with time. The error bars shown at lower right corner are for a typical analysis.

8 0 3 3 3 5 3 2 2

2 3 3 5

9 0 9 3 8

Sample YF SL2

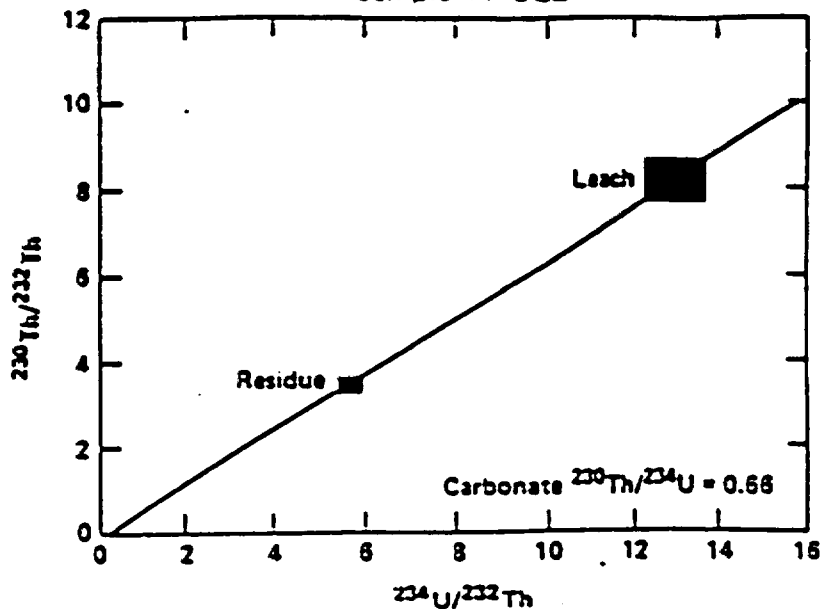


FIG. 2a. Graphical calculation of the $^{230}\text{Th}/^{234}\text{g}$ activity ratio in carbonate.

Sample YF SL2

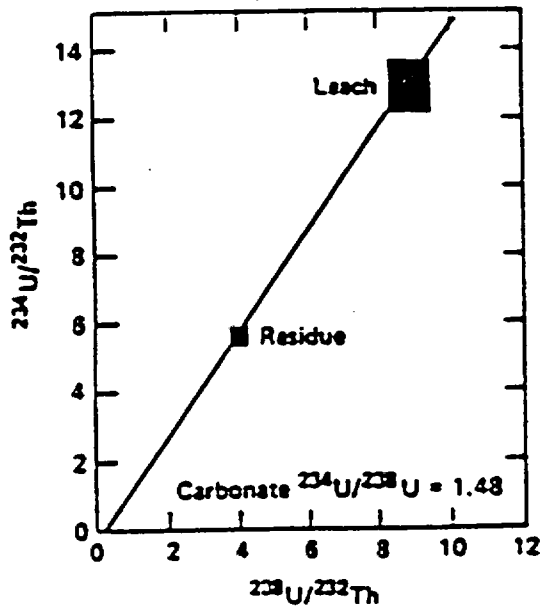


FIG. 2b. Graphical calculation of the $^{234}\text{g}/^{238}\text{g}$ activity ratio in carbonate.

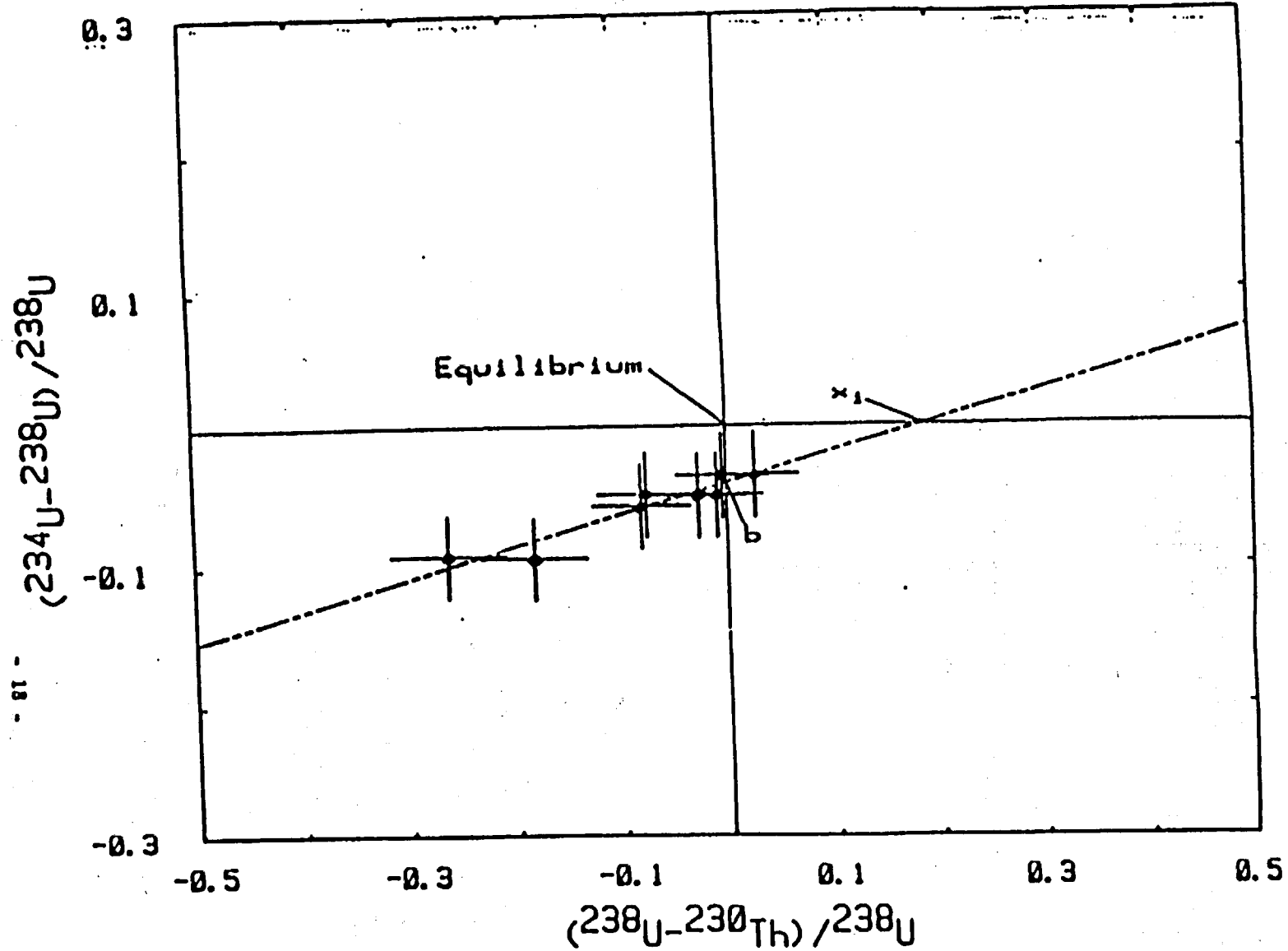


Figure 3. Uranium trend plot of FD unit, Outer Bull Lake till, Sublette County, Wyoming, as an example. Age of the sample can be calculated from the x-intercept (x_i) and slope of the plot.

9 0 8 3 3 2 3 3 6

Half period of $F(t)$, Ka

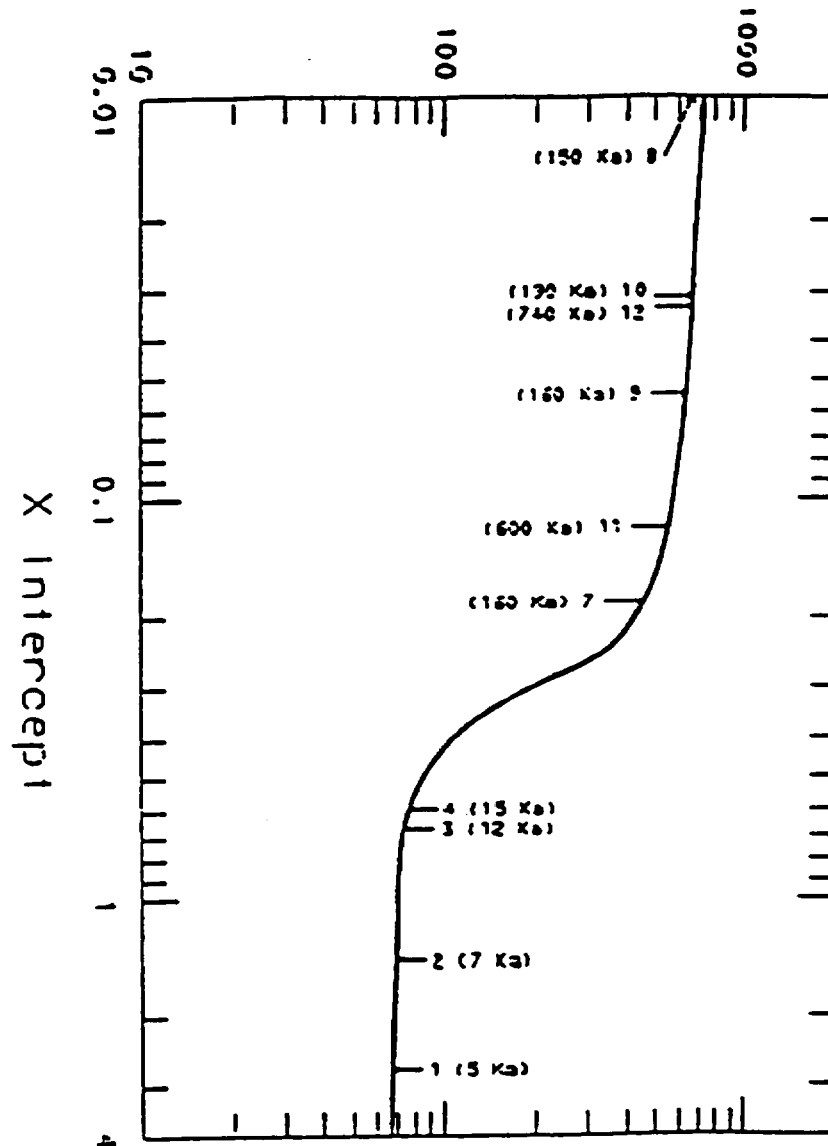
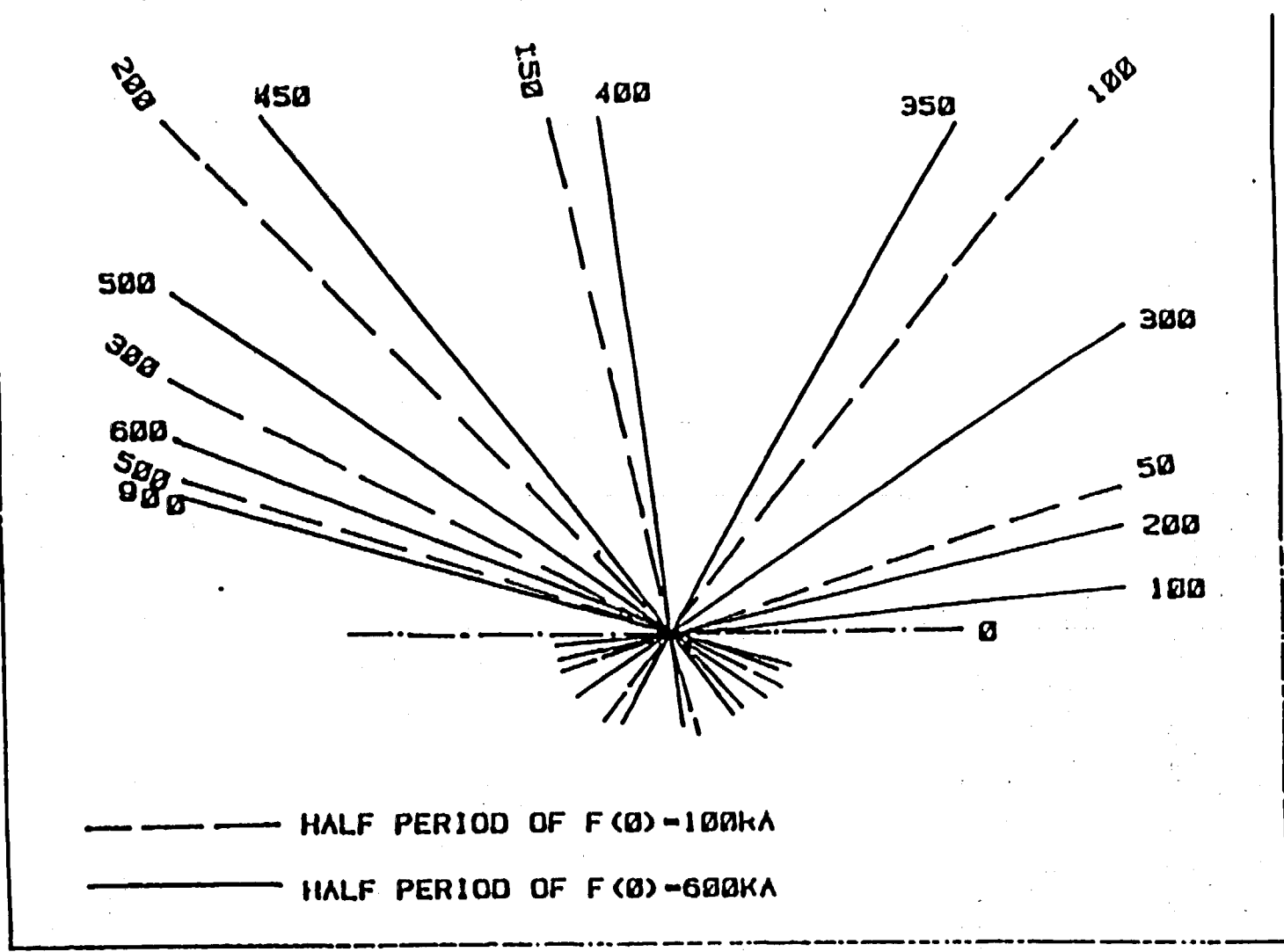


Fig. 4. Empirically derived curve for determination of $F(t)$ from x-intercept value. The primary calibration points are 3, 8, 11, and 12; the remainder are "secondary" calibration points. Knowing $F(t)$ and slope of plots as shown in Fig. 3, the age of the deposit to be dated can be ascertained from plots such as Fig. 5.

$(^{234}\text{U}-^{238}\text{U}) / ^{238}\text{U}$

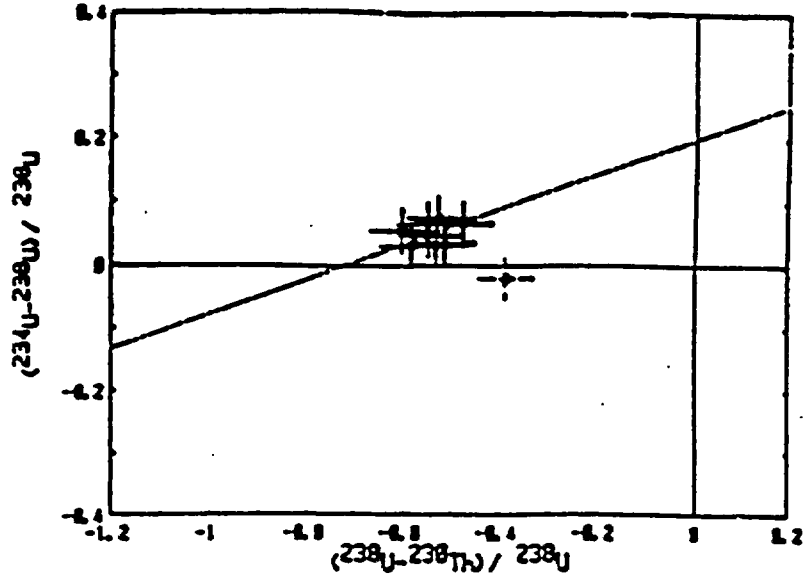
- 02 -



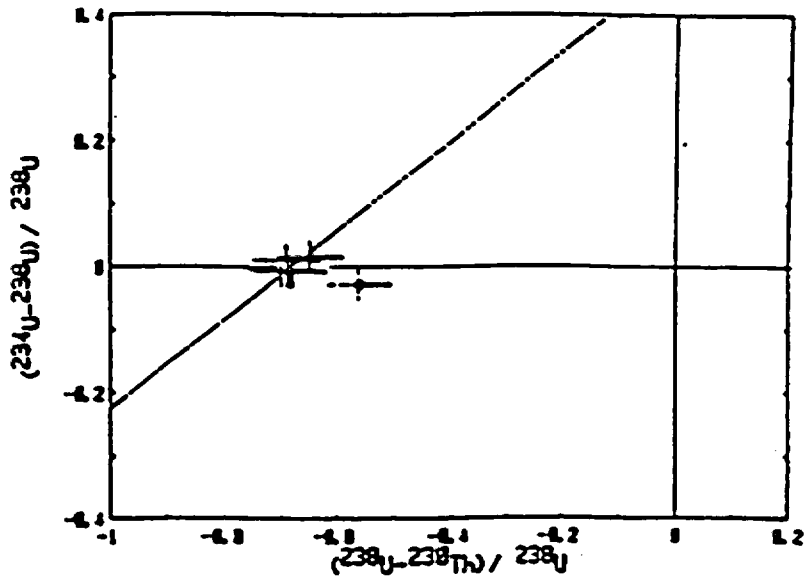
$(^{238}\text{U}-^{230}\text{Th}) / ^{238}\text{U}$

Figure 5. Variation of U-trend slope with age of deposition for 100,000 and 600,000 year half periods of $F(0)$.

9 0 3 3 8
2 3 3 8



Plots of FFP6 unit, eolian sand in Frenchman Flat Trench. The uppermost sample, □, is not included in U-trend slope because it may contain material from overlying deposit.



Plots of S1 unit, alluvium in Frenchman Flat Trench. The uppermost sample, □, is not included in the U-trend slope because it may contain material from the overlying deposit.

Fig. 6. Two examples of the U-trend plots for samples from NTS showing ill-defined slope and x-intercept determinations for the data arrays. In the text, we place these samples in the "Category C".

90888 2339

TABLE 2 -- LIST OF PEDONS DESCRIBED IN CRATER FLAT, AND THEIR TAXONOMIC NAMES, LOCATIONS, GEOMORPHIC SURFACES AND ROCK-VARNISH AGE ESTIMATES

Pedon No.	CFP No.	Soil Family / Site Location	Geomorphic Surface/ Rock-Varnish Age YPA/ Hoover Surf. Deposit
1	CFP2	sandy-skeletal, mixed (calcareous), thermic "Camborthidic" Torriorthent Ashton (site) road, Amargosa Valley	Little Cones 7,310 ⁵ Q2
2	CFP26	sandy-skeletal, mixed, thermic Typic Camborthid Little Cones, Crater Flat	Little Cones 11,200 ⁵ Q1
3	CFP26A	sandy-skeletal, mixed, thermic Typic Camborthid adjacent to Pedon 2	Little Cones 11,200 ⁵ Q1
4	CFP27	loamy-skeletal, mixed, thermic Typic Calciorthid Diamond Queen Mine & Solitario Canyon roads	late Black Cone 28,300 ⁵ Q2
5	CFP27A	sandy-skeletal, mixed, thermic Typic Calciorthid Adjacent to Pedon 4	late Black Cone 28,300 ⁵ Q2
6	CFP32	loamy-skeletal, mixed, thermic Haplic Durargid Between Black Cone & Red Cone, along Solitario Canyon. road	late Black Cone 33,400 ⁵ Q2
7	CFP37	loamy-skeletal, mixed, thermic Typic Durargid along "diagonal road" to NE Crater Flat	early Black Cone 128,000 ⁶ Q2
8	CFP29	loamy-skeletal, mixed, thermic Typic Durargid SE corner Solitario Cny. & Trench CFP2&3 roads	early Black Cone 137,000 ⁶ QTa
9	CFP30	loamy-skeletal, mixed, thermic Haplic Durargid SE of Pedon 8, across drainageway, 0.1 mi. along Trench CFP2&3 roads	early Black Cone QTa
10	CFP35	loamy-skeletal, mixed, thermic Haplic Durargid 0.55 mi. SE along Trench CFP2&3 roads; across wash, N, next higher, older surface than Pedon 11	late Black Cone 29,700 ⁵ Q2

9 0 3 3 8 2 3 4 0

TABLE 2 -- Continued.

Pedon No.	CFP No.	Soil Family / Site Location	Geomorphic Surface/ Rock-Varnish Age YPR/ Hoover Surf. Deposit
11	CFP33	loamy-skeletal, mixed, thermic Typic Camborthid 0.65 mi. SE along Trench CF2&3 roads; across wash, S, next lower surface than Pedon 10	late Black Cone 19,000 ⁵ Q2
12	CFP34	loamy-skeletal, mixed, thermic Naplic Durargid 0.75 mi. SE along Trench CF2&3 roads, adjacent to & slightly higher surface than Pedon 11	late Black Cone Q2a
13	CFP41	sandy-skeletal, mixed, thermic Typic Torriorthent 1.2 mi. SE along Trench CF2&3 roads; rav bar & swale inset fan	very late Crater Flat Q1
14	CFP31	loamy-skeletal, mixed, thermic Typic Haplargid 1.27 mi. SE along Trench CF2&3 road; adjacent to and next older surface than Pedon 13	late Black Cone Q2bc
15	CFP36	loamy-skeletal, mixed, thermic Typic Durargid 1.85 mi. SE along CF2&3 road; 30 ft. NE of E end of Trench CF3	late Black Cone 31,800 ⁵ Q2bc

⁵ Minimum radiocarbon age for basal rock varnish; calculated as 10% greater than uncorrected radiocarbon age; see Table 3 for uncorrected ages and error ranges.

9
0
8
8
8
2
3
4
1

9 0 9 3 8 2 3 4 2

Geomorphic Surface/ Rock-Variety Age Tm/ Sooner Surf. Deposit	Soil Family / Site Location	CRP No.	Pedon No.
---	-----------------------------	------------	--------------

Yucca 380,000 6 QTA	"fine-loamy", mixed, thermic typic durargid High, next-to-oldest fan-plateau remnant, NI Crater Plate	CRP38	16
Yucca 360,000 6 QTA	clayey-skeletal, nontronitic (?) thermic typic durargid High, next-to-oldest fan-plateau remnant, 0.7 mi. S of Solitario Cny.	CRP39	17
Solitario 660,000 6 QTA	loamy-skeletal, mixed, thermic typic durargid / typic durargid (complex) Highest, oldest fan plateau remnant, 0.7 mi. S of Solitario Cny.	CRP40	18

Mean minimum cation-ratio age for rock variolity; see Table 3 for error ranges.

TABLE 2 - Continued.

TABLE 3 — LIST OF ROCK-VARNISH AGES FOR PEDONS IN CRATER FLAT⁷

Pedon No.	CFP No.	Uncorrected Age YPB	+10% Corrected Age YPB	Est. Error	Dating Type
1	CFP2	6,645	7,310	± 245	RC
2	CFP26	10,180	11,200	± 270	RC
3	CFP26A				
4	CFP27	25,700	28,300	± 360	RC
5	CFP27A				
6	CFP32	30,320	33,400	± 460	RC
7	CFP37	128,000		106X-153X	CR
8	CFP29	137,000		115X-162X	CR
9	CFP30				
10	CFP35	26,970	29,700	± 375	RC
11	CFP33	17,280	19,000	± 370	RC
12	CFP34				
13	CFP41				
14	CFP31				
15	CFP36	28,920	31,800	± 400	RC
16	CFP38	380,000		260X-550X	CR
17	CFP39	360,000		253X-515X	CR
18	CFP40	660,000		450X-965X	CR

The Av Horizon and Site Selection for Pedon Descriptions

Evidence for recent fault movement is of prime importance in the Yucca Mountain studies, and the Av horizon is one of the most important soil features for establishing relative ages of Modern, or Late-, mid-, or early-Holocene or late-Pleistocene soils that might be broken by faulting. Hoover et al (1981), Swadley and Hoover (1983), Swadley et al (1984), and Taylor (1986) all apparently use the occurrence of an Av horizon as their major criterion for separating Pleistocene from Holocene surfaces. This could be a very effective criterion if the Av horizon were operationally defined and the time is determined for enough dust accumulation to allow the Av to form.

⁷ Ages from Dorn, 1988.

⁸ Dorn (1988) estimates the actual radiocarbon ages are about 10% older than the uncorrected values.

⁹ For radiocarbon dates the probable "plus or minus" error in YPB is given; for cation-ratio dates the "uncorrected age" is the mean value of several cation-ratio age determinations and the "error" is shown as the probable younger to older error-range of age in thousands of years ("K").

¹⁰ RC = radiocarbon dating of basal rock varnish. CR = cation ratio of rock varnish.

9 0 3 8 8 2 3 4 3

None of the previous authors describe their concept of the Av horizon in morphological terms, but the vesicular horizon can be defined as a genetic horizon (sensu Peterson, 1981, p. 43) that is (a) a surficial horizon that (b) crusts and cracks into coarse "polygons" (i.e., coarse prismatic structure) when dry, that (c) that are either massive or massive in their upper part and platy in their lower part; (d) the horizon has coarse vesicular pores in at least its upper part; (e) the horizon can be under a desert pavement, but regardless, is less gravelly than the subjacent horizon if the original parent material was gravelly and the subjacent horizon is not clayey; the horizon (f) is light colored and low in humus, it (g) is a sandy loam, fine sandy loam, very fine sandy loam, silt loam, or occasionally a loam or sandy clay loam or clay loam, but in any case has a high percentage of very fine sand and/or silt that encourages "dilatancy" when the soil is saturated. The Av horizon also commonly is (h) a "ruptic" horizon, i.e., it starts and stops horizontally, interchanging with an ordinary A horizon that is not crusting and lacks coarsely-vesicular pores, because of their microtopographically higher positions where they are not apt to saturate surficially.

The "Av horizon" is a peculiar genetic epipedon that is characteristic of many desert soils (Peterson, 1977, Eckert et al, 1978, Nettleton and Peterson, 1983), but it is not officially recognized in Soil Taxonomy as a kind of horizon, in the sense a mollic epipedon, petrocalcic horizon, or duripan are kinds of pedogenic horizons. Rather, it is merely one of several types of ochric epipedons; the "v" postscript in the "Av" designation even is illegal for National Cooperative Soil Survey pedon-description standards! } True

An Av horizon that formed in originally coarse-textured parent material, such as that on the piedmont slopes of Crater Flat, is the result of long-term dust-fall on the originally coarsely-porous soil surface followed by recurrent dust-infiltration to the depths of rapid, "gravitational" water infiltration during large storms, i.e., to some 12-18 inches depth in the Crater Flat vicinity. When the coarse interstitial pores between sand grains become plugged with the very fine sand, silt, and (minor) clay of the infiltrated dust and water infiltration becomes slow "capillary" movement, subsequent dust accumulation is at the surface, i.e., between and immediately below any desert pavement that might be present. Animal activity mixes some gravel and sand with the dust into this thin surficial horizon and ejects some gravel onto the surface to join the pavement, but regardless, the surficial layer becomes more silty-loamy and less sandy and gravelly.

Formation of the Av horizon's coarsely-vesicular pores and its diagnostic crusting behavior depend on additional factors after sufficient dust has accumulated for the horizon to form: The surficial horizon must have remained low in humus content and unstructured, so that when it is strongly wetted it will have a slow infiltration rate, hence saturate and act as a thickly-viscous liquid that allows entrapped air bubbles to migrate and join together to form progressively larger bubbles, i.e., vesicular pores (Miller, 1971). Saturation also causes the horizon to consolidate enough that on drying the saturated part becomes a crust (Hillel, 1960). The high percentage of silt and very fine sand in the accumulated dust encourages this sort of "dilatant" behavior when saturated, but limited biological activity in the surface layer is essential to prevent formation of soil structure that would increase infiltration rates, decrease dispersion, and hence decrease the probability of periods of surficial saturation.

9 0 3 3 8
2 3 4 4

Conditions for Av horizon formation are best in the barren, paved areas between desert shrubs. Under the shrubs, coppice dunes of eolian-sand accumulate; they are the site of litter accumulation and the greatest insect and animal activity. Low but significant amounts of humus accumulate and the soil is mixed to some depth; soil structure may be formed, but regardless, the soil material remains pervious to water and does not saturate under heavy rainfall. Within the creosote bush vegetation of the Mojave Desert (Crater Flat is at the northern edge of that desert) accumulation of eolian sand occurs not only as single coppice dunes under single shrubs, but as thin sheets joining several, spaced-apart shrubs and their coppice dunes. These slightly-raised microtopographic features, or biocoppices, to coin a term, also are the site of the most intense rodent digging and the least likely spots for Av horizons to form undisturbed over long periods of time. Between the biocoppices, the barren soil is flattish, if not microtopographically slightly-concave, and if a desert pavement is present, it is most prominent in the flattish or depressed spots. Such paved spots are called pavettes here, to coin another term. They are least frequently mixed, become saturated in their surface few centimeters during heavy storms or snow melt, and have the most closely-packed, best size-sorted, darkly-varnished desert pavement, and most prominent Av horizon. } B.S.

It is not unreasonable to conclude that the effects of slow dust infiltration, accumulation, and Av horizon formation will be best preserved in the pavette microtopographic position, and that is where soils were described for this study unless otherwise noted. } B.S.

Crater Flat Surface and Soils

The active and recently-active washes, inset fans, and fan skirts that show no significant formation of genetic soil horizons comprise the later-Holocene and historic Crater Flat surface. The soils are thermal Typic Torriorthents. Alluvium in Crater Flat is ubiquitously very to extremely gravelly, or cobbly, or stony sand or loamy sand, so the soils are in sandy skeletal families. On the piedmont slope directly below the limestones of Bare Mountain, these soils are in carbonatic mineralogy classes, whereas the Torriorthents of the piedmont slope below the volcanic rocks of Yucca Mountain are in mixed mineralogy classes. Pedon 13 is a representative soil from an inset fan (a Swadley & Hoover Q1b deposit).

2
? Within the Crater Flat geomorphic surface age-span, age distinctions are best made by microtopography, and are quite effectively reflected by Swadley & Hoover's Q1a (raw channels), Q1b (raw, rough, bar & swale inset fans with little "smoothing"), and Q1c (inset fans with "muted" bar & swale microtopography and proto-desert-pavement) distinctions. With the exception of the large area of Little Cones surface in southwestern Crater Flat, Swadley et al.'s (1984) mapping of their Q1 deposit (i.e., Q1a + Q1b + Q1c + Q1s + Q1e) quite correctly shows, at their small scale, the distribution of the Crater Flat surface.

The "muting", or smoothing of the rough bar & swale microtopography that occurs from Q1a to Q1b to Q1c surfaces possibly is caused by rodent digging that lowers stones by undercutting and by accumulation of eolian sand in swales. An open, poorly sorted, "proto-desert-pavement" has formed in the } silt

5
4
3
2
8
8
8
0
9

swales of Q1c areas, but there is only a morphological hint of dust accumulation in the surface horizon, i.e., the surficial few mm of some Q1c areas barely coheres in the weakest of crusts, and in some situations there is effervescence associated with a slight "graying" due to slight dust accumulation at a few cm depth in sand whereas the surficial sand is noneffervescent, or "leached"; in this area calcium carbonate and soluble sodium salts obviously are being added by dust fall.

At most, microtopographic-muting is accompanied by slight dusting of, or filaments of pedogenic calcium carbonate on pebble bottoms at 20-50 cm depths, i.e., Stage I carbonate accumulation (Gile et al, 1966). There is no apparent opal accumulation.

A "Crater Flat age soil" could not be distinguished from raw alluvium by its morphology in a trench. Such a soil has identity only by its location under a Crater Flat-age surface.

Little Cones Surface and Soils

The Little Cones surface comprises one large fan-skirt remnant surrounding Little Cones in southwestern Crater Flat (Fig. 1, shown by Swadley et al (1984) as a Q1 area), and several low basin-floor remnants in adjacent, northern Amargosa Desert that are shown as Q2 areas by Swadley et al. The remnant surrounding Little Cones is bounded on the east by the main wash from northwestern Crater Flat and an extensive area of bar and swale Crater Flat surface formed by this wash and the main wash from the northeast. To the west and southwest the Little Cones remnant is bounded by the lateral drainageway at the base of the Bare Mountain piedmont slope. To the northeast, just to the west of Red Cone, this Little-Cones fan-skirt remnant stands some seven feet above the Q1b bar-and-swales of the main wash¹² and is inset into and some eight feet below the dissected, Black Cone-age fan piedmont sloping down from Bare Mountain. The scarp between the Black Cone and Little Cones surfaces feathers out in an arc to the southwest.

The inset relationships demonstrate that the Little Cones surface is a younger surface than the Black Cone surface (most of Swadley and Hoover's Q2 areas are Black Cone surface remnants) and an older surface than the Crater Flat surface (most of Swadley and Hoover's Q1 is Crater Flat surface). The clear-cut morphogenetic differences between the Typic Camborthids of the Little Cones surface and the Typic Calciorthids of the Black Cone surface or the Typic Torriorthents of the Crater Flat surface demonstrates that the three surfaces are different enough ages that they should be recognized as separate

¹¹ Taylor's (1986) classification of pedogenic stages of opal accumulation will not be used here since it is a too simplistic analogy to Gile, Peterson, and Grossman's (1966) stages of calcium carbonate accumulation. Otherwise, Taylor's study is excellent.

¹² Beneath the Black Cone surface, thick layers of carbonate-silica cemented gravel outcrop on the wash scarp, whereas below the Little Cones surface the sandy-skeletal alluvium has only Stage I or II carbonate accumulation on pebbles.

9
0
3
3
8
2
3
4
6

geomorphic surfaces. At Little Cones, Swadley et al (1984) did not separate the Little Cones surface remnant from their large Q1 delineation to the east, even though it has a fully-smoothed surface with abstracted, though shallow drainageways, and an evident, though only slightly varnished desert pavement, and with a clearly pedogenic soil. Since they accurately drew the boundary of the Q2 area to the north, they must have wittingly included this Little Cones remnant in their Holocene Q1 unit; perhaps they did not think its Av horizon "strongly enough developed" to be a Pleistocene soil feature or recognize that it has a cambic horizon and evident Bk horizon.

Pedon 2 (in a pavette) and Pedon 3 (in a biocoppice) illustrate the soil features of the Little Cones surface at Little Cones (Appendix, II). The Av horizon is only 3 cm thick and barely exhibits the dilatancy¹³ of the usual Av horizon, but it crusts¹⁴, is cracked into polygons, and has coarsely-vesicular pores. The Av horizon occurs only under the pavettes; under the biocoppices it either has been mixed by animals, or is buried by a few inches of eolian sand and has lost its vesicularity and crustiness, though it retains its color and takes on a prominent tubular porosity. There is a prominent but non-cemented, late-stage I, 2Bk horizon that has relatively thick pebble-bottom carbonate coatings. It underlies a roughly 60-cm thick layer that I consider to be loamy due to dust infiltration and that now comprises the Av horizon, an Ak horizon of recent carbonate accumulation, and a Bwk, or cambic horizon that has had carbonate leached through it (the 2Bk is evidence) even though it still has thin pebble-bottom coatings of carbonate in transit to the 2Bk. A very few, very thin, pustulose, brittle, carbonate-laminae occur on the bottom of some of the Av horizons coarse prisms (polygons); such carbonate laminae are common in the lower Av horizons of soils on the Black Cone, Yucca surfaces and are interpreted as evidence of shallow carbonate accumulation during, perhaps, later Holocene to present. The high pH values just below the Ak horizon are evidence of eolian addition of soluble sodium salts and their accumulation just below the current depth of carbonate accumulation.

Pedon 1, from a basin-floor remnant in the Amargosa Desert basin, that was mapped by Swadley as a Q2 deposit, is quite similar to Pedon 2. It has been identified as a "Camborthidic" Torriorthent, rather than as a Typic Camborthid, only because its 22 cm-deep Bwk horizon is 3 cm shy of the arbitrary 25 cm depth required by Soil Taxonomy for diagnostic cambic horizons. Rock varnish from pavement pebbles on Pedon 1 gives a 7,310 YPB minimum age for the surface and soil, whereas varnish from pebbles on Pedon 2 give a 11,200 YPB age (Table 2, 3). The 8-22 cm deep Bwk horizon of Pedon 1 contains some greyish layers that are considered buried Av horizons; the about 4,000 year younger date of Pedon 1, compared to Pedon 2, may reflect a late addition of sediment.

¹³ "Dilatancy" is a term attributed to soil mechanics, perhaps incorrectly, that describes the viscous-liquid-like behavior of saturated soil material with high contents of silt and very fine sand. A blob of the saturated material will collapse and flow out into a broad disk, or "dilate", when jiggled; it also will drool from the fingers.

¹⁴ Operationally, a soil crust is a layer that forms at the surface when a soil dries and that will break out as plate-like fragments that can be handled without breaking.

9 0 8 3 8
2 3 4 7

The rock varnish dates, the thinness of the varnish, and the minimal Bk and Av horizon differentiation of Pedons 1, 2, and 3 all suggest either a very early-Holocene or latest-Pleistocene age for the Little Cones surface and soils. Similar soils under creosote bush vegetation on the Leasburg surface at Las Cruces, New Mexico, are about 10,000 years old and are considered latest-Pleistocene (Gile and Grossman, 1979, p. 166).

Black Cone Surface and Soils

In the Crater Flat basin, the Black Cone surface (much of Swadley and Hoover's Q2 deposits) comprises small to large fan-piedmont remnants that in aggregate are about as extensive as the Crater Flat surface. Defining the Black Cone surface is difficult because mapping the surface is difficult. Boundaries to younger surfaces are readily mapped because they commonly are at an erosional scarp, or at the least are at the boundary from the unvarnished or slightly varnished pavement of Crater-Flat or Little-Cones-surface soils to the blackish-shiny-varnished desert pavement of the soils of the Black Cone surface. However, boundaries to older Yucca or Solitario surface remnants are difficult to determine, unless there is a scarp reflecting an inset relationship, because the darkness of rock-varnishing or closeness or extensiveness or sorting of desert pavements are not consistently different. There are soil differences between the Black Cone and Yucca or Solitario surfaces that are due to confirmable age differences, i.e., that can be observed where there is an inset-surface relation. But, between various remnants of the Black Cone surface there are noticeable differences in soil development that can be related to confirmable surface age differences in the field in only a few cases. However, progressively older rock varnish dates do seem to correlate with these differences in degree of development of the Black-Cone-surface soils.

Late-Black-Cone Age Soils from Limestone Alluvium

Pedons 4 & 5: Pedon 4 (in a biocoppice) and adjacent Pedon 5 (in a pavetta) are on a lower-fan-piedmont remnant that was mapped Q2 by Swadley and Hoover. The remnant has two more somewhat lower and younger levels, but they have soils so similar to Pedons 4 and 5 that these younger levels are included in the Black Cone surface. This remnant is to the north of Pedons 2 and 3 of the Little Cones surface and near Bare Mountain (Fig. 1). Pedons 4 and 5 represent the Typic Calciorthids that form from mixed limestone-volcanic fan-alluvium on the Black Cone surface. Limestone pebbles in the pavement (Pedon 5) are deeply solution-etched whereas volcanic pebbles are darkly-varnished; the pavement is well-sorted and closely-spaced. Under the pavement, there is a moderately thick, fully dilatent, prominently crusted and coarsely-vesicular Av horizon that is notably grayer than the underlying cambic horizon. This Av horizon is easily distinguished from the thinner, less-silty Av horizon of the Little Cones surface. In the non-animal-aided Pedon 5, the cambic horizon (Bvk1, Bvk2) has non-calcareous parts indicating that it was once fully leached, and that the calcareousness of the Av horizon (which has thin, brittle, pustulose carbonate laminae on plate bottoms) represents later, probably Holocene carbonate accumulation. The 2Bk horizon contains about 20% volume of Stage II-III, weakly carbonate-cemented gravel lenses in a Stage I matrix; the 2Bk horizon has enough pedogenic carbonate to be a calcic

9 0 3 3 8 2 3 4 8

horizon, but not a petrocalcic horizon. Rock varnish age is about 28,300 YPB. In southern New Mexico, one would expect at least a minimal petrocalcic horizon to have formed in a soil this old.

There are Paleorthids with petrocalcic horizons on the Bare Mountain fan piedmont on surface remnants that look to be within the Black Cone age-spread, but I did not study them. There also are Petrocalcic Paleargids high on that limestone fan piedmont on probably Yucca-age fan remnants.

Late-Black-Cone Age Soils from Volcanic Alluvium

Pedon 6: Pedon 6 is a Black-Cone-age Haplic Durargid formed from volcanic-rock alluvium from Yucca Mountain that has no admixed limestone. It is between Red and Black Cones (Fig. 1) on an elongate, low, fan-piedmont remnant that Swadley and Hoover mapped Q2, and that is just above Q1c Torriorthents. It is some 33,400 years old, by rock varnish dating, and has a very gravelly sandy loam, minimal, argillic horizon and a haplic (i.e., minimal) duripan rather than the cambic and calcic horizons of Pedon 5, which had limestone in its parent material. The Av horizon of Pedon 6 is fully-dilatant, moderately thick, and leached of carbonates. An underlying Ak horizon reflects Holocene carbonate accumulation, since parts of the Bt are noncalcareous, i.e., previously leached. A pH of 9.4 and dark, 1-2 mm thick bands of alkali-solubilized humus in the Ak horizon indicate soluble sodium salt accumulation as well.

This soil represents one the younger, less-differentiated Durargids of the Black Cone surface. Its argillic horizon has clay skins, but a relatively low clay content. Its duripan has only a single thin laminae on top, and though coherent in place, is only weakly cemented when tested as broken-out chunks. Since this soil is about the same age as Pedon 5, a Calciorthid, the two demonstrate that, in later Pleistocene soils, moderate amounts of limestone in the original parent material will prevent the formation of an argillic horizon, a relationship well known in Nevada.

Pedons 10, 11, 12, 14, 15: These soils (and Pedons 8, 9, & 13) were sampled along a transect from the corner of the Solitario Canyon road and the dozer road to USGS Trenches CF2 & 3, along the CF2 & 3 road (Fig. 1). This transect was intended to determine the soil properties of the Q1a and Q2 deposits, and to test if Swadley and Hoover had consistently mapped these two deposits across this dissected fan piedmont. Swadley et al (1984) mapped most of the large fan-piedmont-remnant summits along this transect as Q1a deposits on their generalized 1:62,500 map, but they did cut out some inset-fan-remnant summits as Q2 deposits. On Swadley and Hoover's (1983) more detailed, larger-scale map of the CF2 & 3 trenches site, they cut out additional, small Q1ab, Q1c, and Q2bc areas from the broad Q1a areas.

In my assignments of Swadley and Hoover's surficial-deposit designations in Table 2, I have attempted to give them the benefit of the doubt where one would think they should have identified deposits as Q2 rather than Q1a because their map is small scale and necessarily generalized. In Table 4, my geomorphic surface and their surficial-deposit designations are repeated for ease of reading.

9
0
3
8
8
2
3
4
9

TABLE 4 -- AGE ASSIGNMENTS FOR PEDONS

Pedon No.	Geomorphic Surface	Rock Varnish Age YBP ¹⁵	Surficial Deposit ¹⁶
1	Little Cones	7,310	Q2
2	Little Cones	11,200	Q1
3	Little Cones	11,200	Q1
4	late Black Cone	28,300	Q2
5	late Black Cone	28,300	Q2
6	late Black Cone	33,400	Q2
7	early Black Cone	128,000	Q2
8	early Black Cone	137,000	QTa
9	early Black Cone	137,000	QTa
10	late Black Cone	29,700	Q2
11	late Black Cone	19,000	Q2
12	late Black Cone	n.d.	QTa
13	very late Crater Flat	n.d.	Q1
14	late Black Cone	n.d.	Q2bc
15	late Black Cone	31,800	Q2bc
16	Yucca	380,000	QTa
17	Yucca	360,000	QTa
18	Solitario	660,000	QTa

Pedons 10, 11, and 12, respectively, are on a highest fan-piedmont remnant, an obviously lower and younger inset-fan remnant, and another highest fan-piedmont remnant, all adjacent to each other along this north-to-south transect. Inasmuch as I could determine in the field, Pedons 10 and 12 are on what looked to be positions that Swadley and Hoover would have mapped as QTa deposits on this particular part of the dissected fan piedmont, even though Pedon 10 appears to be in a mapped Q2 area on the 1:62,500 map; Pedon 12 is mapped as QTa. Pedon 11 looked as if it should be on mapped Q2 and is. All soils have gravelly sandy loam B horizons, but Pedons 10 and 12 are Eaplic Durargids with weak argillic Bt horizons and duripans, whereas Pedon 11, in keeping with its younger relative-geomorphic and rock-varnish age, is only a Typic Camborthid with a cambic Bw horizon and no pan. According to its rock-varnish age, Pedon 11 is some 7,000 years older than Pedon 2, which also is a Typic Camborthid but is on the Little Cones surface. Except for the rock-varnish ages, I would put Pedon 11 together with Pedon 2 as Little Cones age. Pedons 10 and 12, compared with Pedons 8 and 9, demonstrated to me that the Black Cone surface (Q2) could not be separated from the Yucca surface (QTa)

¹⁵ Corrected radiocarbon age or cation ratio age of rock varnish (Dorn, 1988).

¹⁶ Surficial deposit as mapped by Swadley & Hoover (1983) or Swadley et al (1984).

¹⁷ Age assumed to be the same or somewhat younger than adjacent Pedon 8 because Pedon 8 and 9 are on remnants that are at the same level.

9 0 3 8 8
2 3 5 0

during mapping on this broadly-convex, deeply dissected fan piedmont without careful examination of the soils.

Undated Pedon 14, a Typic Haplargid somewhat farther south on the CF2 & 3 road transect, is similar to Pedons 10 and 12, but has so few cemented lenses in its Bk horizon that it cannot be said to have a duripan. It is on a true inset-fan-remnant summit that was mapped by Swadley and Hoover (1983) as Q2bc and is inset into what they called QTa deposits.

Pedon 15, a Typic Durargid next to the USGS CF3 trench, is on a mapped Q2bc deposit. It has a rock-varnish date of 31,800 YPB, but its profile, particularly its duripan, is more like those of the "early-Black Cone" Pedons 7, 8, and 9 than the late-Black Cone Pedons 10, 12, and 14.

All of the soils on this CF2 & 3 road transect have well developed Av horizons. They also have Holocene-age zones of accumulation of carbonate in the lower A horizon. Except for obviously inset-fan remnants, there are no consistent visual clues in the field for separating these late-Black Cone soils and surfaces from the early-Black Cone ones during mapping; the soils must be examined.

Early-Black-Cone Age Soils from Volcanic Alluvium:

If the Pedon 4, 6, 10, 11, and 14 rock-varnish, radiocarbon ages are correct (28,300 YPB, 33,400 YPB, 29,700 YPB, 19,000 YPB, 31,800 YPB, respectively), and the rock-varnish, cation-ratio ages of Pedon 7 and 8 are correct (128,000 YPB, 137,000 YPB, respectively), then one could argue for splitting the Black Cone surface into two geomorphic surfaces. However, I did not split it because I know of no place in the field where the younger and older surfaces are juxtaposed and show an inset or overlapped relation, therefore there is no evidence independent of the rock-varnish dates and comparative soil morphology to argue for splitting the Black Cone surface.

Pedon 7, 8, 9: Pedon 7 is a Typic Durargid (128,000 YPB, cation ratio age). It is along the main, diagonal road to northeastern Crater Flat, on the summit of an elongate, fan-piedmont-remnant that is prominently inset below the large Yucca-age fan-piedmont remnants in northern Crater Flat. Swadley and Hoover mapped the Pedon 7 remnant as a Q2 deposit and the higher Yucca-age remnants as a QTa deposit. The texture of the argillic horizon of Pedon 7 (very sticky, plastic very-extremely gravelly clay loam) suggests that it is older than the very gravelly sandy loam Bt horizons of the late-Black Cone Durargids. The duripan has only a single laminae on top, but strongly to weakly cemented lenses are closely enough fabricated below it that I called it a typic pan.

Pedon 8 is a Typic Durargid described in the southeast corner of the Solitario Canyon and CF2 & 3-Trenches road corners. It has a rock-varnish, cation-ratio date of 137,000 YPB. Pedon 9, was described directly to the south, across a wash on another "highest" fan-piedmont-remnant summit that appears to be at the same level and of the same age surface as that of Pedon 8. However, Pedon 9 is only a Haplic Durargid, because its duripan is not as continuously or strongly cemented as that of Pedon 8. Both soils were identified as in QTa deposits by Swadley and Hoover (1983), but the rock-varnish

1
5
3
2
8
8
8
9
0
9
0
9

date for Pedon 8 forces it into the next younger than Yucca surface, and the argillic horizon and pan development of Pedon 9 are not as great as those of Yucca-age soils.

The argillic horizon of Pedon 8 is distinctly reddish hued (a full 7.5YR), sticky, plastic, and a clay loam at least. It has been opalized, particularly in its platy lower subhorizon, and has the "crunchy" feeling, moist, of strongly opal-agglomerated, clayey Bt horizon material. This argillic horizon opalization is a prominent feature of Yucca-age Pedon 16, and is noted for QTa-age soils by Hoover et al (1981). But, the argillic horizon of Pedon 9, though also a clay loam and crunchy, is not opalized strongly enough to make it platy. Pedons 8 and 9 could be older than their rock-varnish dates suggest.

Yucca Surface and Soils

The Yucca surface can be readily distinguished from the Black Cone and Crater Flat surfaces (and by implication, the Little Cones surface) by aerial-photo patterns, by topographic separation, and by soil differences. On both color and black & white photos, transverse bands of darkly-varnished desert pavement on low, Av-horizon slump-steps contrast with light-colored biocoppice areas to give a distinctively banded photo pattern for the Yucca surface remnants. This contrasts with the photo pattern of the Black Cone surface fan-piedmont remnants--for both the Black Cone's younger and older remnants--where the dark patches of desert pavement are irregularly-shaped, or tend to be longitudinally-elongated and the light-colored biocoppices are semi-circular spots, or "dots." The Crater Flat, Holocene surface is raw sediment and hence distinctively light colored on the aerial photos, compared to either Black Cone or Yucca surface remnants.

The Yucca surface comprises three areas of fairly-extensive, relatively-high, deeply-dissected, flattish-topped (transverse to the slope), fan-piedmont remnants. Yucca-age Pedon 16 is on the area of Yucca remnants in north-eastern Crater Flat (color photo ELM 24 NV80BC 8-44-20, southeast 1/3). The extensive Black-Cone age, dissected fan-piedmont remnant that is just to the northwest of the Yucca fan-piedmont remnants has Pedon 7 on it and is prominently inset into and some 10-20 feet below the Yucca remnants. This inset relationship demonstrates the relative ages of the Black Cone and Yucca surfaces and soils. There are well-preserved remnants of two younger erosion surfaces that were cut into this Yucca-age fan piedmont near the heads of the deep gullies that dissect it. The desert pavement, Av, and upper Bt horizon of the remnants are similar to those of the Yucca surface, so the remnants probably reflect there being more than one level of Yucca-age remnants. The lowest remnants could be of Black-Cone age, but they were not traced-out.

Yucca-age Pedon 17 is on the southernmost of three remnantal Yucca areas immediately southeast of the mouth of Solitario canyon on the east side of Crater Flat (black & white photo GS-VFDT 10-6, northeast 1/3). Black-Cone age fan-piedmont remnants are inset into and below these Yucca remnants. The third group of presumed Yucca remnants is in the northwest corner of Crater Flat, just above the main drainageway (color photo ELM 24 NV80BC 8-43-20A). I got only one look at the edge of this third area, and could only note that the

2
5
3
2
8
8
3
0
9

soil apparently has an argillic horizon and a thick, strongly-indurated duripan.

Both Pedons 16 and 17 have strongly differentiated Av horizons that are very dilatant. Note that Av horizons are not significantly thicker than the Av horizons of the Black-Cone age soils, even though the ages of these pedons (380,000, 360,000 YBP) are several times older. Since the formation of the Av horizon is attributed largely to dust accumulation by most current workers in soil genesis, one would expect thicker Av horizons in the older soils on well-preserved surface remnants. There are two problems with applying this theory. First, the fine earth in the Ak and Bv or Bt horizons (in this area) also probably is largely of eolian origin, therefore measuring the thickness of the Av horizon alone must be a poor measure of dust accumulation. The Av horizon is a morphologically distinct layer of very-coarsely-prismatic ("polygons"), coarsely-vesicular, internally massive or platy, light colored, crusting soil material. Its morphology reflects currently on-going processes that will recreate the morphology if it is disturbed. It is the depth of effect of these processes, not dust accumulation, that determines the depth of the Av horizon once dust accumulation has exceeded the depth of effect of Av-forming processes.

Secondly, all of the surfaces older than the raw Crater Flat surface have abstracted drainages. That is, at least occasionally water sheets off the soil surface rapidly enough to have led to formation of shallow, dendritic, "on-fan" drainage systems. It is reasonable to conclude, as Taylor (1986) suggests, that there has been some sheet erosion of the Av, at least on the older surfaces.

The vertical pattern of leached Av horizon over calcareous Ak, over partly-carbonate-leached Bt horizon again demonstrates recent, relatively shallow, presumably Holocene-age carbonate accumulation in soils that were leached of carbonates in the Pleistocene. High pH values in the Ak again show that soluble sodium salt accumulation from dust fall is occurring.

Both Pedon 16 and 17 have thick (60 and 40 cm), basically clay-textured argillic horizons. In Pedon 16, opal "agglomeration" has weakly cemented the Bt horizon; it is very brittle-crunchy throughout and prominently platy and firm and "orangish-looking" in its lower part--all well known effects of silica accumulation. The apparent texture is a loam in the upper part of the Bt and loamy sand in the lower part, but the "sand" is merely weakly silica-cemented aggregates of clay. Pedon 17 has not had its argillic horizon opalized, and feels like a clay without as long and vigorous a working as Pedon 16's Bt requires to begin feeling clayey. In my experience, opalization of argillic horizons is some sort of evidence of considerable age, but it is so variable within and between polypedons that it is not a consistently-applicable criterion for identifying a particular age of soil.

Both Pedon 16 and 17 have a foot or two of strongly-cemented duripan; the former has several prominently opaline surficial laminae, whereas the latter apparently has a single surficial laminae. I do not know if this apparent difference in degree of opalization of Bt and Bqka horizons is a reflection of age or environmental differences between the two pedons. Decent exposures of the pans were not possible in my hand-dug pits, and gully-wall outcrops must be distrusted because of "case-hardening." Regardless, the

duripans on well-preserved Yucca surface remnants are as thick and as strongly cemented, or more so than on Black Cone remnants.

Solitario Surface and Soils

The Solitario surface comprises a single ballena, or fully-rounded, ridge-line remnant, just to the southwest of the mouth of Solitario Canyon. There are, however, spur-remnants up Solitario Canyon and in valleys in Yucca Mountain above the northeast side of Crater Flat that suggest the Solitario surface was once much more extensive. The ballena-form remnant near Solitario Canyon, where Pedon 18 was described, is 5+ feet higher than the adjacent, well preserved Yucca-age fan remnant where Pedon 17 was described. The Yucca-age fan piedmont clearly is inset into and below the pre-existing Solitario-age fan-piedmont remnant.

No actual, Solitario-age soil was found. Rather, there is a complex of more extensive Typic Durorthids and small spots of Typic Durargids on the ballena that results from stripping of the original A and Bt horizons, mixing with part of the duripan, and later dust accumulation. Pedon 18 is a Typic Durargid that represents the truncated remnants of the original soil. It was described on a ballena crest that marks the position of the former Solitario surface. The ballena is littered with chips of the duripan lamina, showing that animals have been vigorously scraping at the duripan. The 19-cm, Av-Ak-Btk solum of Pedon 18 was found in a slight depression of the duripan. In a second pedon location, there is a Typic Durorthid that has only a 0-5 cm Av and 5-19 cm Ak over the duripan. In a third pedon location, the Durorthid is only a 0-7 cm Av over the duripan. In one of the larger, raised biocoppices on the ballena crest, under a pale wolfberry shrub, the Durorthid comprises 40 cm of rodent-mixed earthy material over the pan.

The duripan has 1-3 cm thick, opalized lamina on top of it. USGS fault-trench CF1 is dug into the side of the ballena and shows that the duripan extends on over the sides of the ballena, but that the strongly-cemented part is thickest (a couple of feet) at the ballena crest and thinner on the younger sideslopes.

On color aerial photos, this ballena-form remnant of the Solitario surface is notably lighter colored, and tan colored, apparently due to the common chips of duripan lamina scattered across its surface. A similar, duripan-chip-strewn, but lower ballena is just northeast of USGS fault-trenches CF2 & 3, and may be another Solitario remnant, or could be a stripped, rounded Yucca remnant. The hillock on the upthrown, eastern side of USGS fault-trenches CF2 & 3 could have either a Solitario or Yucca-age duripan in it.

9
0
3
3
8
2
3
5
4

BEST AVAILABLE COPY

CONCLUSIONS

- (1) There are five major geomorphic surfaces, i.e., groups of land-surface remnants, in the Crater Flat basin: the Crater Flat, Little Cones, Black Cone, Yucca, and Solitario surfaces. Each has a distinctive aerial photo pattern. There is, somewhere in Crater Flat, a situation where remnants of each surface are topographically separated from remnants of surfaces higher (older) and lower (younger) than themselves, thus demonstrating inset relations and relative ages.
- (2) The soils of each surface have distinctive differences from those of the other major surfaces:
- (2A) The soils of the Crater Flat-age surfaces are Torriorthents without genetic horizons.
- (2B) In pavettes, the soils of the Little Cones-age surfaces have slightly-dilatent Av horizons, that are more sandy than those of older surfaces, and have cambic horizons and Stage I Bk horizons.
- (2C) In pavettes, the soils of the Black Cone-age surfaces all have prominent Av horizons that are dilatent. Those from limestone-containing parent material have cambic horizons and Stage I-III calcic horizons, whereas those from solely volcanic alluvium have sandy loam or loam textured argillic horizons and haplic (discontinuously or weakly cemented) to barely typic duripans. Some of the youngest Black-Cone age remnants have soils with cambic horizons, rather than argillic horizons, and no duripan, and some with argillic horizons lack the weak duripan.
- (2D) In pavettes, the soils of the Yucca-age surfaces all have prominent Av horizons that are dilatent and have soliflucted into broad, low, slump-steps that show a transversely-banded pattern on aerial photos. The soils have relatively-thick, clay-textured, or opalized-clay argillic horizons. Their duripans are relatively more strongly cemented than those of the Black Cone surface. Black Cone-age argillic horizons are not as thick or as clayey as those of Yucca-age soils.
- (2E) The Typic Durorthids of the Solitario-age surface remnants, which are ballenas, have a distinctive litter of duripan-lamina chips across their surface and are very shallow to a strongly-cemented duripan that has thick opal lamina on its top. The ballena surface has been stripped of the original A and Bt horizons, so there is only a shallow, dilatent Av, or Av and Ak horizon except where a thin, very gravelly clay loam Bt horizon has been preserved in a shallow depression in the duripan. Where the Bt horizon is preserved, the spot is a Typic Durargid.

9 0 0 3 8 2 3 5 5

- (3) Av horizon formation depends on dust-fall, dust-infiltration, and plugging of macropores that then causes surficial dust accumulation. There has been enough dust fall during, or during and since early Holocene to form the minimal, slightly dilatant Av horizon of the Little Cones soils, but no Av horizon in the mid-Holocene to Modern Crater-Flat age Torriorthents. Dust-fall must have been significant in the Pleistocene because all of the soils on the Black Cone, Yucca, and Solitario surfaces have prominent, very dilatant Av horizons; there probably has been erosion of Pleistocene Av horizons, since there are well-abstracted, on-fan drainage systems on the old fan remnants.
- (4) There has been shallow, limited, Holocene to Modern carbonate and sodium-salt accumulation in the A horizons of all soils. The A and B horizons of the Pleistocene-age soils were once leached of carbonate, and have not been completely re-carbonated.
- (5) Swadley and Hoover's (1983), and Swadley et al's (1984) mapping of "surficial deposits" in Crater Flat failed to distinguish three clearly separate geomorphic surfaces and related soils in their QTA unit (my Black Cone, Yucca, and Solitario surfaces), and in their Q2 unit included two separable geomorphic surfaces, the Little Cones and Black Cone surface.
- (6) Hoover and Swadley's "surficial deposits" concept and mapping are fatally flawed, and should be abandoned. Geomorphic surfaces, defined and mapped in terms of soils and stratigraphic relations, should be used as the geomorphic dating tool for neotectonic studies.

905382356

LITERATURE CITED

- Dorn, R.I. 1988. A Critical Evaluation of Cation-Ratio Dating of Rock Varnish, and an Evaluation of Its Application to the Yucca Mountain Repository by the Department of Energy and Its Subcontractors. Final Report for the Nevada Bureau of Mines and Geology for the Period January 1987-June 1988.
- Eckert Jr., R.E., M.K. Wood, W.H. Blackburn, F.F. Peterson, J.L. Stephens, M.S. Meurisse. 1978. Effects of surface soil morphology on improvement and management of some arid and semi-arid rangelands. Proc. 1st Int. Rangeland Congress, Denver, Color., Am. Soc. Range Manage., pp. 299-302.
- Gile, L.H., F.F. Peterson, and R.B. Grossman. 1966. Morphological and genetic sequences of carbonate accumulation in desert soils. Soil Sci. 101:347-360.
- Gile, L.H., and R.B. Grossman. 1979. The Desert Project Monograph. U.S. Dept. Agr., Soil Conserv. Service., Washington, D.C. 984 pp.
- Hillel, D. 1960. Crust formation in loessial soils. Trans. 7th Int. Congress Soil Sci. 1: 330-339.
- Hoover, D.L., W.C. Swadley, and A.J. Gordon. 1981. Correlation characteristics of surficial deposits with a description of surficial stratigraphy in the Nevada Test Site region. U.S. Geol. Surv. Open-File Rept. 81-512. Denver, Colorado. 27 pp.
- Miller, D.E. 1971. Formation of vesicular structure in soil. Soil Sci. Soc. Am. J. 35:635-637.
- Nettleton, W.D., and F.F. Peterson. 1983. Aridisols. In: Wilding, L.P., N.E. Smack, and G.F. Hall (Eds.). Pedogenesis and Soil Taxonomy. Vol. II: The Soil Orders. Elsevier, Amsterdam. pp. 165-216.
- Peterson, F.F. 1977. Dust infiltration as a soil forming process in deserts. Agron. Abstr., Meetings, Am. Soc. Agron., Los Angeles, Calif., p. 172.
- Peterson, F.F. 1981. Landforms of the Basin & Range Province Defined for Soil Survey. Nev. Agr. Exp. Sta. Tech. Bul. 28., Univ. Nevada-Reno.
- Swadley, W.C., and D.L. Hoover. 1983. Geology of faults exposed in trenches in Crater Flat, Nye County, Nevada. U.S. Geol. Surv. Open-File Report 83-608. Denver, Colorado.
- Swadley, W.C., D.L. Hoover, and J.N. Rosholt. 1984. Preliminary report on late Cenozoic faulting and stratigraphy in the vicinity of Yucca Mountain, Nye County, Nevada. U.S. Geol. Surv. Open-File Report 84-788.
- Taylor, E.M. 1986. Impact of time and climate on Quaternary soils in the Yucca Mountain area of the Nevada Test Site. M.S. Thesis. University of Colorado, Boulder, Colorado.

908882357

APPENDIX I -- SCIENTIFIC NAMES OF COMMON PLANTS IN THE
CRATER FLAT, NEVADA, AREA

Common Name	Scientific Name	Acronyms
Blackbrush	<i>Coleogyne ramosissima</i>	CORA
Creosotebush	<i>Larrea divaricata</i>	LAD12
Joshua-trees	<i>Yucca brevifolia</i>	YUBR
Needlegrass	<i>Stipa</i> spp.	STIPA
Nevada sormon tea	<i>Ephedra nevadensis</i>	EPNE
Pale wolfberry	<i>Lycium pallidum</i>	LTPA
Range ratany	<i>Krameria parvifolia</i>	KRPA
Shadscale	<i>Atriplex confertifolia</i>	ATCO
Spineflower	<i>Chorizanthe</i> spp.	CHOR12
Spiny manodora	<i>Manodora spinescens</i>	MESP2
White bursage	<i>Franseria dumosa</i>	FSDU

2 3 5 8

9 0 3 8 8

¹⁸ Alternative name: *Ambrosia dumosa*.

APPENDIX II -- FROM DESCRIPTIONS

Pages 1 to 18

2 3 5 9

8 0 3 3 8

100-100000-100000

PEDON No. 14 (CFP31) -- TABULAR DESCRIPTION

Taxonomic 1-D: loamy-skeletal, mixed, thermic Typic Haplargid. Est. Min. Age: Because an inset-lan remnant similar to Pedon 11⁶, hence age: 17,200 +/- 370 (uncorrected radiocarbon) 19,000 YBP (+10% correction). Geomorphic Surface: late Black Cone Pedon 1, Bt 1-FFP-1-CFP31-1 to 5. Date: 8/21/87 By: F.F. Peterson Location: Crater Flat, Nevada, 1.27 mi. SE from intersection of Solitaria Cay. and Trench CF243 roads, just S and next older surface from Pedon 13. Physiographic Position: True inset-lan-remnant summit. Parent Material: Tolian dust and volcanic alluvium. Native Vegetation: White bursage, Nevada mormon tea, creosote bush, pale wolfberry, range rattle. Slope: 4% Aspect: 235° Elevation: 3,300 ft. 1,006 m Latitude: 36.70° N Longitude: 116.519° W Microrelief Position: PAVETTE Surficial Gravel: 80 %-area Surficial Cobbles: 1 %-area Surficial Stones: 0 %-area Total Surficial Rock Fragments: 81 %-area Other Surficial features: Many pavement pebbles darkly varnished.

No.	Horizon	Depth cm	Color		Texture	Estimated			Estimated			Argillite
			Dry	Moist		Gravel	Cobble	Stone	Sand	Silt	Clay	
					% vol.			% vol.				
1 ^a	Av	0-6	10YR 7/2	10Y 4/2	L	25	0	0	43	45	12	none
2	Ah	6-19	10YR 6.5/2	10YR 5/3	VGSL	40	0	0	63	25	10	none
3	Btk	19-33	10YR 6.5/3	10YR 4/3	L	25	0	0	45	35	20	IMPC
4	2Bt	33-52	10YR 6/4	10YR 4/4	ECCL	65	0	0	40	30	30	none
5	2Bk	52-99	10YR 6/3	10YR 5/3	EC/S	65	15	0	87	10	3	none

No.	Structure	Consistence			Consentation	CaCO ₃ Effervescence		pH	Pores	Roots	Lower Boundary
		Dry	Moist	Moist		& Morphology					
1	3COPR	SH	VFR	SO/PS	none	EO & E	8.4	3F-MV	none	AS	
2	1FPL & 1VFSBK	SH	FR	SO/PO	none	ES-SPB	8.8	n.d.	vivf	AV	
3	1VFSBK	SH	FR	SS/PS	none	E	8.8	n.d.	1Vf-f	CM	
4	2VFSBK	SH	FR	S/P	none	EO & E	8.2	n.d.	vivf	CM	
5	SO	LO	LO	SO/PO	none	EO & ES-SPB	8.4	n.d.	none	N	

COMMENTS: ^a A few dark grey bands in Av horizon; some pebbles with pustulose bottom carbonate coatings. ^b The 2Bk horizon contains a few thin carbonate-cemented lenses.

2 3 6 0

8 3 8 0 6

BEST AVAILABLE COPY

9 0 3 9 8

2 3 6 1



"BEST AVAILABLE COPY"

PEDON No. 15 (CFP36) — TABULAR DESCRIPTION

Taxonomic I.D.: loamy-skeletal, mixed, thermic Typic Durargid. Est. Min. Age: 28,920 +/- 400 YBP (uncorrected radiocarbon) 31,800 YBP (+10% correction). Geographic Surface: late Black Cone. Pedon I.D.: 1-FFP-1-CFP36-1 to 6. Date: 8/21/87 By: F.F. Peterson
 Location: Crater Flat, Nevada, 1.85 mi. SE from intersection of Solitario Cwy. and Trench CF283 roads and 0.15 mi. NE of CF283 road; 30 ft. NE of E end of Trench CF3, which is across the Windy Wash fault. Physiographic Position: Remnant surface of beheaded Black Cone ("Q2") inset fan. Parent Material: Eolian dust and volcanic alluvium. Native Vegetation: White bursage, creosote bush, shadescale, Nevada wormwood, pale wolfberry, range ratony. Slope: 3% Aspect: 270° Elevation: 3,300 ft. 1,006 m Latitude: 36.782° N Longitude: 116.510° W Microrelief Position: PAVETIE Surficial Gravel: 80 %-area Surficial Cobbles: 5 %-area Surficial Stones: 1 %-area Total Surficial Rock fragments: 86 %-area Other Surficial features: Many pavement pebbles, cobbles, stones darkly varnished.

No.	Horizon	Depth cm	Color		Texture	Estimated			Estimated			Argillines
			Dry	Moist		Gravel	Cobble	Stone	Sand	Silt	Clay	
					%			%				
1	Av	0-7	10YR 7/2	10YR 4/3	GL	25	0	0	42	45	13	none
2	A	7-15	10YR 7/2	10YR 4/3	L	10	0	0	40	40	20	none
3	ABk	15-21	10YR 6/3	10YR 4/4	VGL	50	0	0	39	38	23	none
4	Bt	21-31	7.5YR 6/3	7.5YR 4/4	EGL	65	0	0	62	20	18	IMPEC
5	Bk	31-40	7.5YR 6.5/4	7.5YR 5/4	EGSL	75	0	0	72	20	8	none
6	Bqkm	40-82	10YR 7/1 & 10YR 7/2	10YR 6/3 & 10YR 5/3	n.s.	75	5	0	n.s.	n.s.	n.s.	none

No.	Structure	Consistence			Consolation	CaCO ₃ Effervescence		Poros	Roots	Lower Boundary
		Dry	Moist	Wet		Morphology	pH			
1	3COPR	SH	FR	SO/PS	none	E	8.6	3F-MV	none	AS
2	2COPR & IMPL	SH	FR	SS/PS	none	E	8.6	n.d.	v1VF	AS
3	1FSBK	SH	FR	SS/PS	none	EV-SPB	9.8	n.d.	1VF	AM
4	1FSBK	SH	FR	SS/PS	none	EV	8.6	n.d.	2VF	CM
5	SO	SO	VFR	SO/PO	none	EV-SPB	8.2	n.d.	1VF	vAM
6	M	VH	VFI	brittle	CS	EV	n.d.	n.d.	none	M

COMMENTS: ^aThe Av is dilutant, has pustulose pebble-bottom carbonate coatings. ^bThe A horizon is dilutant. ^cThe ABk horizon is dilutant. ^dThe Bk horizon has prominent carbonate pebble-bottom coatings. ^ePan comprised of 15-20 cm thick lenses with thin laminae on tops of lenses; similar to Pedon 7; this pan could include older cemented materials not removed during formation of the Black Cone inset fan at this site.

2 3 6 2

9 0 8 8 8

BEST AVAILABLE COPY

PEDON No. 16 (CFP38) — TABULAR DESCRIPTION

Taxonomic I.D.: "lino-lacey", mixed, thermic Typic Durargid. Est. Min. Age: 300,000 YPB (cation ratio). Geomorphic Surface: Yucca. Pedon I.D.: 1-FFP-1-CFP38-1 to 5. Date: 8/18/87 By: F.F. Peterson Location: Crater Flat, Nevada, 4.2 mi. NNE of Black Cone. Physiographic Position: Upper-fan-plateau-remnant summit; moderately-wide remnant with wide, low, soil/luccion steps. Parent Material: Eolian dust and volcanic alluvium. Native Vegetation: Spiny monardra, blackbrush, Nevada nornon tea, creosote bush, white bursage, pale wolfberry, Joshua-tree, Stipa spp. Slope: 5% Aspect: 210° Elevation: 3,885 ft. 1,184 m Latitude: 36.873° N Longitude: 116.542° W Microrelief Position: PAYETTE Surficial Gravel: 80 %-area Surficial Cobbles: 3 %-area Surficial Stones: <1 %-area Total Surficial Rock Fragments: 83 %-area Other Surficial Features: Cobbles and some pebbles darkly-vernished, many pebbles not so; stones weathering-spalled where not darkly vernished; no more prominent rock vernish than on early Black Cone surface; black banding on photo is elongate pavettes above low, vegetated scarps of soil/luccion steps.

No.	Horizon	Depth cm	Color		Texture	Estimated			Estimated			Argillans
			Dry	Moist		Gravel	Cobble	Stone	Sand	Silt	Clay	
						% vol.			% wt.			
1	Av	0-7	10YR 6.5/1	10YR 4.5/2	GL	20	0	0	50	35	15	none
2	Ah	7-17	10YR 6/2	10YR 4.5/2	GL	20	0	0	42	40	18	none
3	Bt	17-28	7.5YR 6/4	7.5YR 4/6	FG=LS	20	0	0	n.d.	n.d.	n.d.	4KPF, BR, CO
4	Btqhm	28-72	7.5YR 6/4	7.5YR 4/4	G=LS	15	0	0	n.d.	n.d.	n.d.	3KPF
5	Bqhm	72-77+	10YR 8/1 & 10YR 7/2	10YR 7/3 & 10YR 7/3	n.d.	30	0	0	n.d.	n.d.	n.d.	n.d.

No.	Structure	Consistence			Cementation	CaCO ₃ Effervescence		Pores	Roots	Lower Boundary
		Dry	Moist	Wet		Morphology	pH			
1	SCOPR	H-SH	YR	S/P	none	EO & E	8.6	3F-MV	vivf	AW
2	IMPL & 2YFSBK	SH	YR	SS/PS	none	ES-SPB	9.0	n.d.	ivf, vim	AW
3	IMPL & 3YFABK	H	F1	SS/P	YCW pods	EO	8.4	n.d.	2YF, IM	VAM
4	IMPL	H	F1	SO/PO	CW	EO & EV	8.4	n.d.	none	VAM
5	H	VH	EF1	n.d.	CS	EV	n.d.	n.d.	none	N

COMMENTS: The Av is very dilutant. The Ah is dilutant and banded with (10YR 6/2D 4/2H) illuvial "humus" and browner (10YR 7/3D 4/4H) material, possibly illuvial clay. The Bt is opalized and "crunchy" but hasn't macroscopic opal, so not designated Btq, i.e., individual pods very weakly cemented; actual texture it could be dispersed should be a CLAY. The Btqhm is not part of the duripan proper, though it is as a mass (i.e., the platy pods) brittle, "crunchy", and weakly cemented; actual texture probably a CLAY; calcite accumulation is on the bottoms of platy pods only; contains some gypsum crystals. Based on gully-wall exposures to the N, the duripan proper, i.e., the Bqhm horizon has an about 68 cm thickness (72-140 cm depths) of strongly-cemented material; it has opaline surficial laminae and is densely-impregnated with opal and some calcite cement.

2363
88886

BEST AVAILABLE COPY

PEDON No. 17 (CFP39) — TABULAR DESCRIPTION

Taxonomic I.D.: clayey-skeletal, montmorillonitic (T), thermic Typic Durargid. Est. Min. Age: 360,000 YBP (cation ratio) Geographic Surface: Yucca Pedon I.D.: 1-FFP-1-CFP39-1 to 5. Date: 8/19/87 By: F.F. Peterson Location: Crater Flat, Nevada, about 0.7 mi. S of mouth of Solitario Cay, between road to GM10 & 11 and Solitario Wash. Physiographic Position: Moderately-wide, upper-terrace-piedmont-remnant summit. Parent Material: Eolian dust and volcanic alluvium. Native Vegetation: White bursage, Nevada Mormon tea, pale wolfberry, creosote bush, shadscale, range ratony, needlegrass. Slope: 5% Aspect: 180° Elevation: 3,675 ft. 1,120 m Latitude: 36.809° N Longitude: 116.492° W Microrelief Position: PAVETTE Surficial Gravel: 80 %-area Surficial Cobbles: 3 %-area Surficial Stones: 0 %-area Total Surficial Rock Fragments: 83 %-area Other Surficial Features: Many pebbles and most cobbles darkly varnished.

No.	Horizon	Depth cm	Color		Texture	— Estimated —			— Estimated —			Argillaceous
			Dry	Moist		Gravel	Cobble	Stone	Sand	Silt	Clay	
						— % vol. —			— % wt. —			
1 ^a	Av	0-8	10YR 7/2	10YR 4/2	L	5	0	0	53	35	18	none
2	Ah	8-17	10YR 6.5/3	10YR 5/3	L	10	0	0	50	35	15	none
3 ^b	Bt	17-38	7.5YR 5/4	7.5YR 4/6	VCC	30	10	0	28	30	42	4KPF
4 ^b	Btk	38-57	10YR 6/6	10YR 4.5/6	VCC	45	2	0	22	38	40	4KPF&CO
5 ^c	Bqhm	57-61 ^d	10YR 8/1 & 10YR 7/4	10YR 7/4 & 9YR 5/4.5	n.s.	50	n.d.	0	n.d.	n.d.	n.d.	n.d.

No.	Structure	— Consistence —			Cementation	CaCO ₃ Effervescence		pH	Pores	Roots	Lower Boundary
		Dry	Moist	Moil		& Morphology					
1	3COPR & 1MPL	SH	VFR	SS/P	none	EO & E	8.8	3F-MV	none	AM	
2	1MPL & 2VFSBK	SH	VFR	SS/PS	none	ES-SPB	9.0	n.d.	1VF-F	CM	
3	3VF-FABK	SH	FR	VS/VP	none	E	8.8	n.d.	1VVF	CM	
4	2VFSBK	II	FI	VS/VP	none	EO & E-SPB	8.6	n.d.	none	VAM	
5	M	EH	EFI	brittle	CS	ES	n.c.	n.d.	none	M	

COMMENTS: ^aThe Av with low-contrast, dark-grey, probable illuvial-humus banding. ^bThe Bt and Btk horizons do not have the "crunchy", very weak opalization-cementation that Pedon 16 has. ^cExposures of the Bqhm pan in adjacent gullies suggest a 2-3 ft. thickness of strongly cemented material; only a thin surficial-lamina is present on this pan. ^dRock fragment content of pan estimated from adjacent gully exposures.

2 3 6 4

9 0 8 8 8

"BEST AVAILABLE COPY"

PEDON No. 18 (CFP40) -- TABULAR DESCRIPTION

Taxonomic I.D.: loamy-skeletal, mixed, thermic Typic Durargid / Typic Durorthid (complex) Est. Min. Age: 660,000 YBP (cation ratio)
 Geographic Surface: Solitario. Pedon I.D.: 1-FFP-1-CFP40-1 to 4 Date: 8/19/87 By: F.F. Peterson Location: Crater Flat, Nevada, about 0.7 mi. S of mouth of Solitario Canyon on road to gull 10 & 11, and on W side of Solitario Wash from Pedon 17. Physiographic Position: Broad crest of a bajana. Parent Material: Eolian dust, volcanic alluvium, and fractured duripan fragments. Native Vegetation: White bursage, Nevada Mormon tea, shadscale, creosote bush, pale wolfberry, spiny monardra. Slope: 5% Aspect: 180° Elevation: 3680 ft. 1,122 m Latitude: 36.809° N Longitude: 115.495° W Microrelief Position: PAYETTE Surficial Gravel: 85 %-area Surficial Cobbles: 2 %-area Surficial Stones: 0 %-area Total Surficial Rock Fragments: 85 %-area Other Surficial Features: Many volcanic cobbles and pebbles are darkly varnished; some 10-45% of the pavement is pale brown, indurated, gravel-size chips of the duripan surficial laminae; variation in number of pan chips probably reflects previous rodent activity.

No.	Horizon	Depth cm	Color		Texture	Estimated			Estimated			Argillous
			Dry	Moist		Gravel	Cobble	Stone	Sand	Silt	Clay	
						% vol.			% wt.			
4 3 2 1	Av	0-5	10YR 7/2	10YR 4.5/3	VFSL	10	0	0	67	25	8	none
	Ah	5-9	10YR 7/3	10YR 5/3	L	8	0	0	42	35	23	none
	Btk	9-19	7.5YR 6.5/4	7.5YR 5/4	VOCL	50	0	0	30	35	35	?
	Bqhm	19-211	10YR 8/2-3	10YR 7/3	n.a.	50 ^a	0	0	n.a.	n.a.	n.a.	n.d.

No.	Structure	Consistence			Consentation	CaCO ₃ Effervescence		pH	Pores	Roots	Lower Boundary
		Dry	Moist	Met		Morphology					
1	3COPR	SH	VFR	SO/PS	none	E & E0	8.8	SF-MV	none	AS	
2	3COPR	SH	FR	S/P	none	EV	8.8	n.d.	none	AM-B	
3	1VFSBK	SH	FR	S/P	none	E0 & EV	8.8	n.d.	1VF-F	VAN	
4	M	EH	EFI	brittle	CI	EV	n.d.	n.d.	3VF-F	M	

COMMENTS: ^aThe Av is dilutant; surface littered with pan-laminae chips. ^bThe Ah is dilutant and has a few thin, pustulose carbonate laminae, some hollow carbonate nodules and some carbonate pebble-bottom coatings. ^cThe Btk is a DISCONTINUOUS, REMNANTAL HORIZON PRESENT ONLY IN DEPRESSIONS IN THE DURIPAN where it has not been stripped off; MOST OF SOIL LACKS THIS REMNANTAL ARGILLIC HORIZON; gravel in the Btk is about half pan-laminae-fragments and half carbonate-coated pebbles. ^dThe duripan has an about 1 cm thick, continuous, indurated laminae cap that breaks off on top of 1-2 cm thick platy fragments. ^eRock fragment content estimated. ^fRoots are matted between the upper plates of the duripan.

2365
98806

"BEST AVAILABLE COPY"

V.C.5. Other Concerns and Other Tests

Another test of the method is to divide the varnish into layers and assess the AMS ages of the different layers. On Death Valley Canyon Fan, Death Valley, CA, the basal layer on a fan unit has an age of 4350 ± 88 (AA-2017). The outer composite layer of the varnish gave a net, cumulative age of 2308 ± 71 (AA-2135). This trend of older/lower layer to younger/upper layer is what would be expected if the method is correct.

Operator error could be a problem, if an individual attempted to sample and process varnishes without being properly trained. The effect of operator error (by trained persons) was tested at a few sites. Table 2 present 2 samples of the 8001 ft cone of Hualalai by different operators and different laboratories. The results are similar. In addition, tests at Meteor Crater, AZ, on varnishes collected from the same boulder yielded statistically identical results (R.I. Dorn, D.L. Tanner, D. Roddy, in preparation). The effect of operator error by a relatively untrained person is still being evaluated.

Varnish radiocarbon dating shows potential for assessing the ages of buried varnishes. For example, the varnish on Cima flow A-1 (Table 8) at ca. $14,600 \pm 800$ can be compared with a varnished pavement that was buried by the flow. The radiocarbon age on the top layer of the varnish on a desert pavement buried by the lava flow has an AMS radiocarbon date of $19,520 \pm 240$ (Beta 17536).

V.D. Preliminary Varnish Radiocarbon Date on Lathrop Well Cinder Cone

Rock varnishes were collected from the tops of 19 bombs on the rim of the crater at the cinder cone near Lathrop Wells, NV. The depth of the varnish is illustrated in Figures 14A and 14B. The samples were processed for AMS radiocarbon dating, as described in the method section. Figure 14C illustrates the basal layer of varnish before removal, and Figure 14D after removal. No observable organic matter was detected in the control sample of the underlying rock. About 15 mg of organic matter was extracted and sent to Beta Analytic for processing and analysis at Zurich (Suter et al., 1984). The analytical date is $19,940 \pm 270$ (Beta 17866).

This AMS radiocarbon date should be viewed only as a tentative age-estimate. There may be special concerns to dating cinder cones. For example, there is a possibility that

9
0
3
8
8
2
3
6
6

PEDON No. 2 (C/P26) -- TABULAR DESCRIPTION

Taxonomic I.D.: sandy-skeletal, mixed, lithalic Typic Camborthid. Est. Min. Age: 10160 +/- 270 YBP (uncorrected radiocarbon) 11,200 YBP (110% correction). Geomorphic Surface: Little Cones. Pedon I.D.: 1-FFP-IC/P26-1 to 6. Date: 6/04/87 By: F. Peterson
 Location: Crater Flat, Nevada, 0.2 mi. ENE of northernmost cone of Little Cones, 1.05 mi. E of N-S road to Diamond Queen Mine on trail. Physiographic Position: Summit of very broad basin-floor remnant that has a few, shallow, on-flat flutes. Parent Material: Eolian dust and mixed Tertiary and volcanic alluvium. Native Vegetation: Creosote bush, white bursage, shadscale, pale willowberry (all in coppices off of pavement), spineflower (on pavement). Slope: 2% Aspect: 180° Elevation: 3000 ft. 914 m Latitude: 36.774° N Longitude: 116.399° W Microrelief Position: 946 m, BARREN PAVETTE Surficial Gravel: 80 % area Surficial Cobbles: 0 % area Surficial Stones: 0 % area Total Surficial Rock Fragments: 80 % area Other Surficial Features: 1-3 cm pebbles form pavement; only lightly varnished; 2-3 mm of fine sand mulch between pebbles; one layer of 2-3 cm pebbles embedded in underlying Av horizon.

No.	Horizon	Depth cm	Color		Texture	Estimated			Estimated			Argillans
			Dry	Moist		Gravel	Cobble	Stone	Sand	Silt	Clay	
						% vol.			% wt.			
1	Av	0-5	10YR 7/3	10YR 4/3	GVFSL	20	0	0	58	35	7	none
2	Ak	5-19	10YR 7/3	10YR 5/3	GSL	30	0	0	68	25	7	none
3 ^b	Buk	19-29	10YR 7/3	10YR 5/3	GSL	30	0	0	74	20	6	none
4 ^b	Bk	29-54	10YR 7/3	10YR 5/3	YGSL	50	0	0	76	19	5	none
5 ^b	2Bk1	54-78	10YR 7/3	10YR 5/3	EGSL	65	0	0	80	15	5	none
6	2Bk2	78-100	2.5Y 7/1	2.5Y 5/2	VGCDS	50	5	0	95	3	2	none

No.	Structure	Consistence			Cementation	CaCO ₃ Effervescence		pH	Pores	Roots	Lower Boundary
		Dry	Moist	Wet		Morphology					
1	2VCOPR	SH	VFR	SO/PS	none	ES	8.6	3VF-MV	none	AS	
2	1FSBK	VSH	VFR	SO/PO	none	ES-CISFASPB	8.8	n.d.	v1VF	CS	
3	M	SO	VFR	SO/PO	none	EV-CISFASPB	9.0	n.d.	1VF	GS	
4	M	SO	VFR	SO/PO	none	EV-CSPB	9.0	n.d.	1VFv1F	CW	
5	M	SO	VFR	SO/PO	none	EV-CSPB	8.4	n.d.	1VFv1F	CW	
6	SG	LO	LO	SO/PO	none	ES-CSPB	8.2	n.d.	none	M	

COMMENTS: Technically, this Buk is the cobbic horizon, but both the Ak and Buk horizons could be considered the cobbic horizon with in-transit, pedogenic carbonates; carbonate in the Ak is considered a more recent accumulation than that in the Bk horizons, hence evidence of polygenesis in the Holocene. Pebble bottoms with 0.5 mm, some 1-2 mm thick lime pendants; sand grains and very fine gravel in 2Bk2 barely carbonate-coated; since both 2Bk horizons have less than 5% (vol.) pedogenic carbonate, do not comprise a calcic horizon.

2368

88806
 "BEST AVAILABLE COPY"

PEDON No. 1 (CFP2) -- TABULAR DESCRIPTION

Taxonomic I.D.: sandy-skeletal, mixed (calcareous), thermic "Camborthidic" Torriorthent Est. Min. Age: 6845 +/- 245 YBP (uncorrected radiocarbon) 7,310 YBP (10% correction). Geomorphic Surface: Little Cones. Pedon I.D.: 1-FFP-1-CFP2-1 to 4 Date: 8/17/87 By: F.F. Peterson Location: Amargosa Valley, Nevada; 1.35 mi. W of US Hwy 95 on road to Ashton (site). Physiographic Position: Broad, low, basin-floor-remnant summit; broad Miocene (?) remnant is widely-dissected by 1-4 ft. deep, very gently-sloped, on-flat fluvial, is abruptly cut by modern Amargosa River's anastomosing distributary-floodplain. Parent Material: Eolian dust & mixed volcanic, limestone, metamorphic alluvium. Native Vegetation: Creosote bush (70-95%), white bursage (isolated patches). Slope: 1% Aspect: 180° Elevation: 2685 ft. 818 m Latitude: 36.727° N Longitude: 116.662° W Microrrelief Position: Broad pedette, adjacent creosote-bush coppice dunes only 4-6" high. Surficial Gravel: 75 % area Surficial Cobbles: 0 % area Surficial Stones: 0 % area Total Surficial Rock Fragments: 75 % area Other Surficial features: Pavement is fine gravel, only slightly varnished, has thin underlying Av horizon.

No.	Horizon	Depth cm	Color		Texture	Estimated			Estimated			Argillines
			Dry	Moist		Gravel % vol.	Cobbles	Stones	Sand % wt.	Silt	Clay	
1 ^a	Av	0-8	10YR 6.5/2	10YR 4.5/2	GSL	25	0	0	64	28	8	none
2 ^{abc}	Bvk	8-22	10YR 6.5/2	10YR 4.5/2	GSL	33	0	0	74	18	8	none
3	Bh	22-42	10YR 6.5/2	10YR 4/3	YGSL	50	0	0	78	12	10	none
4 ^d	2CBqk	42-70	10YR 5-6/2	10YR 4/2	EGCOS	75	0	0	94	5	1	none

No.	Structure	Consistence			Cementation	CaCO ₃ Effervescence		pH	Pores	Roots	Lower Boundary
		Dry	Moist	Wet		% Morphology					
1	2COPR	SH	YFR	SO/PS	vsd dilutant	EQLE	8.6	SW	none	AW	
2	1FPL	VSH-H	YFR	SO/PO	none	EQLE	8.6	n.d.	IF	CM	
3	M	SH	YFR	YSS/PS-PO	none	EQLES-D4SPD	9.0	n.d.	IF	CM	
4	SG	LO	LO	SO/PO	none	EQLE	8.6	n.d.	none	N	

COMMENTS: ^a Zone of dust infiltration is Av + Bvk, 0-22 cm. ^b Some parts of Bvk YSS/PS, but not enough clay to make Bt.; Bvk is 1COPR structure in adjacent, old pit. Bottom of Bvk horizon is 3 cm short of >25 cm rule for cambic horizon, so keys to Torriorthent, an using implied "Camborthidic" subgroup to indicate almost-cambic horizon. ^c The Bvk contains 2-4 cm thick, hard lenses of finely-tubular pored, gray, apparently dust-impregnated material that is similar to buried Av horizons. ^d With thin pebble-bottom coatings of opal and carbonate, carbonate even less than in overlying Bh

2369

90888

"BEST AVAILABLE COPY"

PEDON No. 4 (CFP27) -- TABULAR DESCRIPTION

Taxonomic I.D.: loamy-skeletal, mixed, thermic Typic Calcicorthid Est. Min. Age: SAME AS ADJACENT PEDON #5: 25,700 +/- 360 YBP (uncorrected radiocarbon) 28,300 YBP (+10% correction). Geographic Surface: Black Cone; here there are two parts, or remnant-levels comprising this Black Cone surface, that have similar degrees of Av horizon thickness and horizon differentiation; a second, younger surface (Little Cones?) is inset below the Black Cones surface. Pedon I.D.: 1-FFP-1-CFP27-1 to 4. Date: 6/09/87 By: F.F. Peterson Location: Crater Flat, Nevada, in SE corner of Diamond Queen Mine & Solitario Canyon roads; ca 160 m ESE on, ca 25 m S from Solitario Canyon road; ADJACENT TO PEDON #5. Physiographic Position: lower-fan-piedmont-remnant summit; remnant deeply dissected by axial-stream channel here. Parent Material: Colluvial dust and mixed limestone-volcanic alluvium. Native Vegetation: Creosote bush, white bursage, range ratany, mormon tea, shadscale, pale wolfberry (all in biocoppices). Slope: 3% Aspect: 180° Elevation: 3190 ft. 972 m Latitude: 36.810° N Longitude: 116.602° W Microrrelief Position: In BIOCOPPICE. Surficial Gravel: 50 %-area Surficial Cobbles: 0 %-area Surficial Stones: 0 %-area Total Surficial Rock fragments: 50 %-area Other Surficial features: surficial pebbles mostly 1-2 cm dia., a few 3-5 cm, few with any varnish, some with carbonate pebble-bottom coatings indicating excavation from Bk horizon by rodents; surficial 1 cm of LFS A1 horizon only weakly-coherent crusted, no evidence of Av character as expected for modern colluvial deposit.

No.	Horizon	Depth cm	Color		Texture	Estimated			Estimated			Argillans
			Dry	Moist		Gravel	Cobble	Stone	Sand	Silt	Clay	
						% vol.			% wt.			
1	A1	0-9	10YR 6/3	10YR 4/3	LFS	10	0	0	87	10	3	none
2	Avkb	9-32	10YR 7/3	10YR 4/3	L	12	0	0	47	35	18	none
3	Buk	32-54	10YR 6.5/3	10YR 4.5/3	YGSL	50	0	0	72	20	8	none
4	2Bk	54-120	10YR 7/2 & 10YR 6/1	10YR 5/3 & 10YR 7/3	EGLS	70	15	0	87	10	3	none

No.	Structure	Consistence			Consentation	CaCO ₃ Effervescence		pH	Pores	Roots	Lower Boundary
		Dry	Moist	Mo		Morphology					
1	1COPRLMPL	VSH	VFR	SO/PO	none	E-D	8.6	1,P	vIV-F	CS	
2	1COPRLFSBK	SH-H	FR	SS/P	none	ES-SPBAD	8.8	3VFT,1,P	IV-F	CM	
3	1F-KSBK	VSH	VFR	SO/PO	none	EV-SPBAD	8.8	1,P	IV-F	CM	
4	M	VSH-H	FR-FI	SO/PO	20% CM lenses	EV-SPBAD	8.2	1	IV-F	M	

COMMENTS: ^aThe A1 horizon is bioturbated, colluvial LFS collected in a biocoppice; material nondiluted. ^bThe Avkb horizon is somewhat dilated; its finer texture is attributed to its being a buried Av horizon, not to illuvial clay accumulation. ^cThe Buk is only slightly dilated, presumably due to slight dust-infiltration; it shows less pedogenic carbonate than the subjacent 2Bk and is considered a cambic horizon with in-transit pedogenic carbonate; the Avkb can also be considered a part of the currently operative cambic horizon. ^dThe 2Bk horizon is considered a calcic horizon: limestone pebbles and pedogenic carbonate estimated >15% wt.; some 20% vol. is weakly cemented lenses with K-fabric fine earth and 2-4 mm thick carbonate pedants on pebbles; estimate total pedogenic carbonate >5% vol.

2370
88806

BEST AVAILABLE COPY

PEDON No. 3 (ICFP26A) -- TABULAR DESCRIPTION

Taxonomic I.D.: sandy-skeletal, mixed, thermic Typic Camborthid. Est. Min. Age: SAME AS ADJACENT PEDON 2: 10180 +/- 270 YBP (uncorrected radiocarbon) 11,200 YBP (+10% correction). Ocosmorphic Surface: Little Cones. Pedon I.D.: 1-FFP-ICFP26A-1 to 4. Date: 6/08/87 By: F.F. Peterson Location: ADJACENT TO PEDON 2, Crater Flat, Nevada, 0.2 mi. ENE of northernmost cone of Little Cones, 1.05 mi. E of N-S road to Diamond Queen Mine on trail. Physiographic Position: Summit of very broad basin-floor remnant that has a few, shallow, on-flat flutes. Parent Material: Eolian dust and mixed limestone and volcanic alluvium. Native Vegetation: Creosote bush, white bursage, shadscale, pale wallberry (in coppices), spiniflow (on pavette). Slope: 2% Aspect: 180° Elevation: 3000 ft. 914 m Latitude: 36.774 N Longitude: 116.599 W Microrrelief Position: BIODOPPICE-INTERSPACE Surficial Gravel: 50 % area Surficial Cobbles: 0 % area Surficial Stones: 0 % area Total Surficial Rock Fragments: 50 % area Other Surficial Features: This four-meter wide biodoppice is covered with several cm of eolian LFS with some intermixed gravel; pebbles on surface have been recently dug up by rodents, few have any varnish, many have thin, partial carbonate coatings showing they were dug from a Bh horizon.

No.	Horizon	Depth cm	Color		Texture	Estimated			Estimated			Argillines
			Dry	Moist		Gravel	Cobble	Stone	Sand	Silt	Clay	
						% vol.			% wt.			
1 ^a	A1	0-9	10YR 6/2	10YR 5/2	LFS	5	0	0	90	8	2	none
2 ^b	Avhb	9-20	10YR 7/2	10YR 4/3	CFSL	25	0	0	64	28	8	none
3	Bsh	20-60	10YR 6.5/2	10YR 5/3	VGSL	50	0	0	62	30	8	none
4	2Bh	60-65+	As in Pedon #2									

No.	Structure	Consistence			Consentation	CaCO ₃ Effervescence Morphology	pH	Pores	Roots	Lower Boundary
		Dry	Moist	Wet						
1	vMPL-M	YSH	YFR	SO/PO	none	EDGE ^a	n.d.	IFT	vIVF	AS
2	INSDK	SH	VFR	SO/PS	none	ES-CISF	n.d.	2YF-FT	IVF-M	AS
3	INSDK	SH	VFR	SO/PS	none	EY-CISFCSPB	n.d.	IFT	IFT	Cu
4	As in Pedon #2									

COMMENTS: ^a The A1 horizon is bioturbated eolian fine sand and gravel dug from rodent burrows; it is the analogue of the 2-3 cm of sand which between pavement-pebbles on the pavette. The Avhb horizon was traced laterally into the adjacent pavette, where it is the Av horizon; the Avhb horizon has the grayness and slight dilatancy of the adjacent Av horizon, but has tubular macropores (root channels) rather than vesicular pores (due to capillary bubbles), presumably due to burial and lack of periodic saturation subsequently.

2371

86808

BEST AVAILABLE COPY

PECCON No. 6 (CFP32) -- TABULAR DESCRIPTION

Tamamoc 1-Da: loamy-skeletal, mixed, thermic haplic Durargid. Est. Min. Age: 30,320 +/- 420 TBP (uncorrected radiocarbon) 33,400 TBP (1105 correction). Geomorphic Surface: Black Cone. Pedon 1-Da: 1-FFP-1-CFP32-1 to 5. Date: 6/11/87 By: f.f. Peterson Location: Grater Flat, Nevada, between Black Cone and Red Cone, ca 2.25 mi. ESE from corner with Diamond Queen Mine road on, and ca 75 m N of Solitario Canyon road. Physiographic Position: Summit of a low-relief, moderately-broad, elongate, lower-footholdment remnant; dissection by 2-3 ft. deep, near-fluvial, shoulders rounded. Parent Material: Eolian dust and volcanic alluvium. Native Vegetation: Pale willowberry, shade-scale, white burrage, range rafter, creosote bush (all in biocrop). Slope: 45 Aspect: 225 Elevation: 3,165 ft. 965 m Latitude: 36.787°N Longitude: 116.566°W Microrelief Position: 100x3-40 m wide PAVETTE. Surficial Gravel: 80 % area Surficial Cobbles: 1 % area Surficial Stones: all 5-area Total Surficial Rock Fragments: 81 % area Other Surficial Features: Moderately dark varnish on many pavement pebbles; 1-3 cm pavement pebbles; no apparent embedded-pebble layer.

No.	Horizon	Depth cm	Color		Texture	Estimated		Argillaceous			
			Dry	Moist		Gravel	Silt Clay				
1 ^a	Av	0-6	10YR 7/2	10YR 4/3	L	13	0	48	40	12	none
2 ^b	Ah	6-15	10YR 6.5/2	10YR 4.5/3	GSL	20	0	64	28	8	none
3 ^c	Bt	15-33	10YR 6/3	8YR 4.5/3	VGSL	50	0	60	25	15	IMPBC & PO
4 ^d	Bth	33-51	7.5YR 6/3	7.5YR 4/4	EGSL	64	0	0	70	20	10
5 ^e	Bqhm	51-71	10YR 8/1 & 10YR 6/2	10YR 7/2 & 10YR 4/3	EGLSP	637	0	0	n.d.	n.d.	n.d.

No.	Structure	Consistence		Mol	Comestation	CaCO ₃ Effervescence & Morphology	pH	Pores	Roots	Lower Boundary
		Dry	Moist							
1	2YCOpr	SH	VFR	SS/PS	none	EO	8.6	3VF-FV, 2HV	none	AS
2	1YFL & 1YFSBK	VSH-SO	VFR	SO/PO	none	ESLEV- D, SPB, SF	9.4	n.d.	1YF-F	CM-1
3	1YF-FSBK	SH	FR	VSS/VPS	none	EOLE	8.4	n.d.	1YF	CM
4	1YFSBK	VSH	VFR	VSS/PO	none	ESLEVED-D, SP	8.4	n.d.	none	AM-1
5	2YCOPL	EH	SFI	n.e.	CS (CM?)	EY-D, SP	n.d.	n.d.	none	N

COMMENTS: ^a Soil material is fully diffluent, leached of carbonates. ^b Soil material only slightly diffluent; some 1-2 mm thick, dark bands of etch-etchified organic matter reflecting Mn-sulf accumulation. ^c Somewhat redder chroma and a few claystias confirm argillic horizon status, but is barely enough more clayey than A horizon. ^d No evidence of opalization in lower argillic horizon. ^e A single carbonate and/or opal laminae on top of pan; cementation appears strong in place, but fragments of pan appear only weakly cemented; as presumed there is enough opal cement to make this a duripan rather than a petrocalcic horizon.

"BEST AVAILABLE COPY"

2 3 7 2 9 0 8 8 8

PEDON No. 5 (CFP27A) — TABULAR DESCRIPTION

Taxonomic I.D.: sandy-skeletal, mixed, thermic Typic Calcorthid Est. Min. Age: 25,700 +/- 360 YBP (uncorrected radiocarbon) 28,500 YBP (110% correction). Diastrophic Surface: Black Cone; two remnant-levels having similar Av thickness, horizon differentiation, comprise Black Cone surface here; a younger surface (Little Cones?) is inset below Black Cone surface. Pedon I.D.: 1-PPP-1-CFP27A-1 to 4. Date: 6/09/87 By: F.F. Peterson Location: Crater Flat, Nevada, in SE corner of Diamond Queen Mine & Solitaria Canyon roads; ca 160 m ESE on, ca 55 m SSE from Solitaria Canyon road, ADJACENT TO PEDON #4. Physiographic Position: Lower-lan-plateau-remnant summit; remnant deeply dissected by axial-stream channel here. Parent Material: Eolian dust and mixed limestone-volcanic alluvium. Native Vegetation: Creosote bush, white bursage, range ratany, Mormon tea, shadscale, pale wolfberry (all in blocoppices). Slope: 3 S Aspect: 180° Elevation: 3190 ft. 972 m Latitude: 36.810° N Longitude: 116.602° W Microrelief Position: in 20 x 5 m PAYETTE. Surficial Gravel: 80 %-area Surficial Cobbles: 1 %-area Surficial Stones: 0 %-area Total Surficial Rock Fragments: 81 %-area Other Surficial Features: Many pavement pebbles, stones in adjacent "bare" area moderately-darkly varnished; pavement limestone fragments are deeply etched; mostly 1-2 cm pebbles, some 4-8 cm; 1 mm FS much; surficial pebbles loose, over a 1-pebble thick (1-3 cm) layer embedded in Av; loose surficial pebbles without SPB-carbonate coating, a few of embedded pebbles with SPB-carbonate coating.

No.	Horizon	Depth cm	Color		Texture	Estimated Gravel Cobble Stone % vol.			Estimated Sand Silt Clay % wt.			Argillines
			Dry	Moist								
1	Av	0-10	10YR 7/2	10YR 4/3	GL	25	0	0	45	40	15	none
2	Buk1	10-20	10YR 6/3	10YR 4/3	GL	25	0	0	50	35	15	none
3	Buk2	20-32	10YR 6/3	10YR 4/3	YOSL	38	0	0	67	25	8	none
4	2Bk	32-65+	10YR 7/2	10YR 5/2	EGCOS	80	5	0	94	5	1	none

No.	Structure	Consistence			Consentation	CaCO ₃ Effervescence & Morphology		pH	Pores	Roots	Lower Boundary
		Dry	Moist	Wet							
1	ZYCOPR&IMPL	H	FR	SS/PS	none	E-D	9.4	3F-MY	none	AS	
2	1FSBK	SH	FR	SS/PS	none	EG&E-D,SPB	9.6	n.d.	1VF-F	CW	
3	1FSBK	SO	VFR	SO/PO	none	EG&E-D,SPB	9.4	n.d.	2VF,1F	GW	
4	M&SB	LO	LO	SO/PO	CW lenses	ES-D,SPB	9.4	n.d.	1VF	H	

COMMENTS: The lower Av horizon with 2-3, 0.2 mm thick, smooth-topped, pustulose-bottomed, hard-brittle CaCO₃-laminae that are between the platy pods; these thin, brittle carbonate laminae are characteristic of Av horizons in many, if not most Black Cone age and older soils; occasionally seen in Little Cones age Av horizons; soil is fully dilatant; do not have the Avhb horizon of adjacent blocoppice pedon #4, hence is 22 cm shallower to presumably continuous 2Bk horizon, and the family particle size class is only sandy-skeletal rather than loamy skeletal. Soil material is only slightly dilatant, indicating little infiltrated eolian YFS & S1; non-effervescent parts infer that Buk1 once fully leached, that carbonate in Av is later cycle. The 2Bk horizon has the same clean tops and 2-5 mm carbonate-pendants on pebble bottoms as in adjacent pedon #4; only lenses are cemented; considered a calcic horizon.

2373
8888
9

BEST AVAILABLE COPY

PEDON No. 8 (CFP29) — TABULAR DESCRIPTION

Taxonomic I.D.: loamy-skeletal, mixed, thermic Typic Durargid Est. Min. Age: 137,000 YBP (cation-ratio age) Geomorphic Surface: early Black Cone Pedon I.D.: 1-FFP-1-CFP29-1 to 5 Date: 6/10/87 By: F.F. Peterson Location: Crater Flat, Nevada, SE corner of Solitario Cay. & Trench CF243 roads. Physiographic Position: Mid-lan-plateau-remnant summit Parent Material: Eolian dust & volcanic alluvium. Native Vegetation: Creosote bush, white bursage, pale wolfberry, Nevada Mormon tea, range ratony, shedscale. Slope: 45 Aspect: 235° Elevation: 3,360 ft. 1,024 m Latitude: 36.802° N Longitude: 116.532° W Microrelief Position: PAVETTE Surficial Gravel: 80 S-area Surficial Cobbles: 3 S-area Surficial Stones: 0 S-area Total Surficial Rock Fragments: 83 S-area Other Surficial Features: Many pebbles & cobbles dark varnished.

No.	Horizon	Depth cm	Color		Texture	Estimated			Estimated			Argillaceous
			Dry	Moist		Gravel	Cobble	Stone	Sand	Silt	Clay	
						%			%			
3 ⁰	Av	0-5	10YR 7/2	10YR 4.5/2	CL	20	0	0	48	40	12	none
	Ak	5-12	10YR 6.5/3	10YR 4.5/3	SL	10	0	0	74	18	8	none
	Big	12-24	7.5YR 6/3	7.5YR 4/4	OCL	20	2	0	27	35	38	2M/PF
4 ⁰	Big	24-47	7.5YR 6/3	7.5YR 4/4	*SL*	50	5	0	n.d.	n.d.	n.d.	4 PO
5 ⁰	Bqka	47-55+	10YR 8/1 &	10YR 7/3 &	n.d.	60	10	0	n.d.	n.d.	n.d.	4 PBC
			10YR 7/2	10YR 4.5/3								

No.	Structure	Consistence			Cementation	CaCO ₃ Effervescence & Morphology		pH	Pores	Roots	Lower Boundary
		Dry	Moist	Wet							
1	2COPR	SH	VFR	SS/SP	none	ED & E	8.8	3VF-MV	none	AS	
2	1VFSBK	SO	VFR	SO/PO	none	ES	8.4	n.d.	1VF	AW	
3	2VFCR->ABK	SO->SH	VFR	S/P	none	ED & ES	8.2	n.d.	none?	AS	
4	1COPL & 3FABK	H-VH	VFI	SO/PO	CM	ED	8.2	n.d.	none	CM	
5	M	VH-EH	V-EFI	brittle	CS	ES-D, SP, SF	8.2	n.d.	none	M	

COMMENTS: The Av is fully dilatant; has 3-8 mm (10YR 5/1D 3/1M) bands and small, pale brown, thin, brittle, pustulose carbonate laminae at bottom. The Ak is not dilatant. With 1-2 mm soft gypsum masses and salt-flocculated in upper part; with a few pebble-bottom opal coats. The Big is notably crunchy-opalized; coarse plates are weakly cemented. Pan is 1-3 ft. thick where exposed in adjacent arroyos; thin lamina on top.

8 8 BEST AVAILABLE COPY 2 3 7 4

PEDON No. 7 (CFP37) — TABULAR DESCRIPTION

Tenonic I.D.: loamy-skeletal, mixed, thermic Typic Durargid. Est. Min. Age: 120,000 YBP (cation-ratio age) Geomorphic Surface: early Black Cone. Pedon I.D.: 1-FFP-1-CFP37-1 to 5 Date: 8/17/87 By: F.F. Peterson Location: Crater Flat, Nevada, ca 2.1 mi. NNE of Diamond Queen Mine & Saliterno Cny. roads corner on E side of dirt road to N & NE Crater Flat. Physiographic Position: fan-piedmont-remnant summit; clearly inset below Yucca fan-piedmont remnants to NE. Parent Material: Volcanic alluvium with a bit of limestone. Native Vegetation: Creosote bush, white bursage, pale wolfberry, shadscale, Nevada Mormon tea, needlegrass, Joshua-tree (very few). Slope: 3% Aspect: 180° Elevation: 3,374 ft. 1,028 m Latitude: 36.836° N Longitude: 116.579° W Microrelief Position: small PAYETTE Surficial Gravel: 80 %-area Surficial Cobbles: 2 %-area Surficial Stones: 0 %-area Total Surficial Rock fragments: 82 %-area Other Surficial Features: Pavement pebbles commonly darkly varnished.

No.	Horizon	Depth cm	Color		Texture	Estimated			Estimated			Argillous
			Dry	Moist		Gravel % vol.	Cobble	Stone	Sand	Silt	Clay	
1	Av	0-5	10YR 7/2	10YR 4/2	L	10	0	0	45	40	15	none
2 _a	AB	5-11	10YR 6/2	10YR 4.5/3	EGCL	15	0	0	36	35	29	none
3 _a	Btk1	11-35	7.5YR 6/4	7.5YR 4/4	YGCL	50	0	0	37	25	38	2MCO
4 _a	Btk2	35-48	7.5YR 6/4	7.5YR 5/4	EGLCOS	65	2	0	80	15	5	none
5 _a	Btkn	48-130	10YR 8/1	10YR 7/3	n.d.	70	5	0	n.d.	n.d.	n.d.	none

No.	Structure	Consistence			Cementation	CaCO ₃ Effervescence		pH	Pores	Roots	Lower Boundary
		Dry	Moist	Wet		& Morphology					
1	SCOPR	SH	YFR	SS/PS	none	EO & EV	8.4	3FV	none	AS	
2	SCOPR & IMPL	SH	YFR	S/P	none	EO & EV	8.4	1VFV	v1VF	AM	
3	3VFABK	SH	FR	VS/P	none	EO & ES	8.6	n.d.	1VF, v1F	CM	
4	1VFSOK	LO	YFR	SO/PO	none	EO & EV	8.8	n.d.	1VF	VAW	
5	M	SH-VH	LO-VFI	n.a.	none-CS	EV	n.d.	n.d.	v1VF-M	M	

COMMENTS: ^a AB designation because of finer texture than Av. ^b Btk1 with very thin, discontinuous SPD carbonate; EO parts and some places entirely EO indicate this Btk once leached, now accumulating carbonate; in half of pit is EGCL rather than YGCL. ^c Btk2 is continuous horizon; 1 mm thick SPD carbonate; some parts EGOCSL rather than EGLCOS; most of Bt-clay in Btk1. ^d Proseum enough opal cement to call this pan a duripan; some 20-35% vol. of strongly cemented lenses with only slight pebble-separation, 15% vol. loose, remainder weakly-cemented pebble-bridges; only a single, discontinuous laminae at top of pan, but lenses fabricated so use Typic subgroup, though close to Haplic; roots enter deeply into pan.

2375

8880

BEST AVAILABLE COPY

PEDON No. 10 (CFP33) — TABULAR DESCRIPTION

Tamassic l.D.: loamy-skeletal, mixed, thermic Haplic Durargid. Est. Min. Age: 26,970 +/- 375 YPB (uncorrected radiocarbon) 29,700 YBP (+10% correction). Conomorphic Surface: late Black Cone. Pedon l.D.: 1-FFP-1-CFP33-1 to 5. Date: 6/12/87 By: F.F. Peterson
 Location: Crater Flat, Nevada, 0.55 mi. SE from intersection of Solitario Cny. and Trench CF2&3 roads; across wash to N and on next higher, older surface than Pedon 11. Physiographic Position: fan-piedmont-remnant summit. Parent Material: Eolian dust and volcanic alluvium. Native Vegetation: Creosote bush, pale wolfberry, white burrage, shadscale, Nevada nornon tea, range ratony. Slope: 3% Aspect: 247° Elevation: 3,370 ft. 1,027 m Latitude: 36.786 N Longitude: 116.526 W Microrelief Position: PAVETIE Surficial Gravel: 80 %-area Surficial Cobbles: 1 %-area Surficial Stones: all %-area Total Surficial Rock Fragments: 81 %-area Other Surficial features: Well sorted pavement of 0.5-2 cm pebbles, some dark-varnished.

No.	Horizon	Depth cm	Color		Texture	Estimated			Estimated			Argillans
			Dry	Moist		Gravel	Cobble	Stone	Sand	Silt	Clay	
						% vol.			% wt.			
1 ^a	Av	0-7	10YR 7/2	10YR 4.5/2	GL	30	0	0	50	40	10	none
2 ^b	Ak	7-28	10YR 6.5/3	10YR 4.5/3	VGSL	40	0	0	65	25	10	none
3 ^c	2Bt	28-43	10YR 6/3	10YR 4/3	VGL	50	0	0	59	25	16	?
4 ^d	2Bqk	43-68	10YR 6/3	10YR 4/3	EGSL	60	0	0	72	20	8	none
5 ^d	2Bqkm	68-73*	10YR 6/1 & 10YR 7/2	10YR 7/2 & 10YR 6/2	n.s.	80	0	0	n.s.	n.s.	n.s.	none

No.	Structure	Consistence			Cementation	CaCO ₃ Effervescence		pH	Pores	Roots	Lower Boundary
		Dry	Moist	Moist		Morphology					
1	2COPR & IMPL	SH	VFR	VSS/PS	none	EO	8.4	3F-MV	none	CS	
2	1VFSBK-M	SO	VFR	SO/PO	none	ES-D&SPB	8.8	n.d.	1-2vf,F	CS	
3	1VFSBK-M	SO	VFR	SS/PS	none	EO&E-SPB	8.4	n.d.	1VF	GS	
4	SO	LO	VFR	SO/PO	none	EO&E-SPB	8.4	n.d.	?	AM	
5	M	H	VFI	brittle	CM	ES	n.d.	n.d.	none	M	

COMMENTS: ^aTop 2/3 of Av is EO, lower 1/3 is E with a couple thin, brittle, pustulose-bottomed carbonate laminae. ^bArgillic horizon assignment by relatively finer texture than A horizon; only carbonate is a few pebble-bottom coatings. ^cThe loose, extremely gravelly 2Bqk is noncalcareous except some pebbles with opal and some carbonate on bottoms, tops clean. ^dFan lacks an evident upper laminae cap, weakens notably when moistened, may be a single ca. 5-cm thick lens; opal-yellowing on pebble bottoms; at best a HAPLIC pan.

2 3 7 6
8 8 8 0 6

BEST AVAILABLE COPY

PEDON No. 9 (CFP30) — TABULAR DESCRIPTION

Tamomeic 1.0.1 (sooty-shale), mixed, thermal Haplic Durargid. Est. Min. Age: Same as Pedon 8's est. 137,000 YBP (cation-ratio age) because are on adjacent fan-pledment remnants that appear to be same level and age. Cosmorphic Surfaces: early Black Coas. Pedon 1.0.1 1-FFP-1-CFP30-1 to 5 Date: 6/11/87 Dpt: F.F. Peterson Location: Crater Flat, Nevada, 0.1 mi. SE from intersection of Sallierio Cr. and Trench C7283 roads. Physiographic Position: Mid-lan-pledment-remnant (small); apparently same as Pedon 9 surface. Parent Material: Eolian dust and volcanic alluvium. Native Vegetation: Creosote bush, shadscale, white bursage, pale wolfberry, Nevada wormwood. Slope: 4 S Aspect: 235 Elevation: 3,370 ft. 1,027 m Latitude: 36.801 N Longitude: 116.530 W Micromorphic Position: PAVEITE Surficial Gravel: 80 S-area Surficial Cobbles: 2 S-area Surficial Stones: 0.5 S-area Total Surficial Rock Fragments: 83 S-area Other Surficial Features: Pavement pebbles 1-3 cm, many with dark varnish.

No.	Horizon	Depth cm	Color		Moist	Texture	Estimated		Argillous			
			Dry	Moist			Gravel Cobble Stone % vol.	Sand Silt Clay % wt.				
1 ^a	Av	0-7	10YR 7/2	10YR 4.5/3	GL	20	0	0	50	40	10	none
2 ^b	Ah	7-21	10YR 7/3	10YR 4.5/3	GSL	25	0	0	65	25	10	none
3 ^c	Bt	21-37	7.5YR 6/3	7.5YR 4.5/4	OCL	25	0	0	35	35	30	none
4 ^c	BtHq	37-49	10YR 6/4	7.5YR 4.5/4	YGSLo	50	0	0	65	20	15	IMDC & PF
5 ^d	Bqba	49-62	10YR 7/2	10YR 5.5/4	n.a.	60	5	0	n.a.	n.a.	n.a.	none

No.	Structure	Consistence		Moist	Consistation	CaCO ₃ Effervescence & Morphology	pH	Pores	Roots	Lower Boundary
		Dry	Moist							
1	SCOPR	SH	FR	SS/PS	none	ED	8.6	3YF-W	none	AS
2	1FPL & 1VFSK	YSH	VTR	SO/PO	none	EV	9.0	n.d.	ZYF	CH
3	1VFSK	SH	FR	S/P	none	ED	8.8	n.d.	1VF	CH
4	1VFSK	SH	FR	SO/PO	none	ES-SFB	8.6	n.d.	IF	AM
5	M	WH	EFI	brittle	CH-CS	EV	n.d.	n.d.	none	N

COMMENTS: ^aThe Av is fully dilatant. ^bLowest Av and upper half of Ah with several, thin, brittle, petiolate-bottomed carbonate lenses; Ah is only slightly dilatant. ^cThe BtHq is opalized; thin opal coats on pebble bottoms, fine earth is "crunchy." ^dFor hor only a thin, discontinuous upper lamina; brittle but only very firm when moist; opal on pebble bottoms; cementation is weak enough, apparently lumpy enough that will call this a HAPLIC Durargid.

BEST AVAILABLE COPY

PEDON No. 12 (CP34) - TABULAR DESCRIPTION

Tammonic ls.: loamy-shale, mild, thermic haplic durigid. Est. Mm. Agr: On similar surface, hence similar to Pedon 101 higher, older surface than that of Pedon 11. Pedon 101: 1-ff-1-CP34-1 to 7. Date: 8/20/87 By: J.F. Peterson Location: Crater flat, Nevada, 0.75 mi. SE from intersection of Sollarie Cay, and trench C283 roads. Physiographic Position: fan-plateau-remnant summit. Parent Material: Eolian dust and volcanic alluvium. Native vegetation: White bur sage, creosote bush, pale willowberry. Sandstone, Nevada normal fan, range rainey. Slope: 45 Aspect: 250 Elevation: 5,370 ft. 1,027 m Latitude: 36.753 N Longitude: 116.524 W Microrelief Position: PAYETTE Surficial Gravel: 80 5-area Surficial Cobble: 0 5-area Surficial Stones: 0 5-area Total Surficial Rock Fragments: 80 5-area Other Surficial Features: Many of fine pebbles in pavement are darkly varnished.

No.	Horizon	Depth cm	Color		Texture	Estimated			Argillous			
			Dry	Moist		Gravel Cobble Stone	Sand Silt Clay	5 vol. —				
1	Av	0-5	10YR 7/3	10YR 5/3	VC/SL	30	0	0	37	35	0	none
2	Ah1	5-13	10YR 7/3	10YR 5/3	VOL	40	0	0	47	40	13	none
3	Ah2	13-21	10YR 7/3	10YR 5/3	VC/SL	30	0	0	67	25	8	none
4	Bt	21-30	10YR 6/4	9YR 4/4	CL	30	0	0	50	33	17	none
5	Bt	30-46	7.5YR 5.5/4	7.5YR 4.5/4	VC/SL	35	0	0	70	15	15	VINER
6	Bt	46-64	10YR 6/4	10YR 5/3	VCS	50	5	0	93	5	2	none
7	Bt	64-75	10YR 6/1	2.5YR 7/2	n.s.	80	15	0	n.s.	n.s.	n.s.	none

No.	Structure	Dry Moist	Moist	Consistence	CaCO ₃ Effervescence			Morphology	pH	Pores	Roots	Boundary
					—	—	—					
1	XOpr	SH	WFR	50/PS	none	E & EO	0.4	M-NV	none	AS	AS	AS
2	1HrL & 1fSBK	SM-H	FR	SS/PS	none	ES	0.6	n.d.	none	AV	AV	AV
3	1HrL & 1fSBK	VSH	WFR	VSS/PO	none	EA-SPB	0.0	n.d.	none	CV	CV	CV
4	1fSBK	SH	WFR	SS/P	none	E	0.6	n.d.	none	CV	CV	CV
5	1fSBK	SM-H	FR	SS/PS	none	EO	0.6	n.d.	none	CR	CR	CR
6	SO	LO	LD	SO/PO	none	EO	0.6	n.d.	none	VAL-B	VAL-B	VAL-B
7	M	EH	EFI	Wtillite	CS lenses	EV	n.d.	n.d.	none	M	M	M

COMMENTS: The Av is somewhat different. The Ah1 is different. Soluble salts efflorescing on the pit wall from the Ah2 a few weeks after thunderstorm. Ped consists of 5-7 cm thick lenses that are network of pebbles with many interstices open; thin leaden cap only on top of lenses; interpret as a MULLIC podzol. Comment to call it a duripan.

"BEST AVAILABLE COPY" 9 0 8 8 8 2 3 7 8

PEDON No. 11 (CFP33) -- TABULAR DESCRIPTION

Taxonomic I.D.: loamy-skeletal, mixed, thermic Typic Camborthid. Est. Min. Age: 17,280 +/- 370 YBP (uncorrected radiocarbon) 19,000 YBP (10% correction). Diomorphic Surface: late Black Cone. Pedon I.D.: 1-FFP-1-CFP33-1 to 5 Date: 6/12/87 By: F.F. Peterson
 Location: Crater Flat, Nevada, 0.65 mi. SE from intersection of Solitario Cny. and Trench CF283 roads; across wash to S from Pedon 10.
 Physiographic Position: True inset-lan-remnant summit; next younger surface than that of Pedon 10. Parent Material: Eolian dust and volcanic alluvium. Native Vegetation: Shadscale, creosote bush, white bursage, pale wolfberry, Nevada Mormon tea, range ratony.
 Slope: 35 Aspect: 247 Elevation: 5,360 ft. 1,024 m Latitude: 36.794 N Longitude: 116.526 W Microrelief Position: PAVETTE
 Surficial Gravel: 85 %-area Surficial Cobbles: 2 %-area Surficial Stones: 0.3 %-area Total Surficial Rock Fragments: 87 %-area
 Other Surficial Features: Pavement of 0.5-2 cm, only thinly-varnished pebbles.

No.	Horizon	Depth cm	Color		Texture	Estimated			Estimated			Argillans
			Dry	Moist		Gravel	Cobble	Stones	Sand	Silt	Clay	
						% vol.			% wt.			
1	Av	0-5	10YR 7/2	10YR 4.5/3	GFSL	25	0	0	55	35	10	none
2	AA1	5-11	10YR 7/3	10YR 5/3.5	GL	25	0	0	42	40	18	none
3	AA2	11-27	10YR 7/3	10YR 4.5/3	GFSL	30	0	0	62	30	8	none
4	Buk	27-60	10YR 6/3	10YR 4/3	OSL	30	0	0	55	30	15	none
5	ZBh	60-95	10YR 7/2	10YR 4.5/3	EGSL	70	10	0	67	25	8	none

No.	Structure	Consistence			Consistation	CaCO ₃ Effervescence Morphology	pH	Pores	Roots	Lower Boundary
		Dry	Moist	Wet						
1	2COPR & 1F-MPL	VSH	VFR	YSS/YPS	none	E0	8.2	MF-MV	none	AS
2	2COPL	SH	VFR	SS/PS	none	ES-D,SPD	8.4	n.d.	vlyf	AS
3	1FSBK	SO	VFR	SO/PO	none	EV-SPD,D	9.0	n.d.	2YF	CW
4	1FSBK-M	SO	VFR	YSS/YPS	none	EV-SPD,D	8.8	n.d.	lyf	CW
5	M-SO	LO	VFR	SO/PO	none	EV-SP,SPD	9.0	n.d.	?	M

COMMENTS: Only slightly dilated Av; evidence of limited dust accumulation. A few, faint, slightly darker lamellae may reflect some clay accumulation or gibbii-organic matter; only very slightly dilated. The AA2 is slightly dilated; evidence of some dust infiltration? Note pick-up of clay in Buk, but no suggestion of argillans (clayskins) and color not reddened, so keep as a cambic horizon with in-transit carbonates rather than an argillic horizon; in adjacent old SCS pit is slightly redder and clayey, might call it a Bt horizon. Described in adjacent old SCS pit.

9 0 8 8 8 8 2 3 7 9

"BEST AVAILABLE COPY"

An important test of the closed system of dated VOM is in progress. Varnishes from surfaces far, far older than the 40 ka limit of radiocarbon were collected and processed from areas close to open-air bomb explosions near the Nevada Test Site and the Trinidad Site, NM. If the varnish system for the extracted organics is truly closed, bomb carbon should not affect the date. If it is open, the bomb carbon could affect the date. The AMS analyses have not been completed. Away from the immediate influence of bomb carbon, a volcanic flow in the Big Pine Volcanic Field was sampled for radiocarbon analysis. At the time of collection, it was thought that the flow might be around 25 ka (B.D. Turrin, personal communication, 1985). As the results in Table 8 indicate, the AMS age was > 40,800 and the K-Ar age for the basalt flow turned out to be around 250 ka. In other words, at a site known to be "dead" by K-Ar dating, the varnish radiocarbon age did indeed turn out to be at background.

V.C.4. Assessing the Importance of Stability of Rock Varnish

Even if the varnish has not been completely eroded by chemical dissolution or aeolian abrasion, partial erosion may change an AMS radiocarbon date. This could be the reason for the greater lags at more humid sites in Table 8.

An example using the role of microcolonial fungi illustrates this. Microcolonial fungi are fairly common on varnishes in the southwestern U.S. (cf. Staley et al., 1982; Taylor-George et al., 1983) and Australia (Staley et al., 1983). They appear to erode varnishes (Dorn, 1986; Figure 7), and they can affect a varnish cation-ratio (Table 2). Table 9 illustrates the effect of microcolonial fungi on the stable carbon isotope values of varnishes on an altitude transect near Crater Flat. When the microcolonial fungi are present, the $\delta^{13}\text{C}$ values are affected. Note how the values change beneath the eroding microcolonial fungi as compared to varnish beneath the microcolonial fungi that are not appearing to erode the varnish.

It, therefore, seemed logical to investigate the possibility that abundant, eroding microcolonial fungi could affect the varnish radiocarbon signal. Based on one example, it appears there can be an effect. In Table 8, the ca. 9 ka age for black subaerial varnish on shoreline B of Lake Mojave, CA. (cf. Wells et al., 1984) contrasts with the 4320 ± 105 (AA-2133) age for the varnish beneath the microcolonial fungi. Both samples were processed the normal way, as listed in an earlier section.

PEDON No. 13 (CFP41)— TABULAR DESCRIPTION

Taxonomic I.D.: sandy-skeletal, mixed, thoracic typic Torriorthent. Est. Min. Age: Modern, <1000 years? Geomorphic Surface: very-late Crater Flat. Pedon I.D.: 1-PPP-1-CFP41-1 to 2. Date: 8/20/87 By: F.F. Peterson Location: Crater Flat, Nevada, 1.2 mi. SE from intersection of Solitaria Cny. and Trench CF243 roads. Physiographic Position: Row inset fan with prominent bar & subtle microtopography. Parent Material: Volcanic alluvium. Native Vegetation: White bursage, creosote bush, range raton, Nevada amaranth, pale wolfberry, shadscale. Slope: 3 S Aspect: 225° Elevation: 3,290 ft. 1,003 m Latitude: 36.788° N Longitude: 116.519° W Microrelief Position: Proto-pavette between stone bars. Surficial Gravel: 65 S-area Surficial Cobbles: 3 S-area Surficial Stones: 1 S-area Total Surficial Rock Fragments: 49 S-area Other Surficial Features: Surficial pebbles, cobbles, stones clean of rock varnish; no evidence of dust infiltration in top of AC horizon.

No.	Horizon	Depth cm	Color		Texture	--- Estimated --- Gravel Cobble Stone			--- Estimated --- Sand Silt Clay			Argillines
			Dry	Moist		% vol.			% wt.			
1	AC	0-19	10YR 6/2	10YR 4/2	EGS	65	0	0	95	3	2	none
2 ^a	Ch	19-100	10YR 6/2	10YR 4/2	EGS	65	3	0	95	3	2	none

No.	Structure	--- Consistence ---			Cementation	CaCO ₃ Effervescence & Morphology		pH	Pores	Roots	Lower Boundary
		Dry	Moist	Wet							
1	SO	LO	LO	SO/PO	none	EO & E	8.6	no V's	IVF	GM	
2	SO	LO	LO	SO/PO	none	E	8.6	n.d.	IVF-F, vii	N	

COMMENTS: ^a Very thin, powdery, discontinuous pebble-bottom carbonate coatings in the Ch horizon suggest minimal pedogenesis; roots follow crude 3-8 cm thick stratifications.

2 3 8 1

9 0 8 8 8

BEST AVAILABLE COPY



IN REPLY REFER TO:

INFORMATION ONLY
United States Department of the Interior

GEOLOGICAL SURVEY
Box 25046 M.S. 425
Denver Federal Center
Denver, Colorado 80225

February 27, 1995

Stephan J. Brocoum
Assistant Manager for Suitability and Licensing
Yucca Mountain Site Characterization Project Office
U.S. Department of Energy
P.O. Box 98608
Las Vegas, NV 89123-8608

WBS: 1.2.5

QA: NA

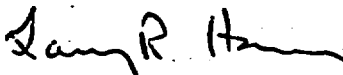
SUBJECT: Map unit descriptions for the preliminary surficial deposits map of the southern half of the Topopah Spring NW quadrangle and the northern half of the Busted Butte quadrangle, Nye County, Nevada, prepared by EG&G *SCPB: 8.3.1.5.1.4*

Dear Steve:

Enclosed is a U.S. Geological Survey (USGS) letter that was requested by T.W. Bjerstedt of your staff. The letter was prepared by Scott Lundstrom and provides introductory text and map unit descriptions to accompany the digitized composite surficial deposits map prepared by EG&G in cooperation with the USGS as part of the Department of Energy's responses to U.S. Nuclear Regulatory Commission (NRC) comments on the Extreme Erosion Topical Report (YMP/91-41-TPR).

The enclosed description is a compilation of work that has already received USGS Director's approval in separate Open-File Reports (OFR). The reports serving as input to this description are OFR-94-341, OFR-95-132, and OFR-95-133 that are now in press. The composite map prepared by EG&G includes map units common to all three OFRs, as well as map units and parts of unit descriptions unique to an individual report. No new data or interpretations have been added to the information included in the three OFRs. This report and the EG&G composite map are specially prepared for the DOE's responses. We would not expect that the DOE needs to review the same material again since the three OFRs referenced above are now in DOE's programmatic review.

This is an unscheduled deliverable, and therefore no milestone is associated with this report


Larry R. Hayes
Technical Project Officer
Yucca Mountain Project Branch

Enclosures

cc:

T. Sullivan, YMSCO, Las Vegas, NV
T. Bjerstedt, YMSCO, Las Vegas, NV
T. Crump, TRW/M&O, Las Vegas, NV
A. Mathusen, WCFS/M&O, Las Vegas, NV

1-367905

Map unit descriptions for the preliminary surficial deposits map of the southern half of the Topopah Spring NW quadrangle and the northern half of the Busted Butte Quadrangle, Nye County, Nevada

This text was prepared to provide an explanation of Quaternary map units for a digitized color map compiled by EG&G from three U.S. Geological Survey Open-File Reports.

Lundstrom, S.C., Wesling, J.R., Taylor, E.M., and Paces, J.B., in press, Preliminary Surficial Deposits Map of the Northeast Quarter of the Busted Butte 7.5-minute Quadrangle: United States Geological Survey Open-File Report 94-341, scale 1:12,000.

Lundstrom, S.C., Mahan, S.A. and Paces, J.B., in press, Preliminary Surficial Deposits Map of the Northwest Quarter of the Busted Butte 7.5-minute Quadrangle: United States Geological Survey Open-File Report 95-133, scale 1:12,000.

Lundstrom, S.C., and Taylor, E.M., in press, Preliminary Surficial Deposits Map of the Southern Half of the Topopah Spring NW 7.5-minute Quadrangle: United States Geological Survey Open-File Report 95-132, scale 1:12,000.

Each of these reports include common map units as well as some unique map units and parts of unit descriptions; this text was prepared to accompany the digitized map (YMP-95-014.1). No new data or interpretations were added to the information included in the three Open-File Reports.

INTRODUCTION

The U.S. Geological Survey is conducting investigations to determine the geologic and hydrologic suitability of Yucca Mountain, in southwestern Nevada, as a potential site for a mined geologic repository for high-level nuclear wastes. These investigations are being conducted in cooperation with the U.S. Department of Energy, under Interagency Agreement DE-AI08-92NV10874, as part of the Yucca Mountain Site Characterization Project.

Mapping of surficial deposits is an integral component of the comprehensive program of site characterization of Yucca Mountain (Department of Energy, 1988). Knowledge of the distribution, characteristics, and history of surficial deposits is needed to assess paleoclimate, tectonics, erosion, surface-water hydrology,

DESCRIPTION OF MAP UNITS

Map units used for the composite map are preliminary informal allostratigraphic units (North American Commission on Stratigraphic Nomenclature, 1983) in which bounding discontinuities of depositional map units are included in their definition. Both the upper and lower bounding unconformities of deposits are used to define the surficial map unit, but the upper surface is much more useful because of its accessibility and characteristics indicative of deposit age and potentially of paleoclimatic variation during exposure since deposition. Subaerial exposure of the upper surface results in soil development and modification of original depositional surface characteristics over time. Lateral discontinuities for surficial deposits range from distinctive fluvial escarpments where one deposit has been inset within another, to an indistinct feather edge. These lateral discontinuities are locally useful in mapping surficial deposit outlines (Peterson, 1981) but are not useful in unit definitions because many surficial deposit margins are laterally variable. Soils near unit margins may differ significantly from soil characteristics described as typical for a given map unit.

The description of each unit represents the predominant surficial deposit occurring within each mapped unit, but map areas may also include other surficial deposits that occur over areas too small to be represented as separate polygons. A combined map symbol (1-3, 3-4, 5f-6f, 5-7) is used where two or three map units are interspersed at such a small scale that separate mapping was impractical; 5-7 denotes a combination of units 5, 6 and 7, and 1-3 denotes a combination of units 1, 2 and 3. Where a surface deposit is so thin that its typical surface characteristics are modified by the underlying deposit, a combined symbol using a slash (5/1, 1/eo) is used.

Deposits are broadly classified by predominant origin inferred from sedimentology and geomorphology. However, this classification is a simplification in that most surficial deposits have complex histories; surface deposits are progressively modified after deposition through subsequent surface processes including eolian deposition or deflation, fluvial reworking by overland flow, colluviation, formation of desert pavement and rock varnish, and pedogenesis. The resulting surficial and pedogenic characteristics (Taylor, 1986; Wesling and others, 1992) are useful for subdividing deposits by relative age, and for correlation and numerical age estimation. Morphologic stages of pedogenic calcite used are based on Gile and others (1966), and stages of pedogenic silica are based on Taylor (1986). Soil horizon nomenclature, especially that of B horizons, follows Birkeland (1984).

3f, 4f, 5f, 6f, and 7f, respectively, is distinguished by the presence of mafic volcanic lithologies, usually vesicular, that typically occur as well-rounded cobbles and boulders. These mafic clasts probably are derived predominantly from the mafic lava flows of Dome Mountain (Christiansen and Lipman, 1965; Lundstrom and Warren, 1994), which is extensively exposed in upper Fortymile Canyon. The non-Fortymile facies of any alluvial unit usually overlies the Fortymile facies to which it grades, but buried soils have not been observed at these contacts. To the east of Fortymile Wash, alluvium derived from the Calico Hills has a distinctly lighter tone and finer grain size, because a significant component of gravel is derived from the hydrothermally altered rhyolite of the Calico Hills, as well as from Paleozoic limestone (Orkild and O'Connor, 1970; McKay and Williams, 1964).

Alluvial units include fluvial sediments and debris-flow deposits (Glancy, 1994; Costa, 1988). The younger alluvial units (5, 6, and 7, defined below) include nonvegetated surficial lobes and bars, which are too small to map separately, of angular cobbles and boulders lacking matrix at the surface. These features are similar to those described by Hooke (1967) as sieve deposits. Exposures through these features, interpreted as debris-flow deposits here and elsewhere (Glancy, 1994; Blair and McPherson, 1992), typically show a matrix of sand and silt that fills the void space between coarse clasts at depths greater than 20 cm, although much of this material may be secondary, infiltrated, eolian sediment. The surficial matrix-free features in alluvium in the Yucca Mountain area are more common in relatively coarse-grained alluvium proximal to steep hillslopes than in finer-grained alluvium at locations more distal from hillslope source areas.

7, 7f Modern alluvium (late Holocene), deposited or modified during latest streamflow events--Predominantly sandy gravel, with interbedded sands; poorly to moderately well sorted; massive to well bedded; clast-supported to matrix-supported. Gravel is angular to subrounded, ranging in size from granules to boulders, but commonly finer grained than adjoining alluvial units, reflecting more limited width of modern channels than of terraces. Unaltered bar-and-swale depositional morphology; vegetation absent to relatively sparse; general absence of desert pavement and rock varnish; no soil development. Clasts with relict, partially eroded, and randomly oriented coats of calcite and silica are common in some channels and accentuate the relatively light tone of modern channels; the coatings were probably formed pedogenically in older deposits from which they were reworked by erosion.

5s Alluvial sand deposits (Holocene to late Pleistocene?)-- Gravelly sand, moderately well-sorted; poorly to well bedded; gravel is angular to subrounded, clasts less than 10 cm in diameter. Surfaces of the deposit are smooth, and lack well-packed desert pavement. Soil has stage I carbonate morphology. Unit occurs in southeast corner of quadrangle as relatively lighter colored areas in swales slightly inset to and reworked from unit 4s and similar sandy alluvial and eolian deposits on the piedmont of the Calico Hills to the northeast.

4, 4f, 4/1

Alluvium (late Pleistocene (?))--Predominantly sandy gravel, with interbedded sands; poorly to moderately well sorted; massive to well bedded; clast-supported to matrix-supported. Gravel is angular to subrounded, ranging in size from granules to boulders. Soil development typically includes a Btj horizon and stage II-III carbonate/silica morphology. In Midway Valley, unit 4 is characterized by a distinctly light-toned surface, with weakly to moderately varnished clasts in a loosely to moderately packed pavement. In Fortymile Wash, unit 4f is characterized by a well packed and varnished surface pavement on a terrace generally about 2 meters above the modern wash. The main basis for correlation of units 4 and 4f is similar soil development, because all occurrences of these units are discontinuous and relatively limited in area. 4/1 designates an area of central Midway Valley in which thin unit 4 only partially buries unit 1 (defined below).

4s Alluvial sand deposits (late Pleistocene (?))--Sand and gravelly sand, light yellowish brown; moderately well-sorted, poorly to well bedded, gravel clasts less than 10 centimeters. Surface is smooth, and has loosely packed, nonvarnished desert pavement, with a darker surface tone on 4s than on 5s. Soil includes a cambic Bw to Btj horizon. Occurs in southeast corner of quadrangle at distal southern edge of piedmont of the Calico Hills to the northeast.

3, 3f, 3/eo

Alluvium (late and middle (?) Pleistocene)--Predominantly sandy gravel, with interbedded sand; poorly to moderately well sorted; massive to well bedded; clast-supported to matrix-supported. Gravel is angular to subrounded, ranging in size from granules to boulders. Surface typically

The surface morphology indicates the original upper depositional surface of unit 1 has been eroded, so that its original depositional thickness is unknown. However, the accordant nature of the more gently rounded surfaces are suggestive of the original depositional top. The occurrence of an ash suggested to be the 0.76 Ma Bishop Ash (Izett and Obradovich, 1991) beneath a buried soil within underlying unit 0 along Yucca Wash (Davis, 1983; see below) constrains surficial unit 1 to be middle Pleistocene in this area. Unit 1 converges with younger alluvial surfaces in central Midway Valley, and may correlate to alluvium associated with a buried soil exposed beneath unit 3f along lower Sever and Fortymile Washes. To east of Fortymile Wash, unit 1/eo designates dissected thin unit 1 gravel derived from the Calico Hills and underlain by eolian sand eo.

- 0 Older gravel along Yucca Wash (middle (?) and early Pleistocene)--Predominantly sandy gravel, with interbedded sands; poorly to moderately well sorted; massive to well bedded; clast-supported to matrix-supported. Gravel is angular to subrounded, ranging in size from granules to boulders. Erosional upper surface consists of rounded ridges; complete absence of depositional microrelief. Includes several areas of gravel older than unit 1, but which may not correlate to each other. Four areas of 0, which occur along the tributary of Yucca Wash from Pinyon Pass, have rounded erosional surfaces. The most extensive of these areas occurs along the west side of the main modern channel, as a ridge of gravel with an even but markedly steeper grade which results in the southward convergence of the ridge with younger alluvium. Along the north bank of the central part of Yucca Wash, an older gravel sequence, also designated as 0, is exposed beneath terraces of surficial map units 1, 3 and 5. Unit 0 includes a buried soil with stage III silica/carbonate morphology. The predominantly pebble gravel which underlies this buried soil contain several reworked ash lens; preliminary chemical analyses are consistent with a correlation to the Bishop Ash (Z.E. Peterman, USGS, written commun., 1993), which is about 760 ka in age (Izett and Obradovich, 1991). This ash may be the same as ash along Yucca Wash that was described and analyzed by Davis (1983). Also includes small area of lag gravel at the northern tip of Alice Ridge (Wesling and others, 1992), and on ridgetop north of Yucca Wash and west of Fortymile Wash; composed of rounded cobbles and boulders of various rhyolitic lithologies that are consistent with transport from provenance similar to that of modern Yucca Wash; no terrace form.

between gullies; surfaces of slopes between gullies typically have poorly to moderately well packed surface pavement of fine angular gravel that is poorly varnished, underlain by a soil that includes a brown cambic to argillic B horizon, and stage II-III carbonate/silica morphology. The predominant sand component is inferred to be of eolian origin, but the presence of fine angular gravel in unit e and in its surface pavement indicate a substantial colluvial, and possibly sheetwash process during deposition. Gully exposures show that unit e includes multiple buried calcic soils; where best exposed at Busted Butte to the south of this map sheet, at least 4 buried soils are exposed, and are inferred to be stratigraphically above Bishop ash that occurs near the base of the sand ramp section (Whitney and others, 1985; Izett and others, 1988). U-series disequilibrium analyses of these buried soils (Paces and others, 1994) indicates that most of the sand was deposited during the middle Pleistocene with relatively minor sand deposition and major dissection during the late Pleistocene; a buried soil at 3-4 m depth of a maximum exposed thickness of 22 m yielded a date of 221 ± 32 ka. At trench T4 in southern Midway Valley (Swan and others, 1993) thermoluminescence dates of 38 ± 5 ka and 73 ± 9 ka in depositional units separated by buried soils indicate at least 3 m of Late Pleistocene deposition.

Colluvial deposits

Colluvial deposits are subdivided on the basis of surface characteristics that are more indicative of hillslope position, thickness, and origin than of age.

cf Footslope colluvium and alluvium (Holocene to early Pleistocene)--Interbedded colluvial and debris-flow diamictos grading to and interbedded with alluvium, generally on lower, concave-upward footslopes (Peterson, 1981) which are typically partially dissected. Angular gravel ranging in size from granules to boulders; generally supported by a matrix with variable proportions of sand, silt, and clay; matrix material inferred to be at least partly of eolian origin. Includes debris-flow deposits associated with boulder levees adjoining and parallel to modern gullies, and probably correlative to units 5-7. As exposed in trenches, unit is massive to finely bedded, and includes multiple buried soils (Swadley and others, 1984; Menges and others, 1994; Wesling and others, 1993), with U-series and TL dates indicating early, middle, and late Pleistocene episodes of pedogenesis and eolian deposition

desert pavement; on steeper slopes, pavement and rock varnish are less well developed. The fine component is inferred to be eolian material with increased clay content from weathering and pedogenesis. Unit re occurs on gently sloping ridgetops of the northern Yucca Mountain area within areas where the former caprock unit of the Tiva Canyon Member of the Paintbrush Tuff was mapped by Scott and Bonk (1984). Grades to and includes areas of colluvial unit cu; the transition to unit cu includes areas of imbricated clasts in pavements on steeper slopes.

Other map units

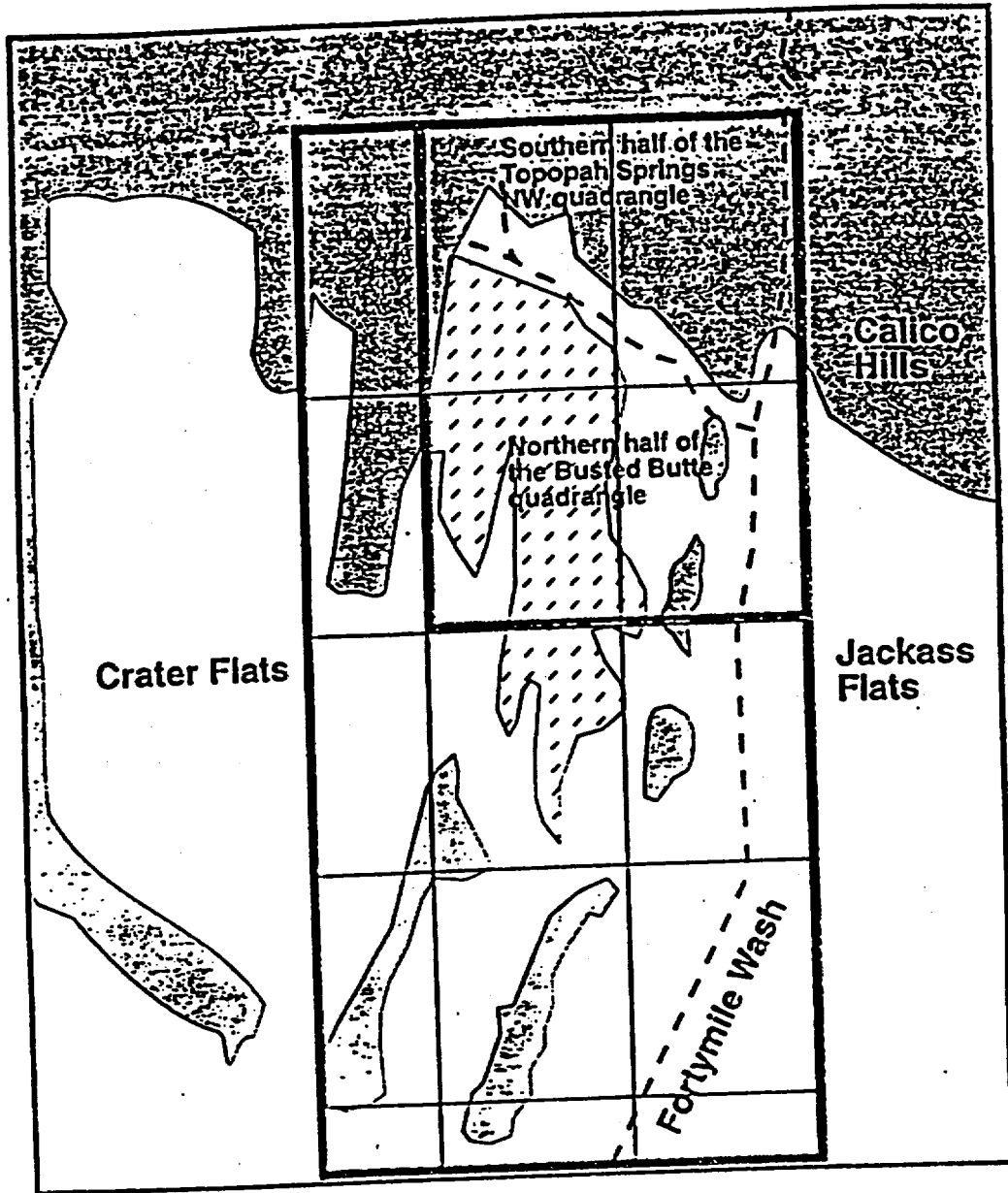
- d Disturbed area (historic)--Includes drillpads, roads and other areas where human activity has removed, buried or otherwise obscured the natural surface deposits; based on March 1990 airphotos (surface disturbance since March 1990 is not mapped).

- r Volcanic bedrock (Late Miocene)--Felsic lava flows and variably welded tuffs that include the Rhyolite of Calico Hills, the Paintbrush Group and the former Rhyolite of Fortymile Canyon (Lipman and Christiansen, 1965; Scott and Bonk, 1984; Warren and others, 1988; Buesch and others, 1994). These volcanic units underlie all surficial deposits, and have outcrops within colluvial units that are too small to map separately. Exposed bedrock exposures mapped as unit r are typically poorly welded tuff.

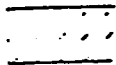
- Glancy, P.A., 1994, Evidence of prehistoric flooding and the potential for future extreme flooding at Coyote Wash, Yucca Mountain, Nye County, Nevada: U.S. Geological Survey Open-File Report 92-458
- Harrington, C.D., and Whitney, J.W., 1987, Scanning electron microscope method for rock-varnish dating: *Geology*, v. 15, p. 967-970.
- Hoover, D.L., 1989, Preliminary description of Quaternary and late Pliocene surficial deposits at Yucca Mountain and vicinity, Nye County, Nevada: U.S. Geological Survey Open-File Report 89-359, 45 p.
- Hooke, R.L., 1967, Processes on arid-region alluvial fans: *Journal of Geology*, v. 75, p. 438-460.
- Izett, G.A., and Obradovich, J.D., 1991, Dating of the Matuyama-Brunhes boundary based on Ar/Ar ages of the Bishop Tuff and Cerro San Luis Rhyolite: *Geological Society of America Abstracts with Programs*, v. 23, p. A106.
- Lundstrom, S.C., and Warren, R.G., 1994, Late Cenozoic evolution of Fortymile Wash: major change in drainage pattern in the Yucca Mountain, Nevada region during late Miocene volcanism, *Proceedings of the Fifth International Conference on High Level Radioactive Waste Management*, p. 2121-2130
- Lundstrom, S.C., Wesling, J.R., Taylor, E.M., and Paces, J.B., in press, Preliminary Surficial Deposits Map of the Northeast 1/4 of the Busted Butte 7.5-minute Quadrangle: United States Geological Survey Open-File Report 94-341, scale 1:12,000.
- Lundstrom, S.C., Mahan, S.A. and Paces, J.B., in press, Preliminary Surficial Deposits Map of the Northwest 1/4 of the Busted Butte 7.5-minute Quadrangle: United States Geological Survey Open-File Report 95-133, scale 1:12,000.
- Lundstrom, S.C., and Taylor, E.M., in press, Preliminary Surficial Deposits Map of the Southern Half of the Topopah Spring NW 7.5-minute Quadrangle: United States Geological Survey Open-File Report 95-132, scale 1:12,000.
- McKay, E.J., and Williams, W.P., 1964, Geologic map of the Jackass Flats Quadrangle, Nye, County, Nevada: U.S. Geological Survey Geologic Quadrangle Map GQ-368, scale 1:24,000.

- Taylor, E.M., 1986, Impact of time and climate on Quaternary soils in the Yucca Mountain Area of the Nevada Test Site, Boulder, University of Colorado, M.S. thesis, 217 p.
- Warren, R.G., McDowell, F.W., Byers, F.M., Jr., Broxton, D.E., Carr, W.J., and Orkild, P.P., 1988, Episodic leaks from Timber Mountain Caldera: new evidence from rhyolite lavas of Fortymile Canyon, southwest Nevada volcanic field: Geological Society of America Abstracts with Programs, v. 20, n. 3, p. 241.
- Wesling, J.R., Swan, F.H., Thomas, A.P., and Angell, M.M., 1993, Preliminary results of trench mapping at the site of prospective surface facilities for the potential Yucca Mountain repository, Nevada: Geological Society of America Abstracts with Programs, v. 25, n. 5, p. 162.
- Wesling, J.R., Bullard, T.F., Swan, F.H., Perman, R.C., Angell, M.M., Gibson, J.D., 1992, Preliminary mapping of surficial geology of Midway Valley, Yucca Mountain Project, Nye County, Nevada: Sandia Report Sand91-0607, scale 1:6000, 55 p.
- Whitney, J.W., and Harrington, C.D., 1993, Relict colluvial boulder deposits as paleoclimatic indicators in the Yucca Mountain region, southern Nevada: Geological Society of America Bulletin, v. 105, p. 1008-1018.
- Whitney, J.W., Swadley, WC, and Shroba, R.R., 1985, Middle Quaternary sand ramps in the southern Great Basin, California and Nevada: Geological Society of America Abstracts with Programs, v. 17, p. 750.

Figure 1
 Yucca Mountain Surficial Deposits Map Area



LEGEND

- | | | | |
|---|-----------------------|--|-------------|
|  | Map Area Boundary |  | Uplands |
|  | Quadrangle Boundaries |  | Yucca Mtn. |
| | |  | Valley Fill |